INTRODUCTION TO MODERN PLANAR TRANSMISSION LINES

PHYSICAL, ANALYTICAL, AND CIRCUIT MODELS APPROACH

ANAND K. VERMA

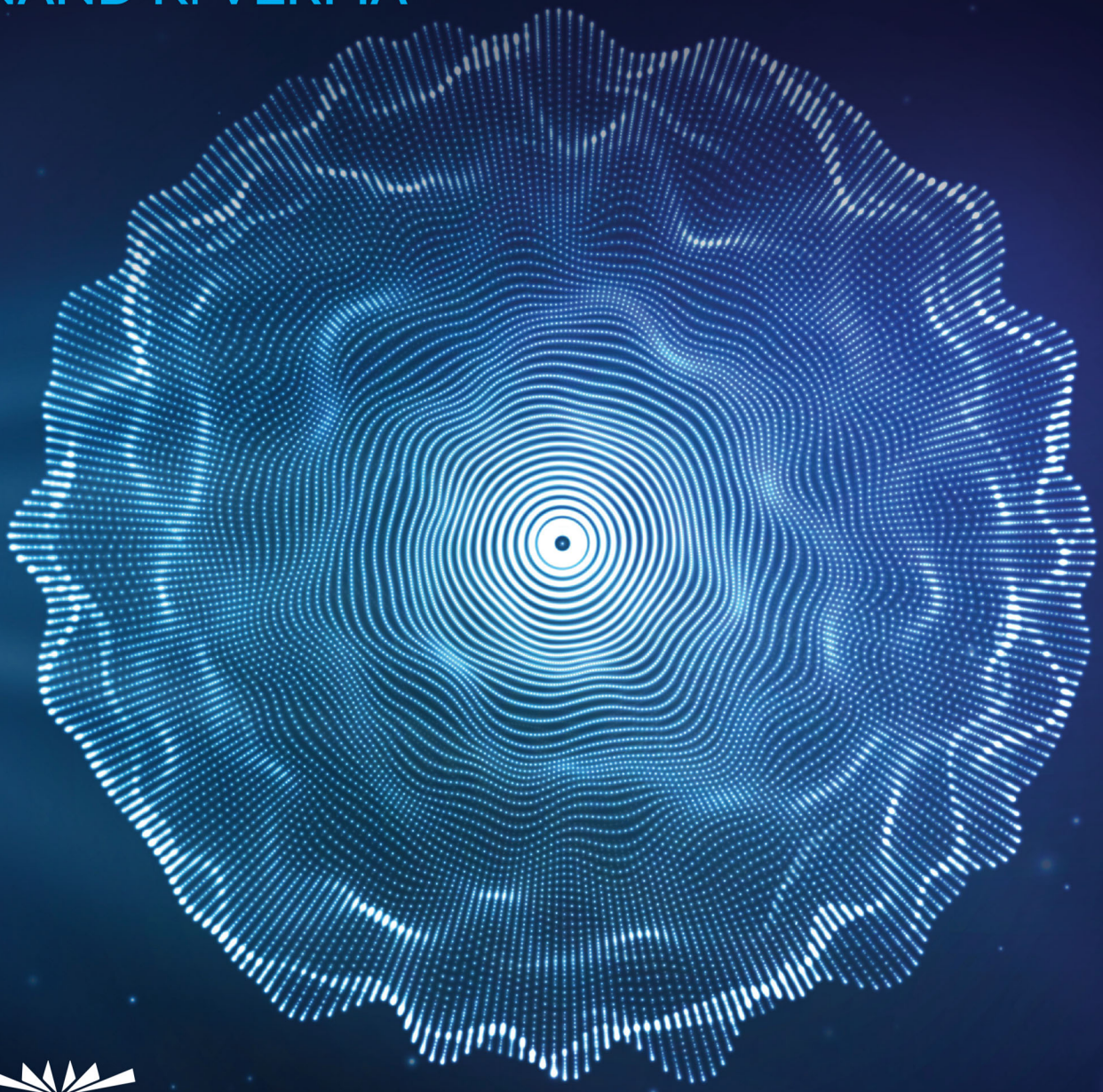

IEEE PRESS

WILEY

Introduction to Modern Planar Transmission Lines

Introduction to Modern Planar Transmission Lines

Physical, Analytical, and Circuit Models Approach

Anand K. Verma
Adjunct Professor, School of Engineering
Macquarie University, Sydney, Australia
Formerly Professor, Department of Electronic Science
South Campus, Delhi University
New Delhi, India

IEEE PRESS

WILEY

This edition first published 2021

Registered Office(s)

John Wiley & Sons, Inc., 111 River Street, Hoboken, NJ 07030, USA

John Wiley & Sons Ltd, The Atrium, Southern Gate, Chichester, West Sussex, PO19 8SQ, UK

Editorial Office

The Atrium, Southern Gate, Chichester, West Sussex, PO19 8SQ, UK

For details of our global editorial offices, customer services, and more information about Wiley products visit us at www.wiley.com.

Wiley also publishes its books in a variety of electronic formats and by print-on-demand. Some content that appears in standard print versions of this book may not be available in other formats.

Library of Congress Cataloging-in-Publication Data:

Names: Verma, Anand K., 1948– author.
Title: Introduction to modern planar transmission lines : physical, analytical, and circuit models approach / Anand K. Verma.
Description: Hoboken, New Jersey : Wiley-IEEE Press, [2021] | Includes bibliographical references and index.
Identifiers: LCCN 2020050198 (print) | LCCN 2020050199 (ebook) | ISBN 9781119632276 (cloth) | ISBN 9781119632450 (adobe pdf) | ISBN 9781119632474 (epub)
Subjects: LCSH: Electric lines.
Classification: LCC TK3221 .V47 2021 (print) | LCC TK3221 (ebook) | DDC 621.3815–dc23
LC record available at https://lccn.loc.gov/2020050198
LC ebook record available at https://lccn.loc.gov/2020050199

Cover Design: Wiley
Cover Image: © DamienGeso/Getty Images

Set in 10/12.5pt STIXTwoText by Straive, Pondicherry, India

10 9 8 7 6 5 4 3 2 1

To my loving and caring wife Kamini Verma and ever-smiling grandchildren Naina, Tinu, and Nupur.

Contents

Preface

The planar transmission lines form the core of modern high-frequency communication, computer, and other related technology. The subject has come up to the present level of maturity over the past three to four decades. The planar transmission lines are used not only as interconnects on the PCB board and IC chips; these are directly needed for the development of microwave and mm-wave components in the form of microwave integrated circuits (MIC). The types of planar transmission lines, i.e. their physical structures and material medium, have been changing with the growth of technology in many other disciplines. Such efforts during recent years propelled the MIC to move in many exotic directions – MMIC, MEMS, LTCC, use of ferroelectrics, and high-temperature superconductors, optically controlled microwave devices, nonlinear planar transmission lines, DGS, EBG, metamaterials, etc. The researchers with varying backgrounds have contributed much to research activities. Already the divergent planar technology has contributed significantly to the advancement of high-frequency electronics and in the near future, more contribution will be made by it. The exotic planar transmission lines are not covered comprehensively in a single book. The present book is an attempt in this direction. *The proposed book aims to provide a comprehensive discussion of planar transmission lines and their applications. It focuses on physical understanding, analytical approach, and circuit models for planar transmission lines and resonators in the complex environment*.

The present book has evolved from the lecture notes, workshop, seminar presentation, and invited lectures delivered by the author at many universities and R&D centers. Some chapters were also initially written for the Ph.D. students to help them to understand the topics. Finally, it has evolved from notes prepared by the author as a scheme for the self-study. The author started his academic career after 17 years of professional experience in the field of electrical engineering, broadcast transmitters, and satellite communication.

At present, the planar transmission lines are taught as part of the course on RF and microwave packaging, advanced electromagnetic field theory, and microwave design. It is also taught as an independent paper. However, a teacher has to consult divergent sources to prepare the lecture notes, as no single source at the teaching-level is available. Moreover, the classroom teaching of the planar transmission lines is not as systematic as the classical metallic waveguide structures. It is due to the very nature of the subject itself. *The available books are usually not classroom oriented. Usually, they can be grouped into two categories – 1. Design-oriented books, 2. Monograph kind of books*. Once we use the first category of books in the classroom, we end up writing only closed-form expressions without any systematic derivation of the expressions. The systematic approach is important in the classroom environment. The second category of books is suitable for an experienced researcher or specialist. It is difficult to use them in the classroom. Thus, a teacher of this subject has to struggle between these two extremes to balance teaching throughout the semester. Finally, a teacher has to depend on personal experience and lecture notes.

There is a need to present, in one cover, the divergent topics of the planar transmission lines in a student-friendly format. The researchers with varying backgrounds in physics, chemistry, engineering, and other fields have joined activities in the expanding area of the planar technology. The early researchers, R&D professionals in the industry, teachers, and students need a text that could be useful in faster acquisition of the physical modeling process and theoretical formulations used in the classical planar transmission lines. Similar treatment is also needed for the modern engineered EBG and metamaterial lines and surfaces.

Therefore, the real motivation for writing this *intermediate-level* book is to fill the gap for a *textbook* on the planar transmission line that caters to the need for classroom teaching, early researchers with divergent backgrounds, and designers working in the microwave industry. The book is intended to help students both at the undergraduate and postgraduate levels. It also serves the purpose of a resource book for self-study. *The detailed derivations of results and physical modeling of the planar transmission lines are two basic concepts followed through the book*. The present book is neither a design-oriented book nor an advanced monograph. The book correlates the physical process with mathematical treatment. The advanced mathematical methods such as the *conformal mapping method*, *variational method, and spectral domain method* applied to planar lines are worked out in adequate details. The book further covers modern topics such as the *DGS/EBG, metamaterial-based planar transmission lines,* and *surfaces*. The approach used in writing the book is perhaps less formal than most available texts. This approach is helpful for classroom teaching. It also assists the reader to follow the contemporary developments in planar technology.

Acknowledgments

The author is thankful to Prof. Karu P. Esselle and Prof. Graham Town, *School of Engineering, Macquarie University, Sydney,* for supporting Adjunct Professorship at Macquarie University. The author is also thankful to Prof. Enakshi K. Sharma, *Department of Electronic Science, South Campus, Delhi University,* for continuous discussions on topics related to EM-Theory, Wave propagation, etc. The author sincerely appreciates the help and guidance provided by Prof. Kai Chang, *Department of Electrical Engineering, Texas A&M University* during the review process of the book. The author also appreciates the active interest taken by Mr. Brett Kurzman and his team of *Wiley Publishing* for the review and friendly administrative support.

The author is particularly grateful to Dr. I.J. Bahl, *Editor-in-Chief, Int. J. of RF & Microwave Computer-Aided Engineering, John Wiley, USA*; Prof. Zhongxiang Shen, *School of Electrical and Electronic Engineering, Nanyang Technological University, Singapore*; and Prof. Ladislau Matekovits, *Department of Electronics and Telecommunications, Politecnico di Torino, Italy,* for reading book chapters and providing valuable suggestions to improve the book.

The author has benefitted from the comments, suggestions, and corrections of many colleagues, teachers, and students. The author would like to thank the following people for their useful contributions toward corrections and useful discussions: Dr. Koteshwar Rao, Dr. Harsupreet Kaur, Dr. Kamlesh Patel, Mr. Amit Birwal, Dr. Ashwani Kumar, Dr. Paramjeet Singh, Dr. Y.K. Awasthi, and Mr. Prashant Chaudhary from the *Department of Electronic Science, Delhi University*; Dr. Raheel Hashmi, Dr. Sudipta Chakraborty, and Dr. Rajas Prakash Khokle of *School of Engineering, Macquarie University, Sydney*; Dr. Nasimuddin of *Institute for Infocomm Research, Singapore*; Prof. Asoke De, Dr. Priyanka Jain, Ms. Priyanka Garg of *Department of Electrical Engineering, DTU, Delhi*; Mr. Shailendra Singh of *Product Development and Innovation Center, Bharat Electronics Ltd., Bengaluru, India*; Dr. Rajesh Singh, *Microwave Radiation Laboratory, University of Pisa, Italy*; Dr. Archna Rajput, *IIT Jammu, India;* Dr. Ravi Kumar Arya, *Dept. of ECE, NIT, Delhi*. The author is especially thankful to his students, Mr. Shailendra Singh and Mr. Prashant Chaudhary for their continuous help in correction of all chapters.

The author expresses his unbounded love and regards to his parents – Late Sh. A.P. Verma and Late Tara Devi, Uncle Late Sh. Hira Prasad, to grandmother Late Radhika Devi, and Uncle and Life-guide Sh. Girija Pd. Srivastava. The author also is grateful to his teacher Prof. M.K.P. Mishra for excellent teaching of Circuit Theory in unique style, and for providing support in many ways. The author is thankful to his family members for their encouragement and support. Finally, I wish to express my heartfelt thanks and deepest appreciation to my wife, Kamini. The smiling faces of my grandchildren, Naina, Tinu, and Nupur have always kept me going on with the tiring work of book writing.

Anand K. Verma
New Delhi, Sydney

Author Biography

Anand K. Verma, PhD, is an adjunct professor in the School of Engineering, Macquarie University, Sydney, Australia. Formerly, he was professor and head, Department of Electronic Science, South Campus, University of Delhi, New Delhi, India. He has been a visiting professor at Otto van Guericke University, Magdeburg, Germany (2002–2003), and a Tan Chin Tuan Scholar (2001) at Nanyang Technological University, Singapore. He holds a German patent on a microstrip antenna. He has introduced *the concept and design method of surface-mounted compact horn antenna* used for high gain, wideband, and ultra-wideband quasi-planar antenna applicable to both linear and circular polarization. He has organized and attended many international symposia and workshops. He has conducted short-term courses and delivered invited lectures at the research institutes in India and several countries. He was also chairman of the TPC, APMC-2004, New Delhi, India. Professor Verma has published over 250 papers in international journals and the proceedings of international and national symposia. He has introduced the *concept of single layer reduction (SLR) formulation* for the CAD-oriented modeling of multilayer planar lines.

1

Overview of Transmission Lines

(*Historical Perspective, Overview of Present Book*)

Introduction

The transmission line is at the core of the communication technology system. It forms a medium for signal transmission, and also helps to develop high-frequency passive components and circuit blocks. Historically, both experimental investigations and analytical theories have played significant roles in the growth of transmission line technology. Each type of distinct line structure is responsible for the development of distinct communication technology. The *single-wire transmission line* with the Earth as a return conductor is responsible for the operation of Telegraphy. It evolved into the *coaxial cable* that made the *Transatlantic Telegraphy* possible. The *two-wire open line* became a medium for the *Telephonic transmission*. These two line structures are behind the development of the monopole and dipole antenna that made possible the growth of the high-frequency communication using the medium wave (MW), short wave (SW), very high-frequency (VHF), and ultra-high frequency (UHF) bands. The microwave and mm-wave transmission systems are developed mostly around the metallic waveguides, and subsequently also using the nonmetallic dielectric waveguides. Finally, it has resulted in modern optical fiber technology. The planar transmission lines are behind the modern advanced microwave communication components and systems.

The present chapter provides a very brief historical overview of the classical and modern planar transmission lines. The chapter presents a historical survey of the development of the electromagnetic (EM) theory also. Next, a brief overview of the organization of the book is discussed.

Objectives

- *To present a survey of the developments of the classical EM-theory.*
- *To present brief historical notes on the classical transmission lines and development of transmission line theory.*
- *To present brief historical notes on planar transmission lines.*
- *To present an overview of the contents of the book.*

1.1 Overview of the Classical Transmission Lines

The classical transmission lines such as a single-wire line with the earth as a return conductor, coaxial cable, two-wire line, multi-conductor lines, and waveguides are reviewed very briefly in this section. The historical development of the *Telegrapher's Equations* is also presented. The developments of the theoretical concepts of EM-theory are reviewed below. The data related to the review of the EM-theory and transmission lines are collected from the published books [B.1–B.7] and journal articles referred at the end of the chapter.

1.1.1 Telegraph Line

The telegraph is the first coded point-to-point electrical communication system. As early as 1747, William Watson showed the possibility of transmitting an electrical current on a wire using the earth as a return conductor. Thus, *overhead single-wire* with the earth as a return conductor is the first transmission line. It is to be noted that even the *voltaic pile*, i.e. the chemical battery of Volta was nonexistent at that time. The *Leiden jar,* a capacitor to store the static electrical charges, was invented just two years before in 1745. However, much earlier in the year 1663, Otto Von Guericke studied the phenomenon of *static electricity* and designed a machine to produce it. Thus, the charged Leiden jar became a source of

Introduction to Modern Planar Transmission Lines: Physical, Analytical, and Circuit Models Approach, First Edition. Anand K. Verma.

electricity, and single-wire transmission was the communication medium. These were two important ingredients to establish the telegraph link. The third ingredient of telegraphy, the *electroscope*, invented by William Gilbert around 1600, acted as the receiver for the coded signals. It is interesting to note that the telegraph was conceived without any theoretical investigations on electricity. Even Coulomb's law was discovered later in 1785. However, the proper telegraphy could be developed only after the invention of *voltaic pile, i.e. a chemical battery* by Volta in 1799. Further development of the telegraph has an involved history. In 1837, Morse patented his telegraph in the United States, and on January 6, 1838, the first telegram was sent over 3 km distance. Cooke commercialized the telegraph in England and established the 21 km link on April 9, 1839. Thus, an era of electrical communication heralded. In 1844, long-distance Morse's telegraph between Washington, DC, and Baltimore, Maryland was established. Before further reviewing the growth of the classical transmission lines, it is useful to have a quick look at the theoretical developments related to electricity [B.5].

1.1.2 Development of Theoretical Concepts in EM-Theory

The ancients unfolded our story of Electromagnetism through careful observations of the phenomena of static electricity and natural magnetism. The developments of basic concepts, analytical modeling, and theoretical formulations used in the EM-Theory are emphasized in the review. The theoretical concepts of the electric and magnetic fields followed the mathematical models developed for the gravitational force by Newton in 1687, and subsequently refined by other investigators. The development of the theoretical models of transmission lines inherited the modeling process, and mathematical method of Fourier developed for the transmission of heat in a rod.

Electrostatics and Scalar Potential

Newton published his theory of gravitation in his monograph *Philosophiae Naturalis Principia Mathematica*. Newton viewed the gravitational interaction between two masses through *force*. The effect of static electricity was known for a long time, at least since 600 BC. However, only in 1600, Gilbert carried out systematic studies of both magnetism and static electricity. The *static electricity* was generated by the rubbing of two specific objects. He suggested the word *electricus* for electricity, and the English word "*electricity*" was suggested by Thomas Browne in 1646. Gilbert also suggested that the electrical effect is due to the flow of a small stream of weightless particles called *effluvium*. This concept helped the formulation of *one- and two-fluid model* of electricity. He also invented the first electrical measuring instrument, the *electroscope*, which helped further experimental investigations on electricity.

In 1733, Fay proposed that electricity comes in two forms – *vitreous* and *resinous,* and on combination, they cancel each other. The flow of the two forms of electricity was explained by the *two-fluid model*. During this time interval, around up to 1745, the electrical attraction and repulsion were explained using the flow of Gilbert's particle effluvium. In 1750, Benjamin Franklin proposed the *one-fluid model* of electricity. The matter containing a very small quantity of electric fluid was treated as negatively charged, and the matter with excess electric fluid was treated positively charged. Thus, the *negative charge* was resinous electricity, and the *positive charge* was vitreous electricity. Now, the stage was ready for further theoretical and experimental investigations on electricity.

In the year 1773, Lagrange introduced the concept of the *gravitational field*, now called *the scalar potential field*, created by a mass. The gravitational force of Newton was conceived as working through the *gravitational field*. The scalar potential field has appeared as a mechanism to explain the gravitational force interaction between two masses. Thus, a mass located in the potential field, described by a function called the *potential function*, experiences the gravitational force. In 1777, Lagrange also introduced the *divergence theorem* for the gravitational field. The nomenclature *potential field* was introduced by Green in 1828. Subsequently, Gauss in 1840 called it "*potential.*" Laplace in 1782 showed that the potential function ϕ (x,y,z) satisfies the equation $\nabla^2\phi = 0$. Now the equation is called *Laplace's equation*.

Following the Law of Gravitation, Coulomb postulated similar inverse square law, now called *Coulomb's law*, for the electrically charged bodies. He experimentally demonstrated the inverse square law for the charged bodies in 1785. Thus, the mathematical foundation of the EM-theory was laid by Coulomb. The law was also applicable to magnetic objects. The interaction between charged bodies was described by the electric force. In the year 1812, Poisson extended the concept of potential function from the gravitation to electrostatics. Incorporating the charge distribution function ρ, he obtained the modified Laplace's equation, written in modern terminology, $\nabla^2\phi = -\rho/\varepsilon_0$. This equation now called *Poisson's equation* is the key equation to describe the potential field due to the charge distribution. In the same year, Gauss

rediscovered the divergence theorem originally discovered by Lagrange for the gravitational field.

In the year 1828, Green coined the nomenclature – the *potential function*, for the function of Lagrange and modern concept of the *scalar potential field* came into existence. Green also showed an important relation between the surface and volume integrals, now known as *Green's Theorem*. Green applied his method to the static magnetic field also. Green also introduced a method to solve the 3D inhomogeneous Poisson partial differential equation where the considered source is a point charge. The point charge is described by the *Dirac's delta function*. The solution of the Poisson's partial differential equation, using Dirac's delta function, is now called *Green's function*. Neumann (1832–1925) extended the *Green's function* method to solve the 2D potential problem and obtained the eigenfunction expansion of 2D Green's function [J.1–J.5, B.2, B.7].

Magnetic Effect of Current

So far, we have paid attention to the electrostatics. At this stage, *Leiden jar* was the only source of static electricity. A source for the continuous electric current was not available. Volta in 1799 invented the *voltaic pile, i.e. a chemical battery*, and the first time a continuous source of electric current came into existence. On April 21, 1820, it led to the *discovery of the magnetic effect of current* flowing in a wire. The electric current became the source of the magnetic field, encircling the current-carrying wire. The magnetic effect of current was discovered by Orsted (Oersted). In the same year, Ampere showed that the co-directional parallel currents flowing in two wires attract each other, and the counter-currents repel each other. It was a very significant discovery, i.e. creation of the attractive and repulsive magnetic forces without any physical magnet. It firmly established the relation between electricity and magnetism. Ampere further developed an equation, presently called *Ampere's Circuital Law*, to connect the current flowing in a wire to the magnetic field around it and developed the right-hand rule. He called the new field of electricity *Electrodynamics* and Maxwell recognized him as the *Father of Electrodynamics*. Ampere further modeled the natural magnetic materials as the materials composed of perpetual tiny circulating electric currents. He demonstrated the validity of his concept using the current-carrying conductor in the helical form called a *solenoid*. The solenoid worked like an artificial bar magnet. In the year 1820 itself, Biot–Savart obtained the equation using the line integral to compute the magnetic field at a position in the space due to the current flowing in a wire [J.2, B.6, B.7].

Ohm's Law

The voltaic pile helped the discovery of the magnetic effect of current; however, surprisingly the relation between the current flowing in resistance and voltage across it, known as the *Ohm's law*, remained undiscovered. The primary reason was the unstable voltage supplied by the voltaic pile. The discovery of *thermoelectricity* by Seebeck in 1822 provided a constant voltage source to supply continuous electric current. Using the thermo-piles in the year 1826, Ohm obtained a simple but powerful relation among voltage, current, and resistance. It was the beginning of the *Electric Circuit Theory*. However, only in 1850 Kirchhoff published his two *circuital laws* and opened the path for the development of the *Network Theory*. Kirchhoff also showed that *Ohm's electroscopic force (voltage)* and classical potential of Lagrange, Laplace, and Poisson are identical. Interestingly, Ohm's law could be viewed as a symbol of the International Scientific unity relating to Italy (Volta), Germany (Ohm), and France (Ampere). Based on the magnetic effect of current, in the same year, Johann Christian Poggendorff invented the *galvanometer* to detect the current in a wire. Kelvin improved its sensitivity by designing the *mirror galvanometer* in 1858 [B.1, B.6, B.7].

Electric Effect of the Time-Varying Magnetic Field

On knowing the magnetic effect created by an electric current, Faraday argued that the magnetic field can also produce the electric effect. After some attempts, he realized that such an effect can't be produced by the stationary magnet. In 1831, he could generate the electric potential (*electromotive force*) and electric current by the time-varying magnetic field of a moving magnet. The phenomenon is called the *induction effect*. The voltage induction effect demonstrated that electricity could be generated by a purely mechanical process, converting the mechanical energy into electrical energy via the medium of the moving magnetic field. The first *DC generator* was demonstrated by Faraday himself, and next year French instrument maker Hippolyte Pixii built the first *A.C. generator* inaugurating the Electrical Age. Now, the electricity was ready to accelerate the growth of human civilization at an unprecedented rate [B.6, B.7].

Concept of the Magnetic Vector Potential

In the process of discovery of induction, Faraday introduced the *concept of fields*, and also suggested that the electric energy resides in the field around the charged body and the magnetic energy resides in the field around the magnetized body. Thus, he viewed that the electric and magnetic energies reside in the space around the charged or magnetized body, not in the charge or magnet.

The *field concept* has greatly influenced the further development of EM-theory. The field provided a mechanism of interaction between charged bodies. Using Ampere-Biot–Savart law of magnetic forces, and electromagnetic induction of Faraday, Neumann in 1845 introduced the concept of the *magnetic vector potential* $\vec{A}$ to describe the magnetic field. Subsequently, Maxwell showed that the time derivative of $\vec{A}$ computes the induced electric field $\vec{E}$. Kelvin in 1847 further extended the concept of the *magnetic vector potential* $\vec{A}$ to compute the magnetic field using the relation $\vec{B} = \nabla \times \vec{A}$. This relation comes as a solution of the Gauss divergence equation $\nabla \cdot \vec{B} = 0$ due to the closed-loop of the magnetic field, showing the nonexistence of a magnetic charge. Kelvin further elaborated on the mathematical theory of magnetism in 1851. It is interesting to note that at any location in the space once time-dependent magnetic vector potential function is known, both the magnetic and electric fields could be computed as,

$$\vec{B} = \nabla \times \vec{A} \qquad \text{(a)}$$

$$\nabla \times \vec{E} = -\partial \vec{B}/\partial t = \nabla \times \left(-\partial \vec{A}/\partial t\right) \qquad (1.1.1)$$

$$\Rightarrow \vec{E} = -\partial \vec{A}/\partial t \qquad \text{(b)}.$$

Maxwell shared the views of Neumann and Kelvin. However, *time-retardation* was not incorporated in the scalar and vector potentials. In 1867, Lorentz introduced the *concept of retardation* in both the scalar and vector potentials to develop the EM-theory of light, independent of Maxwell. The time-retardation only in the scalar potential was first suggested by Riemann in 1858, but his work was published posthumously in 1867 [J.1, J.2, B.6, B.7].

Maxwell's Dynamic Electromagnetic Theory

At this stage of developments in the EM-theory, the electric field was described in terms of the scalar electric potential, and the magnetic field was described by the magnetic vector potential. Several laws were in existence, such as Faraday's law, Ampere's law, Gauss's law, and Ohm's law. Now Maxwell, Newton of the EM-theory, arrived at the scene to combine all the laws in one harmonious concept, i.e. in the *Dynamic Electromagnetic Theory*. He introduced the brilliant concept of the *displacement current,* created not by any new kind of charge but simply by the time-dependent electric field. Unlike the usual electric current supported by a conductor, this new current was predominantly supported by the dielectric medium. However, both currents were in a position to generate the magnetic fields. Thus, Maxwell modified Ampere's circuital law by incorporating the displacement current in it. The outcome was dramatic; the *electromagnetic wave equation*. Despite such success, the concept and physical existence of displacement current created a controversy that continues even in our time, and its measurement is a controversial issue [J.6–J.8].

In the year 1856, Maxwell formulated the *Faraday's law of induction* mathematically, and modified Ampere's circuital law in 1861 by adding the displacement current to it. Finally in 1865 after a time lag of nearly 10 years, Maxwell could consolidate all available knowledge of the electric and magnetic phenomena in *a set of 20 equations* with 20 unknowns. However, he could solve the equations to get the wave equations for the EM-wave with velocity same as the velocity of light. Now, the light became simply an EM-wave. In the year 1884, *Heaviside reformulated the Maxwell equations* in a modern set of four vector differential equation. The new formulation of Maxwell equations was in terms of the electric and magnetic field quantities and completely removed the concept of potentials, considering them unnecessary and unphysical. Hertz has independently rewritten the Maxwell equation in the scalar form using 12 equations without potential function. Hertz worked out these equations only after Heaviside. In 1884, Poynting computed the power transported by the EM-waves. Recognizing the contributions of both Heaviside and Hertz in reformulating Maxwell's set of equations, Lorentz called the EM-fields equations *Maxwell–Heaviside–Hertz equations*. However, in due course of time, the other two names were dropped and the four-vector differential equations are now popularly known as "*Maxwell's Equations*" [J.1, J.6, J.9, J.10, B.5–B.7].

Generation and Transmission of Electromagnetic Waves

Maxwell's EM-theory was a controversial theory, and physicists such as Kelvin never accepted it. Hertz finally generated, transmitted, and detected the EM-waves in 1887 at wavelengths of 5 m and 50 cm. In the process, he invented the *loaded dipole* as the transmitting

antenna, rectangular *wire-loop receiving antenna*, and *spark-gap* both as transmitter and detector to detect the propagated EM-waves. Thus, he experimentally confirmed the validity of Maxwell equations and opened the magnificent gateway of wireless communication.

In the year 1895, Marconi transmitted and received a coded telegraphic message at a distance of 1.75 miles. Marconi continued his works and finally on December 12, 1901, he succeeded in establishing the 1700 miles long-distance wireless communication link between England and Canada. The transmission took place using the *Hertzian spark-gap transmitter* operating at the wavelength of 366m. In the year 1895 itself, J.C. Bose generated, transmitted, and detected the 6 mm EM-wave. He used circular waveguide and horn antenna in his system. In 1897, Bose reported his microwave and mm-wave researches in the wavelengths ranging from 2.5 cm to 5 mm at Royal Institution, London. Of course, the Hertzian spark-gap transmitter was at the core of his communication system. Bose was much ahead of his time as the commercial communication system grew around the low frequency, and the microwave phase of communication was yet to come in the future. In 1902, Max Abraham introduced the concept of the *radiation resistance of* an antenna [J.11–J.13, B.1–B6].

Further Information on Potentials

Hertz is known for his outstanding experimental works. However, as a student of Helmholtz, he was a high ranking theoretical physicist. Although, he considered, like Heaviside, electric and magnetic fields as the real physical quantities, still he used the vector potentials, now called *Hertzian potentials* $\vec{\pi}^{e}$ and $\vec{\pi}^{m}$, to solve Maxwell's wave equation for the radiation problem. These potentials are closely related to the electric scalar potential ϕ and magnetic vector potential $\vec{A}$. Stratton further used Hertzian potentials in elaborating the EM-theory [B.8]. Collin continued the use of Hertzian potentials for the analysis of the guided waves. He also used the $\vec{A}$ and ϕ potentials in the radiation problems [B.9, B.10]. The use of Hertzian potentials gradually declined. However, its usefulness in problem-solving has been highlighted [J.1, J.11, J.12].

Gradually, the magnetic vector potential became the problem-solving tool if not the physical reality. Further, by using the *retarded scalar and vector potentials* and *Lorentz gauge condition* $\nabla\cdot\vec{A} = -\mu\varepsilon\partial\phi/\partial t$ connecting both the vector and scalar potentials, Lorentz formulated the EM-theory of Maxwell in terms of the magnetic vector potential. In his formulation, a current is the source of the magnetic vector potential $\vec{A}$. So, Lorentz considered the propagation of both the magnetic vector and electric scalar potential with a finite velocity that resulted in the retarded time at the field point. However, Maxwell's scalar potential was nonpropagating. Maxwell did not write a wave equation for the scalar potential, as his use of *Coulomb gauge* $\nabla\cdot\vec{A} = 0$ was inconsistent with it. Later on, even *electric vector potential* $\vec{F}$ was introduced in the formulation of EM-theory. The nonphysical magnetic current, introduced in Maxwell's equations by Heaviside, is the source of potential $\vec{F}$. The use of vector potentials simplified the computation of the fields due to radiation from wire antenna and aperture antenna. A component of the magnetic/electric vector potential is a scalar quantity. It has further helped the reformulation of EM-field theory in terms of the *electric scalar* and *magnetic scalar potentials* [B.9, B.10]. Such formulations are used in the guided-waves analysis. In recent years, it has been pointed out that the *Lorentz gauge condition* and *retarded potentials* were formulated by Lorenz in 1867, much before the formulation of famous H. A. Lorentz [J.14, J.15]. However, most of the textbooks refer to the name of Lorentz.

Both Heaviside and Hertz considered only the electric and magnetic fields as real physical quantities, and magnetic vector and electric scalar potentials as merely auxiliary nonphysical mathematical concepts to solve the EM-field problem. Possibly, this was not the attitude of Kelvin and Maxwell. They identified the electrical potential with energy, and magnetic vector potential with momentum. The magnetic vector potential $\vec{A}$ could be considered as the *potential momentum per unit charge*, just as the electric scalar potential ϕ is the *potential energy per unit charge* [J.16]. The potential momentum $\vec{P}$ is obtained as follows:

$$\vec{F} = \frac{d\vec{P}}{dt} = q\vec{E} = -\frac{\partial\left(q\vec{A}\right)}{\partial t}, \Rightarrow \vec{P} = q\vec{A}. \tag{1.1.2}$$

In the above equation, $\vec{F}$ is the force acting on the charge q, and $\vec{E}$ is given by equation (1.1.1b).

Lebedev in 1900 experimentally demonstrated the radiation pressure, demonstrating momentum carried by the EM-wave. The energy and momentum carried by the EM-wave indicate that the light radiation could be viewed as some kind of particle, not a wave phenomenon. A particle is characterized by energy and momentum. Such a dual nature of light is a quantum mechanical duality phenomenon. Einstein introduced the concept of the light

particle, called "photon" to explain the interaction of light with matter, i.e. the *photoelectric effect*. However, Lorentz retained the classical wave model to explain the interaction between radiation and matter via *polarization of dipoles* in a material creating its frequency-dependent permittivity.

It is to be noted that at a location in the space, even for zero $\vec{B}$ and $\vec{E}$ fields, the potentials $\vec{A}$ and ϕ could exist [B.11]. Aharonov–Bohm predicted that the potential fields $\vec{A}$ and ϕ, in the absence of $\vec{B}$ and $\vec{E}$, could influence a charged particle. Tonomura and collaborators experimentally confirmed the validity of Aharonov–Bohm prediction. The *Aharonov–Bohm effect* demonstrates that $\vec{B}$ and $\vec{E}$ fields only partly describe the EM-fields in quantum mechanics. The vector potential also has to be retained for a complete description of the EM-field quantum mechanically [J.3, J.16, J.17]. However, to solve the classical electromagnetic problems, such as guided wave propagation and radiation from antenna, Heaviside formulation of Maxwell equations and potential functions as additional tools is adequate.

EM-Modeling of Medium

The above brief review omitted developments in the electromagnetic properties of the material medium. A few important developments could be summarized. In 1837, Faraday introduced the concept of the *dielectric constant* of a material. In 1838, he introduced the concept of *electric polarization* $\vec{P}$ in dielectrics under the influence of the external electric field. Soon after the discovery of the electron in 1897 by J.J. Thomson, the models around electrons were developed to describe the electromagnetic properties of a material. Around 1898, John Gaston Leathem obtained an important relation $\vec{D} = \vec{E} + \vec{P}$, connecting the displacement of charges in a material with polarization. Kelvin, in the year 1850, developed the concept of *magnetic permeability* and *susceptibility* with separate concepts of $\vec{B}$, $\vec{M}$, and $\vec{H}$ to characterize a magnetic material. In 1900, Drude developed the electrical conduction model, now known as the *Drude model*, after electron theory. Subsequently, the model was extended to the dielectric medium by Lorentz in 1905. The model called the *Drude-Lorentz model* explains the dispersive property of dielectrics. In the year 1912, Debye developed the concept of *dipole moment* and obtained equations relating it to the dielectric constant. These models laid the foundation to study of the electric and magnetic properties of natural and engineered materials under the influence of external fields [B.4, B.6, B.7, B.12]

1.1.3 Development of the Transmission Line Equations

Kelvin's Cable Theory

During the period 1840–1850, several persons conceived the idea of telegraph across the Atlantic Ocean. Finally, in the year 1850, the first *under-sea telegraphy*, between Dover (*Kent, England*) and Calais (*France*), was made operational. However, no cable theory was available at that time to understand the electrical behavior of signal transmission over the undersea cable.

In 1854, Kelvin modeled the under-sea cable as a *coaxial cable* with an inner conductor of wire surrounded by an insulating dielectric layer, followed by the saline seawater acting as the outer conductor [J.18, B.1]. The coaxial cable was modeled by him as a *distributed RC circuit* with the series resistance R *per unit length* (*p.u.l.*) and shunt capacitance C *p.u.l.* It was the time of the *fluid model* of electricity. Kelvin further conceived the flow of electricity similar to the flow of heat in a conductor. Fourier analysis of 1D heat flow was in existence since 1822. Following the analogy of heat equation of Fourier, Kelvin obtained the *diffusion type equation* for the transmitted voltage signal over the under-sea coaxial cable:

$$\frac{\partial^2 v}{\partial x^2} = RC\frac{\partial v}{\partial t}. \tag{1.1.3}$$

This is the first *Cable Theory*; Kelvin called the above equation the equation of electric excitation in a submarine telegraph wire. Kelvin's model did not account for the inductance L *p.u.l.* and the conductance G *p.u.l.* of the cable. The cable inductance L is due to the magnetic effect of current, and G is due to the leakage current between the inner and outer conductors. However, cable theory was a great success. Following the method of Fourier, he solved the equation for both the voltage and current signals. At any distance x on the cable, a definite time-interval was needed to get the maximum current of the received signal. The galvanometer was used to detect the received current. This time-interval called the *retardation time* of the received current signal also depends on the square of the distance. Moreover, the telegraph signals constituted of several waves of different frequencies, and their propagation velocities were frequency-dependent. It limited the speed of signal transmission for long-distance telegraphy. The conclusions of Kelvin's analysis were ignored, and 1858 transatlantic cable worked only for three weeks. It failed due to the application of 2000 V potential pulse

on the cable. The speed of transmission was just 0.1 words per minute. Finally, following Kelvin's advice and using a very sensitive mirror galvanometer invented by him, the *transatlantic telegraph* was successfully completed in 1865 with eight words per minute transmission speed [B.1–B.3].

Heaviside Transmission Line Equation

The limitation of the speed of telegraph signals was not understood at that time. The RC model of the cable, leading to the diffusion equation, and use of the time-domain pulse could not explain it. Moreover, it became obvious that the *RC model* couldn't be used to understand the problems related to voice transmission over telephonic channels. The telephony was coming into existence. The modern telephone system is an outcome of the efforts of several innovators. However, Graham Bell got the *first patent of a telephone* in the year 1874. The transmitted telephonic voice signal was distorted. Therefore, an analytical model was urgently needed to improve the quality of telephonic transmission. Heaviside in 1876 introduced the *line inductance* L *p.u.l.* and reformulated the cable theory of Kelvin using Kirchhoff circuital laws [B1, B.3]. The formulation resulted in the *wave equation* for both the voltage (V) and current (I) waves on the line:

$$\frac{\partial^2 T}{\partial x^2} = RC\frac{\partial T}{\partial t} + LC\frac{\partial^2 T}{\partial t^2}, \quad (\text{where } T = V, I). \tag{1.1.4}$$

In the case of line inductance $L = 0$, the above equation is reduced to the diffusion type cable equation (1.1.3) of Kelvin. Using the Fourier method, Heaviside solved the aforementioned time-domain equation. Only in 1887, he could introduce the *line conductance* G *p.u.l* in his formulation to account for the leakage current in an imperfect insulating layer between two conductors. Finally, Heaviside obtained a set of coupled transmission line equations using all four line constants R, L, C, and G. Subsequently, the coupled transmission line equations were called the *Telegrapher's equations*. At the end, Heaviside obtained the following modified wave equation:

For lossy line:

$$\frac{\partial^2 T}{\partial x^2} = (RC + LG)\frac{\partial T}{\partial t} + LC\frac{\partial^2 T}{\partial t^2} + RG\,T \qquad (a)$$

For lossless line:

$$\frac{\partial^2 T}{\partial x^2} = LC\frac{\partial^2 V}{\partial t^2}, (\text{where } T = V, I) \qquad (b). \tag{1.1.5}$$

To solve the above time-domain equation, Heaviside developed his own intuitive *operational method approach* by defining the operator $\partial/\partial t \rightarrow p$. The use of the operator reduced the above partial differential equation to the ordinary second-order differential equation. Finally, he solved the equation under initial and final conditions at the ends of a finite length line. In the process, he obtained the expressions for the *characteristic impedance* and *propagation constant* in terms of line parameters. Heaviside could obtain results for the line under different conditions. For a lossless line, $R = G = 0$, the equation (1.1.5b) is obtained. Conceptually, the characteristic impedance provided a mechanism to explain the phenomenon of wave propagation on an infinite line. At each section of the line, it behaved like a secondary Huygens's source providing the forward-moving wave motion. Heaviside also obtained the condition for the *dispersionless transmission* on a real lossy line, and suggested the *inductive loading* of a line to reduce the distortion in both the telegraph and telephone lines. Afterward, his intuitive *operational method approach* developed into the formal *Laplace transform method*, widely used to solve the differential equations [J.19, J.20, B.1–B.3, B.13].

The method of Heaviside was further extended by Pupin in 1899 and 1900. Pupin introduced the *harmonic excitation* in the wave equation as a real part of the source $V_0 e^{jpt}$ [J.21, J.22]. This was an indication of the use of the modern phasor solution of the wave equation. Similar analytical works, and also practical inductive loading of the line was done by Campbell at Bell Laboratory. He published the results in 1903 [J.23]. In July 1893, Steinmetz introduced the *concept of phasor* to solve the AC networks of RLC circuits. In 1893, Kennelly also published the use of complex notation in Ohm's law for the AC circuits [J.24]. Carson in 1921 applied the method to solve Maxwell's equations for the wave propagation on closely spaced lines, and also analyzed for the mutual impedances. Carson in 1927 developed the electromagnetic theory of the Electric Circuits, and paved the way for the modeling of the wave phenomena using the circuit models [J.25, J.26].

Peijel in 1918, and Levin in 1927 analyzed the wave propagation on the parallel lines. Levin extended the telegrapher's equations to the *multiconductor transmission lines* using Maxwell's equations [J.27]. In 1931 Bewley presented a set of wave equations on the coupled multiconductor lines. Subsequently, Pipes introduced the *matrix method* to formulate the wave propagation problem on the multiconductor lines [J.28, J.29]. Thus, the theoretical foundation was laid to deal with the complex

technical problems related to transmission lines. Starting with Marconi wireless in 1895, several improvements took place in the long-range wireless telegraphy. Also, the audio broadcasting was developed between 1905 and 1906 and commercially, around 1920–1923, in the long-wave, medium-wave, and short-wave RF frequency bands [B.5]. Now, the time was ripe for microwave and mm-wave communication.

The above discussion shows that the Telegrapher's equations have come in existence due to the contributions of both Kelvin and Heaviside. To recognize their contributions, we call in this book the Telegrapher's equations as the *Kelvin-Heaviside transmission line equations*. Also, as the characteristic impedance behaves as the secondary Huygens's source, so it can also be viewed as the *Huygens's load*. Such Huygens's load distributed over a surface forms the modern *Huygens's metasurface*, discussed in the chapter 22 of this book.

1.1.4 Waveguides as Propagation Medium

Heaviside reformulated Maxwell equation in 1884. He rejected the idea of EM-wave propagation in a hollow metallic cylinder. In his opinion, two conductors, alternatively one conductor and the earth as a ground conductor are essential for the EM-wave propagation. However, in 1893 J.J. Thomson expressed the possibility of the EM-wave propagation in a hollow cylinder [B.12]. Next year, Oliver Lodge verified it experimentally. In the year 1895, J.C. Bose used the waveguide and horn antenna for the mm-wave transmission and reception. In 1897 he reported the work at Royal Institution in London [B.5]. However, it was Rayleigh who carried out a detailed solution of boundary-value problems. He obtained the *normal mode* solution, showing wave propagation in the form of the distinct discrete modes, i.e. the normal modes. He obtained his solutions for both the TE and TM modes, and introduced the concept of the cutoff frequency for modes. He further examined the EM-wave propagation on a dielectric waveguide [J.30]. In 1920 Rayleigh, Sommerfeld and Debye continued the researches in this direction.

However, only in 1930 proper experimental investigations of the wave propagation in the waveguides were undertaken by G. C. Southworth at Bell Labs, and W.L. Barrow at MIT. In 1934, *microwave commercial link* was established, and in 1936, Southworth and Barrow discovered the possibility of using the waveguide as a transmission medium. However, they published their works only in 1936 [J.31, J.32, B.5]. During the same time-period, Brillouin also investigated the wave propagation in a tube [J.33]. Serious analytical work on waveguides was further undertaken by J.R Carson, S.P. Mead, and S.A. Schelkunoff around 1933 [J.34]. Almost forgotten analytical works of Rayleigh was reinvented. Chu and Barrow further investigated the EM-waves propagation in the elliptical and rectangular hollow metallic pipes [J.35]. During 1934, Schelkunoff extended the *concept of impedance* to the EM-wave propagation in the coaxial line, and obtained the transmission line equations using the electromagnetic theory [J.36]. In 1937, he further extended the theory to the TE and TM mode guided wave propagations, and obtained the circuit models of mode supporting waveguides. Finally, Schelkunoff generalized the standard telegrapher's equation, using Maxwell's EM-theory to represent an infinite set of uncoupled and coupled modes of a waveguide by the system of uncoupled and coupled transmission line equations [J.37–J.39]. Subsequently, his method has been extended to planar lines in an inhomogeneous medium supporting the hybrid modes [B.13].

During the World War-II period, important theoretical and practical works were done in the field of waveguide technology for the development of the waveguide-based components and systems. The development of Radar provided the impetus for such research activities.

1.2 Planar Transmission Lines

A brief review of the development of planar transmission lines, influencing modern microwave technology, is presented below. A review is also given for the analytical methods as applied to the planar line parameters.

1.2.1 Development of Planar Transmission Lines

The waveguide is a low-loss transmission medium capable of handling high power transmission. However, it is a bulky structure with limited bandwidth. The fabrication of waveguide-based components is a complex and expensive machining process. The limitations of the waveguide provided an impetus for the growth of planar lines, and technology based on the planar lines. H.A Wheeler, in 1936, developed a low-loss *coplanar stripline*, and in 1942 created parallel plate strip transmission line on a high permittivity substrate. The line structure was compact and suitable at low RF frequency from 150 MHz to 1500 MHz. However, properly documented *stripline* was reported by R.M. Barrett only in 1951. Just next year, i.e. in 1952, Grieg and Engelmann

reported *microstrip* line. Both structures competed with each other. Initially, the stripline in the homogeneous medium was a preferred line, as it is a dispersionless line with a larger bandwidth. It supports the TEM mode propagation. As it is a shielded line, so it also has a higher Q-factor. Whereas, the microstrip in the inhomogeneous medium is a dispersive line as it supports the dominant hybrid mode. It has a smaller bandwidth and lower Q-factor. During 1960, solid-state components started appearing, and microstrip became the preferred line structure for the MIC environment. The microstrip is an open structure that provided easier access for the interconnections. It led to the development of miniaturized *microstrip integrated circuit (MIC)* technology. Gradually, the discrete active devices were combined with the planar passive microwave components, and the *hybrid MIC (HMIC)* came into existence. The sixties were a very creative period for the planar line technology. In 1968, Cohn reported the *slot line* followed by the *coplanar waveguide (CPW)* that became the medium of MMIC. C.P. Wen in 1969 developed the CPW. It is an interesting and unusual coincidence that the abbreviation of both the line name and inventor's name is CPW. The integration of the slot line with waveguide took place in 1972 when Meier reported the quasi-planar *fin line* [J.40–J.44].

Further compactness in the microwave circuits and systems took place through the development of the *monolithic MIC (MMIC)* circuit concept in the year 1964. At this stage, the MMIC was based on *silicon technology*. Unfortunately, the program was not successful due to the very lossy Si-substrate. The semi-insulating Si-substrate deteriorated in the process of the formation of active devices, such as bipolar junction transistors (BJTs) on a Si-substrate. The next phase of MMIC development took place for the GaAs substrate-based technology in 1968. It required nearly 10–12 years for its more meaningful development. The span of 1980–1986 was a period of rapid growth for *MMIC technology*. In 1990s, SiGe based technology was developed that permitted operation of high-efficiency circuits at higher frequencies. The MMIC technology achieved its maturity for the MMIC based on the silicon and indium–phosphide (InP) substrates apart from the GaAs substrate. At the core of the development were the *multilayer planar lines* and new varieties of active devices [J.45].

Another kind of Si-based technology, namely the *micro-electro-mechanical system (MEMS)* gradually came to the fields of RF and microwave. Petersen's reported the MEMS membrane-based switches in July 1979. However, after a long gap, Yao and Chang developed the surface MEMS switch for DC-4 GHz operation and high-quality MEMS inductor chip could be realized in 1997. Subsequent years witnessed a reduction in operating voltage of MEMS switches. The operation of MEMS in the microwave and mm-wave ranges expanded their applications in the field of the antenna and other microwave systems [J.46–J.48].

The robust and compact multilayer ceramic tape-based microwave technology, called the *low-temperature co-fired ceramics (LTCC)* gradually acquired significance for the development of the hybrid integrated circuits. It started in 1950–1960 to develop more robust capacitors. The several layers of different materials are used in a single multilayer laminated package to design multifunctionality circuit-blocks. The planar lines in the LTCC are used in the multilayer and multilevel formats as a medium to develop the components and interconnect [J.49, J.50].

Further innovations in the planar microwave technology were added by incorporating the periodic reactive loading of planar lines and planar surfaces resulting in the *electronic band-gap (EBG) lines and EBG surfaces* for a wide range of applications. Long ago, the theoretical basis for the analysis of the periodic structures was summarized by L. Brillouin [B.14]. The theoretical concept of the *metamaterial* as a double negative (negative permittivity and negative permeability) material medium, and its radical impact on behaviors of the electromagnetic phenomena were worked out by Victor Veselago in 1967. The practical development of the metamaterials is an outcome of a long history of *artificial dielectrics* and *mixture medium*. However, only in 1996–1999, Pendry and co-workers suggested, and further experimentally demonstrated, the artificial negative permittivity below the controlled plasma frequency. It was realized by using the periodic arrangement of thin conducting wires. Further, in 1999 Pendry and co-workers suggested and experimentally produced resonance type magnetic behavior in the split coaxial conducting cylinders. However, only Smith and co-workers worked out the simultaneous negative permittivity and negative permeability in 2000, and experimentally verified it in 2001. Gradually, the concept of metamaterials was added to the planar lines and surfaces resulting in the realization of *metalines and metasurfaces*. These artificial structures have significantly influenced the design and development of unique antenna, components, and circuits with new characteristics and multifunctionality. Present researches in these fields are in progress in many directions [J.51–J.55].

1.2.2 Analytical Methods Applied to Planar Transmission Lines

Assaudourion and Rimai considered the *microstrip* in the quasi-static limit. They assumed the TEM mode propagation on it. They applied, in 1952, the well-established *conformal mapping method* to compute the characteristic impedance, dielectric, and conductor losses. Between the years 1954 and 1955, Cohn also used the conformal mapping method to get the design-oriented results for the characteristic impedance, dielectric and conductor losses of the *stripline*. He further used the conformal mapping method to get the odd-even mode impedances of the *edge-coupled strip lines* in 1955 itself. He further obtained these results for the *broadside-coupled strip lines* in 1960. Following the conformal mapping method, in 1964 and 1965 Wheeler produced more accurate and design-oriented expressions for the computation of characteristic impedance of microstrip line. He extended his analysis to get further results in 1977 and 1978 [J.56–J.64].

In 1969 Cohn suggested another planar line, i.e. the *slot line*. It is a complementary structure of the microstrip line. He also presented the *equivalent waveguide model* of the slot line, and obtained the frequency-dependent propagation parameters of the slot line. Next in the group of the planar lines is the *coplanar waveguide (CPW)* proposed by C.P. Wen. He obtained the initial quasi-static line parameters of CPW using the conformal mapping method. Subsequently, the conformal mapping method was applied to analyze several variants of the planar lines [J.65–J.67].

Other quasi-analytical and numerical methods were also used for the analysis of microstrip lines. For instance, in 1968 Yamashita and Mitra introduced the quasi-analytical *variational method in the Fourier domain* to obtain the quasi-static line parameters of the microstrip line. It was the prelude to the quasi-analytical *dynamic spectral domain analysis* (SDA) of microstrip and other planar lines. The dynamic SDA is a full-wave analysis method that considers the hybrid mode nature of planar lines. After a gap of nearly 10 years, Itoh used the concept of the *discrete Fourier transform* and *Galerkin's method to* get the static line parameters of suspended coupled microstrip lines, and also extended the method to suspended multiconductor microstrip structures. The Fourier domain method was significantly extended by many investigators to other planar structures such as the CPW [J.68–J.71, B.15, B.16].

In 1973 and 1974, Itoh and Mitra introduced the *dynamic SDA* to obtain dispersion characteristics of the slot line, and also microstrip line. Jansen extended the dynamic SDA to analyze the higher order modes in the microstrip. The method is very powerful and analytically elegant. It has been used and improved by other researchers in the field of planar resonators, antenna, and line structures. Other powerful methods, such as *the method of moments*, *finite elements, finite-difference time-domain method,* and so on have also been developed to analyze the 2D and 3D complex planar structures. The contemporary *EM-Simulators* are based on these numerical methods. The *closed-form models* for faster computation of the static and frequency-dependent line parameters of planar lines have also been developed by several investigators. The closed-form models of lines, discontinuities, and so on helped the development of the *Circuit Simulators* [J.72–J.75, B.15, B.16].

1.3 Overview of Present Book

The book presents a seamless treatment of the *classical planar transmission lines* and *modern engineered planar lines* using the concept of the engineered electromagnetic bandgap (EBG) structures and metamaterials. The modern EBG and metamaterials based planar lines are the outcome of the classical researches in the artificial dielectrics and concept of *homogenization of mixing of inclusions in the host medium*. Gradually, the modern microwave planar transmissions became a complex medium of wave propagations on the 1D lines and 2D surfaces. It demanded serious considerations of wave–matter interactions, especially in the engineered materials by the microwaves researchers and engineers. It demanded a physical understanding of various electromagnetic phenomena taking place in the artificially engineered complex medium. It also required the analytical and circuit modeling of the planar transmission lines under the complex environment. The present book: **Introduction to Modern Planar Transmission Lines** (*Physical, Analytical, and Circuit Models Approach*) addresses these problems from the very basics, making it suitable for the early comers to the fields. However, the detailed treatment of topics could be also useful to more experienced professionals and engineers. The numerical methods used in the analysis of the planar structures and basis of the EM-simulators are more specialized topics beyond the scope and line of thought followed in the present book.

The key concept used throughout the book is the modeling, *physical, analytical*, and *circuit,* of the planar

structures. However, what is the meaning of modeling itself? *Scientific modeling is a process of understanding the unknown with the help of known*. The reverse is not possible. The *method of analogy* is a great tool in such a modeling process. The growth of electromagnetic field theories at different stages has evolved from the previously known results of the gravitational field. Likewise, the gradual development of the transmission line theory has used the analogy of heat flow. These are two important illustrative examples discussed in the previous section. The experimental observation and the experimental verification of the theoretically predicted results are further contributors to the modeling process. The scientific modeling process has been examined in depth by the modern educationists [B.17]. The reader can observe such a modeling process in the development of models for the complex planar medium exhibiting unique properties.

1.3.1 The Organization of Chapters in This Book

The chapters of this book are organized into four distinct groups as follows:

i) Introductory transmission line and EM wave theory.
ii) Basic planar lines and Resonators: Microstrip, CPW, Slot lines, Coupled lines, and Resonators.
iii) Analytical Methods: Conformal mapping method, Variational method, Full- wave SDA, and SLR formulation.
iv) Contemporary engineered planar structures: Periodic planar lines and surfaces, Metamaterials – Bulk, 1D metalines, 2D metasurfaces.

The group i reviews the *transmission line and the EM-theory* to assist the reader to follow the rest of the chapters with ease. The groups ii and iii form the *classical transmission lines,* and the group iv is the *modern transmission lines and surfaces*. The book presents a seamless treatment of the classical planar transmission lines and the modern engineered planar lines and surfaces using the concept of EBG and metamaterials. The modern EBG and metamaterials based planar lines are the outcome of the classical researches in the artificial dielectrics and concept of homogenization of mixing of inclusions in the host medium. The topics of the chapters are selected to provide comprehensive coverage of the needed background to understand the functioning of both the classical and modern lines and surfaces. Each chapter follows a uniform style. The topics within a chapter start with simple concepts and move to a higher complexity level. Likewise, the chapters are also arranged from the simpler to complex.

The distribution of the chapters among the groups is discussed below. The key features of the chapters are also summarized.

Introductory Transmission Line and EM-Wave Theory

The six chapters, chapters 2–7, on the transmission lines and various aspects of the EM-theory are introduced in the book before even commencing with the microstrip in chapter 8. These topics provide the essential background to follow smoothly the topics covered in this book. It could be useful in understanding the analysis and modeling of the planar line structures, the EBG based lines, and surfaces, and also the metamaterials and metasurfaces. Moreover, the topics discussed may also help to understand the modern publications in these fields. The usual undergraduate textbooks on the EM-theory do not cover all the topics. However, the reader's familiarity with the transmission line and EM-theory is assumed. The reader interested in a more detailed study of these topics can follow the references given at the end of the chapters. Some contents of the chapters are highlighted below.

The chapters 2 and 3 on transmission lines are written as a review. However, it goes beyond a regular review, although it starts with the familiar notion of oscillation and wave propagation on lines. Usually, the available textbooks present the transmission line equations and wave equations for the uniform lines only, without any source. The present book covers the transmission line equations and wave equations with a source, and the analysis of the multisection transmission lines is also introduced. Such formulation is used in the chapters 14 and 16 to obtain the Green's functions of planar transmission lines used with the variational method and full-wave spectral-domain analysis (SDA) method. The chapter on the transmission line adequately covers the concept of dispersion in the wave supporting medium. Also, the impact of the reactive loading of the line on the nature of wave propagation is discussed. Such treatment prepares a reader for the periodically loaded engineered lines and surfaces, both as the bandgap medium and homogenized metamaterial medium. These topics are discussed in chapters 19–22. Chapter 3 covers various parameters used for the characterization of a line section. Understanding of this topic is essential for understanding the microwave components design, the results obtained from EM-simulation, and to develop the circuit models.

Chapters 4 and 5 cover the wave's propagation in the material medium. Again, primarily it is a review of the

EM-theory. However, its perspective is very broadly applicable to the topics discussed in other chapters. The chapter 4 commences with a basic review of the electromagnetics and elementary electrical properties of the material medium, such as linearity, nonlinearity, homogeneity, inhomogeneity, anisotropy, and losses. It further covers the topic of the circuit modeling of a medium. The known topics of Maxwell's equations in the differential form, as well as in the vector-algebraic form are presented. The wave propagation is discussed not only in the isotropic and conducting media but also in the *anisotropic, uniaxial, gyroelectric*, and *biaxial* media. The complex media are encountered by the wave propagating in the metamaterials. While reviewing the wave polarizations, the *Jones matrix* description of polarization states is also discussed. It is needed to follow the contemporary developments in the metasurfaces. Chapter 4 ends with the concepts of *isofrequency contours* and *isofrequency surfaces*, and the dispersion relations in the uniaxial medium.

Chapter 5 reviews both the normal and polarization-dependent oblique incidence of the waves at the interface of two media. It also presents the equivalent transmission line model of the wave's incidence at the interface of two media. The model can be extended to more number of layers. The formulation has many applications. The model is used for instance in chapter 20 on the EBG surface. The chapter 5 also presents the basic electrodynamics of the engineered metamaterials and formulate the basic characteristics of the wave propagation in the metamaterials. It also discusses some important directions for applications of metamaterials. However, the realization of the bulk metamaterials, metalines, and metasurfaces are followed up in the chapters 21 and 22.

Chapter 6 covers a review of the electrical properties of the natural and artificial dielectric media. It also presents various static and frequency-dependent models of the mixture media. The artificial dielectric medium finds its application in modeling the metamaterials. The Lorentz, Drude, and Debye models applicable to the frequency-dependent permittivity are discussed. Chapter 6 further discusses the interfacial polarization and its circuit model. This important topic is usually not discussed in popular textbooks. The modeling of the substrates, using the single term Debye and Lorentz models, as well as the multi-term and wideband Debye models are elaborated. These models help to get the causal effective permittivity of the planar lines of the substrates, useful in the time-domain analysis of pulse propagation on the planar lines. Finally, the chapter ends with a novel concept of artificial metasubstrate.

Chapter 7 comprehensively treats basic waveguide structures. It begins with the classification of the modal EM-fields, and the sources of their generation. The waveguides are analyzed using the scalar electric and magnetic potentials. The spectral domain analysis (SDA) method discussed in chapter 16 is based on these scalar potentials. The concept of the *perfect electric conductor (PEC)* and the *perfect magnetic conductor (PMC)* with boundary conditions are introduced. The analysis of the rectangular geometry of the waveguides formed with these surfaces is presented. Thus, apart from the usual all metallic walls, i.e. the PEC based waveguides, all PMC and two PEC and two PMC walls waveguides are also discussed. The dielectric slab waveguides and surface-waveguides are also presented. The concept of the odd/even mode analysis is introduced. These concepts are used in the book for the analysis of symmetrically coupled planar lines in chapters 11 and 12. The simple and powerful *transverse resonance method (TRM)* is introduced to get the propagation characteristics of the dielectric-loaded waveguides and the multilayer surface-waveguides. Finally, chapter 7 ends with the contemporary *substrate integrated waveguide (SIW)* developed in the environment of the planar technology.

Basic Planar Lines and Resonators

The planar line structures – microstrip, CPW, and slot line are discussed in chapters 8–10, respectively. The chapters 11 and 12 cover the theory of the coupled transmission lines and their realization and analysis in the planar technology environment. The theory of resonating structures and planar lines version of the resonators are discussed in chapters 17 and 18, respectively. The fabrication technologies – MIC, MMIC, MEMS, and LTCC used in the planar lines and components are reviewed in chapter 13.

The microstrip is the most commonly used planar line in planar technology. It is in the inhomogeneous medium supporting the *hybrid-mode* that is approximated as the dispersive *quasi-TEM mode*. However, at the lower frequency, it is treated in the nondispersive static condition. Chapter 8 introduces the concept of medium transformation from the inhomogeneous medium to the homogeneous medium using *Wheeler's transformation* for the lossy microstrip medium. The results on the static microstrip line parameters are summarized. The *dispersion law* is discussed to get the dispersion model of microstrip. Some other dispersion models are also summarized. The losses and their computation are presented in detail. Finally, chapter 8 ends with the circuit model of the microstrip line giving the complex frequency-dependent characteristic impedance

and propagation constant. The circuit model explains the behavior of the low-frequency dispersion due to the finite conductivity of the conductors. Several topics are covered for the first time in a book form. The derivations of some frequently used expressions are provided.

The *coplanar waveguides (CPW)* and the *coplanar stripline structures (CPS)* and their variations are discussed in chapter 9. The approach used in this chapter is based on the detailed derivation of the results using the *conformal mapping method*. Usually, the available books only summarize the results of the conformal mapping method. However, chapter 9 briefly presents the conformal mapping method as applied to the CPW and CPS. The characteristics of the modes, dispersion, and losses are presented in detail. The results are also presented for the synthesis of the CPW and CPS line structures. Finally, the circuit models of the lossy CPW and CPS are given to get the frequency-dependent complex characteristics impedance and propagation constant.

The modeling of the third important planar line, i.e. the *slot line* is presented in chapter 10. The modeling process is based on the *unique waveguide model* of Cohn. The model provides the frequency-dependent characteristic impedance and propagation constant of the slot line, supporting the hybrid mode. The waveguide model of the slot line treats the hybrid-mode as a linear combination of the TE and TM modes. The equivalent waveguide model is further extended to the multilayer and shielded slot line structures. The chapter ends with the *closed-form integrated model* of the slot line to compute the dispersion and loss parameters.

The next two chapters 11 and 12 cover the basic characteristic of the coupled lines theory and implementation of theory in the planar technology. Chapter 11 discusses the coupling mechanism and the analysis of symmetrical and asymmetrical coupled lines. The wave equation of the coupled transmission is obtained and solved in some cases. Chapter 12 summarizes the design expressions for the edge coupled and broadside coupled microstrip lines. Similar expressions are also summarized for the coupled CPW line structures. The network parameters for both symmetrical and asymmetrical coupled line sections are discussed in detail. Such an analysis is useful for the design of the filters.

At this stage, the further discussion of the planar line structure is discontinued and the fabrication technologies suitable for the planar lines and components are introduced in chapter 13. The chapter 13 discusses, in brief, the four kinds of fabrication technologies – the *hybrid microwave integrated circuit (HMIC)* suitable for the PCB board medium, the semiconductor based *monolithic MIC (MMIC)* technology, the silicon-based *micro-electro-mechanical systems (MEMS)* technology, and the ceramic tape-based *low temperature co-fired ceramic (LTCC)* technology. The typical details of the material and conductor parameters used in these technologies are also summarized. The familiarity of the fabrication process could be useful to the researchers and designers developing planar lines models and circuits.

The basic discussion and basic analysis of the resonator circuits, lumped and distributed line type, are presented in chapter 17. The implementation of the theory of transmission line resonators, and also the patch resonators, is the subject matter of chapter 18. The emphasis is placed on the circuit modeling of the resonating structures. Chapter 18 also discusses the fractal resonators and the dual-mode resonators with the illustrative examples of their applications. The resonating structures are important components for the development of the planar EBG and metamaterials.

Analytical Methods

Most of the discussions on the planar transmission lines and resonators are centered on the physical models and closed-form expression using circuit modeling. However, the analytical and quasi-analytical methods have been developed in the literature for more versatile and accurate modeling of the planar line structures in the multilayered medium. The *conformal mapping method*, as applied to the CPW and CPS line structures, is presented in chapter 9. The chapter 14 presents the *static variational methods*, both in the space-domain and Fourier domain, for the analysis of the microstrip and coupled microstrip. Using the *transverse transmission line (TTL) technique*, the variational method is extended to the multilayer microstrip lines. The method is extended to the boxed microstrip line and CPW using the Galerkin's method. However, the planar lines are both lossy and dispersive medium. The closed-form models are normally not available for the multilayer lossy planar lines. Chapter 15 presents the scheme of the *single-layer reduction (SLR) formulation* that utilizes the variational method and available single layer closed-form expressions to compute the dispersion and losses in the multilayer planar lines. The SLR models could be incorporated in the microwave CAD packages for the synthesis of the planar microwave components in the multilayer environment. Finally, the semi-analytical full-wave method, i.e. the *dynamic SDA* is elaborated in chapter 16. The treatment is at the introductory level with the detailed derivation of expressions. The method also incorporates the multilayered planar lines.

Contemporary Engineered Planar Structures

These are the topics of current interest and have wide-ranging applications in the development of novel devices and antenna structures with controlled functionalities. Chapter 19 is dedicated to the periodically loaded transmission lines and their circuit models. The method of the circuit models based analysis of the *electronic band-gap (EBG) line* is elaborated in detail and applied to the loaded microstrip and CPW line structures. The method is extended to the planar EBG surfaces in chapter 20. The accurate circuit model of the EBG surfaces is presented, and also the process of the EM-simulation and interpretation of the results are discussed.

The analyses of the engineered artificial media called the bulk metamaterials, metalines, and metasurfaces are presented in the chapters 21 and 22. The modeling and parameter extraction of the engineered media are also discussed. The metasurfaces are interesting structures with several possible applications both in the development of the circuits and planar antenna with multi-dimensional functionalities. The unique *generalized Snell's laws* are discussed in chapter 22 that helps to control the wave propagation. The polarization control and conversion of the state of polarization of the incident waves are also achieved with metasurfaces. Several applications of the metasurface are summarized.

1.3.2 Key Features, Intended Audience, and Some Suggestions

Key Features

Possibly, it is the first comprehensive book dedicated entirely to the planar transmission lines. The book covers the microstrip lines, CPW, and other classical resonating structures from basic to advanced form in one cover. The book further covers the EBG and metamaterial-based planar transmission lines and surfaces. These are the topics of current interest. The sequence of the chapter is logical and of increasing complexity.

The emphasis of the book is on the modeling of the planar lines and engineered surfaces using the physical concepts, circuit-models, closed-form expressions, and the derivation of a large number of expressions. It provides an in-depth review of the classical transmission line theory, electromagnetics, modeling of the material medium, and waveguide structures compactly without sacrificing the clarity of presentation.

The advanced mathematical treatment of the topics, such as the variational method, conformal mapping method, and SDA for several kinds of planar line structures is carried out in detail to help the new readers unfamiliar with these topics. A large number of illustrative examples from the published literature are given to clarify the theory and physical principles involved in the contemporary topics of the EBG lines and surfaces, metamaterials, metalines, and metasurfaces.

The multilayer structures useful for the MMIC, MEMS, and LTCC technology are covered. The closed-form modeling of dispersion, frequency-dependent characteristic impedance, and losses in the multilayer planar transmission lines is covered for the first time in a book-form. Also, the basic fabrication technology of the planar transmission lines in the MMIC, MEMS, and LTCC technology is described to help the modelers of the EM-phenomenon and microwave circuit designers.

Thus, the book prepares the reader to follow the modern designs of the planar circuits and also to undertake independent researches in the field of planar microwave technology.

Intended Audience

The book is intended to help undergraduate students of third/fourth year and also postgraduate students. It is useful to the teachers of microwave engineering in preparing lectures, assignments, and projects. The new researchers in the field of microwave engineering will find the book useful to improve their skills in the modeling of the planar structures. It is also suitable for the self-study of the RF/Microwave professionals in the industries. The selected chapters could be used in classroom teaching. It could be the main text for conducting elective courses at the university level. Further, the book can serve as a reference book even to more experienced users in the industry.

Some Suggestions

The students and new researchers can have a fast review of the transmission line theory, EM-theory, and so on from chapters 2–7. Then it will be much easier to follow the remaining text. It will be also helpful in following other advanced books and published current literature. However, experienced readers can read any chapter or topic. The concept for the *forward and backward referencing* of chapters, sections, and subsections are provided to help the reader to skip the chapters or to go back to an intended topic inside the book.

A large number of closed-form expressions are given for the modeling purpose. A reader is encouraged to write the Matlab codes or codes in any other language familiar to him/her. The teacher can assign to students the code development as homework. Such activities will enhance the learning process and skill development. More efforts will be needed to write the codes for the

variational method, Galerkin's method, and the SDA. Of course, the effort is rewarding.

The researchers must look into the journals to follow newer investigations and decide the direction of his/her research activities. Good luck!

References

Books

B.1 Nahin Paul, J.: *Oliver Heaviside, Sage in Solitude: The Life, Work, and Times of an Electrical Genius of the Victorian Age*, IEEE Press, New York, 1988.

B.2 Mahon, B.: *Oliver Heaviside: Maverick Mastermind of Electricity*, IET, London, 2009.

B.3 Yavetz, I.: *From Obscurity to Enigma: The Works of Oliver Heaviside 1872–1889*, Birkhäuser, Basel, Switzerland, 2011.

B.4 Whittaker, E.: *A History of Theories of Aether and Electricity (Two Volumes)*, Dover Publications, Dallas, TX, USA, 1989.

B.5 Sarkar, T.K.; Mailloux, R.J.; Oliner, A.A.; Salazar-Palma, M.; Sengupta, D.L.: *History of Wireless*, John Wiley & Sons, Inc., Hoboken, New Jersey, USA, 2006.

B.6 Elliott, R.S.: *Electromagnetics: History, Theory, and Applications*, IEEE Press, Piscataway, NJ, 1993.

B.7 Lorentz, H.A.: *The Theory of Electrons and Its Applications to the Phenomena of Light and Radiant Heat*, 2nd Edition, B.G. Teubner, Leipzig, 1916.

B.8 Stratton, J.A.: *Electromagnetic Theory*, McGraw-Hill, New York, 1941.

B.9 Collin, R.E.: *Field Theory of Guided Waves*, 2nd Edition, IEEE Press, New York, 1991.

B.10 Harrington, R.F.: *Time-Harmonic Electromagnetic Fields*, McGraw-Hill, New York, 1961.

B.11 Feynman, R.P.; Leighton, R.B.; Sands, M.: *The Feynman Lectures on Physic, Vol. II, Electromagnetic Field*, pp. 15-8, 15-14, Addison – Wesley Pub. Co. Inc., Boston, Indian Reprint, B.I. Publications, New Delhi, 1969.

B.12 Thomson, J.J.: *Recent Researches in Electricity and Magnetism*, Clarendon Press, Oxford, 1893.

B.13 Fricke, H.M.: Two rival programme in 19th-century classical electrodynamics action – at- distance versus field theory, Ph. D. Thesis, London School of Economics & Political Science, 1982, London.

B.14 Fache, N.; Olyslager, F.; Zutter, D.D.: *Electromagnetic and Circuit Modeling of Multiconductor Transmission Lines*, Clarendon Press, Oxford, 1993.

B.15 Brillouin, L.: *Wave Propagation in Periodic Structures - Electric Filters and Crystal Lattice*, 2nd Edition, Dover Publications, New York, 1953.

B.16 Itoh, T. (Editor): *Planar Transmission Lines*, IEEE Press, Piscataway, NJ, 1987.

B.17 Khine, M.S.; Saleh, I.M. (Editors): *Models and Modeling in Science Education*, Vol. 6, Springer Dordrecht Heidelberg, London, New York, 2011.

Journals

J.1 Elliott, R.S.: *The history of electromagnetics as Hertz would have known it*, *IEEE Antennas Propag. Soc. Newsl.*, Vol. 30, No. 3, pp. 5–18, June 1988

J.2 Grattan-Guinness, I.: *Why did George Green write his essay of 1828 on electricity and magnetism?*, *Am. Math. Mon.*, Vol. 102, No. 5, pp. 387–397, DOI: 10.1080/00029890.1995.12004591http://about.jstor.org/terms.

J.3 Wu, A.C.T.; Yang, C.N.: *Evolution of the concept of the vector potential in the description of potential interactions*, *Int. J. Mod. Phys. A*, Vol. 21, No. 16, pp. 3235–3277, 2006.

J.4 Eliseo Fernández, E.: *Concepts and instruments: the potential from Green to Kelvin*, The Midwest Junto for the History of Science, March 25–27, 1994.

J.5 Challis, L.; Sheard, F.: *The green of Green's function*, *Phys. Today*, Vol. 56, No. 12, pp. 41–46, 2003.

J.6 John Roche, R.: *The present status of Maxwell's displacement current*, *Eur. J. Phys.*, Vol. 19, pp. 155–16n, 1998.

J.7 French, A.P.; Tessman, J.R.: *Displacement currents and magnetic fields*, *Am. J. Phys.*, Vol. 31, pp. 201–204, 1963.

J.8 Scheler, G.; Paulus, G.G.: *Measurement of Maxwell's displacement current*, *Eur. J. Phys.*, Vol. 36, No. 055048, pp. 1–9, 2015.

J.9 Selvan, K.T.: *Presentation of Maxwell's equations in historical perspective and the likely desirable outcomes*, *IEEE Antennas Propag. Mag.*, Vol. 49, No. 5, pp. 155–160, Oct. 2007.

J.10 Selvan, K.T.: *A revisiting of scientific and philosophical perspectives on Maxwell's displacement current*, *IEEE Antennas Propag. Mag.*, Vol. 51, No.3, pp. 36–46, June 2009.

J.11 Essex, E.A.: *Hertz vector potentials of electromagnetic theory*, *Am. J. Phys.*, Vol. 45, pp. 1099–1101, 1977.

J.12 Kraus, J.D.: *Heinrich Hertz-theorist and experimenter*, *IEEE Trans. Microwave Theory Tech.*, Vol. 36, No. 5, pp. 824–829, May 1988.

J.13 Susskind, C.: *Heinrich Hertz: A short life*, *IEEE Trans. Microwave Theory Tech.*, Vol. 36, No. 5, pp. 802–805, May 1988.

J.14 Bladel, J.V.: *Lorenz or Lorentz?*, *IEEE Antennas Propag. Mag.*, Vol. 33, No. 2, pp. 69, April 1991.

J.15 Jackson, J.D.; Okun, L.B.: *Historical roots of gauge invariance*, *Rev. Mod. Phys.*, Vol. 73, pp. 663–680, July 2001.

J.16 Griffiths, D.J.: *Resource letter EM-1: Electromagnetic momentum*, *Am. J. Phys.*, Vol. 80, No. 1, pp. 7–18, Jan. 2012.

J.17 Aharonov, Y.; Bohm, D.: *Significance of electromagnetic potentials in quantum theory*, *Phys. Rev.*, Vol. 115, pp. 485–491, 1959.

J.18 Thomson, W. (Kelvin): *On the theory of the electric telegraph*, *Proc. R. Soc. London*, Vol. 4, No. 11, pp. 382–399, May 1855.

J.19 Searle, G.F.C., et al. *The Heaviside Centenary Volume*, The Institution of Electrical Engineers, London, 1950.

J.20 Whittaker, E.T.: *Oliver Heaviside*, In *Electromagnetic Theory* Vol. 1, Oliver Heaviside, Reprint, Chelsea Publishing Company, New York, 1971.

J.21 Pupin, M.I.: *Wave propagation over non-uniform cables and long-distance airlines*, *Trans. Am. Inst. Electr. Eng.*, Vol. 17, pp. 445–507, (discussion on pp. 508–512), May 1900.

J.22 Pupin, M.I.: *Propagation of long electrical waves*, *Trans. Am. Inst. Electr. Eng.*, Vol. xv, No. 144, pp. 93–142, March 1899.

J.23 Campbell, G.A.: *On loaded lines in telephonic transmission*, *London, Edinburg Dublin Philos. Mag. J. Sci.*, Vol. 5, No. 27, pp. 313–330, 1903.

J.24 Kennelly, A.E.: *Impedance*, 76th Meeting of American Institute of Electrical Engineers, pp. 175–232, April 1893.

J.25 Carson, J.R.: *Wave propagation over parallel wires: The proximity effect*, *London, Edinburgh Dublin Philos. Mag. J. Sci.*, Vol. 41, No. 244, pp. 607–633, 1921

J.26 Carson, J.R.: *Electromagnetic theory and the foundations of electrical circuit theory*, *Bell Syst. Tech. J.*, Vol. 6, pp. 1–17, Jan. 1927.

J.27 Levin, A.: *Electromagnetic waves guided by parallel wires with particular reference to the effect of the earth*, *Trans. Am. Inst. Electr. Eng.*, Vol. 46, pp. 983–989, June 1927.

J.28 Bewley, L.V.: *Traveling waves on transmission systems*, *Trans. Am. Inst. Electr. Eng.*, Vol. 50, No. 2, pp. 532–550, June 1931.

J.29 Pipes, L.A.: *Matrix theory of multiconductor transmission lines*, *London, Edinburgh Dublin Philos. Mag. J. Sci.*, Vol. 24, No. 159, pp. 97–113, July 1937.

J.30 Rayleigh, J.W.S.: *On the passage of electric waves through tubes, or vibrations of dielectric cylinders*, *Philos. Mag.*, Vol. 43, pp. 125–132, Feb. 1897.

J.31 Southworth, G.C.: *Hyper – frequency waveguides – General consideration and experimental results*, *Bell Sys. Tech. J.*, Vol. 15, pp. 284–309, 1936.

J.32 Barrow, W.L.: *Transmission of electromagnetic waves in hollow tubes of metal*, *Proc. IRE*, Vol. 24, pp. 1298–1328, Oct. 1936.

J.33 Brillouin, L.: *Propagation of electromagnetic waves in a tube*, *Rev. GMn. de l'Elec.*, Vol. 40, pp. 227–239, Aug. 1936.

J.34 Carson, J.R.; Mead, S.P.; Schelkunoff, S.A.: *Hyper-frequency wave guides – mathematical theory*, *Bell Sys. Tech. J.*, Vol. 15, pp. 310–333, 1936.

J.35 Chu, L.I.; Barrow, W.L.: *Electromagnetic waves in hollow metal tubes of rectangular cross- section*, *Proc. IRE*, Vol. 26, 1520, 1938.

J.36 Schelkunoff, S.A.: *The electromagnetic theory of coaxial transmission lines and cylindrical shields*, *Bell Sys. Tech. J.*, Vol. 13, No. 4, pp. 532–579, Oct. 1934.

J.37 Schelkunoff, S.A.: *Transmission theory of plane electromagnetic waves*, *Proc. IRE*, Vol. 25, p. 1437, 1937.

J.38 Schelkunoff, S.A.: *Generalized telegraphist's equations for waveguides*, *Bell Sys. Tech. J.*, Vol. 31, No. 4, pp. 784–801, July 1952.

J.39 Schelkunoff, S.A.: *Conversion of Maxwell's equations into generalized telegraphist's equations*, *Bell Sys. Tech. J.*, Vol. 34, No. 5, pp. 995–1043, Sept. 1955.

J.40 Niehenke, E.C.; Pucel, R.A.; Bahl, I.J.: *Microwave and millimeter-wave integrated circuits*, *IEEE Trans. Microwave Theory Tech.*, Vol. 50, No. 3, pp. 846–857, March 2002.

J.41 Greig D.D.; Engelmann, H.: *Microstrips – A new transmission technique for the kilomegacycle range*, *Proc. IRE*, Vol. 40, pp. 1644–1650, Dec. 1952.

J.42 Barrett, R.M.: *Microwave printed circuits-A historical survey*, *IEEE Trans. Microwave Theory Tech.*, Vol. 3, No. 2, pp. 1–9, Mar. 1955.

J.43 Barrett, R.M.: *Microwave printed circuits - The early years*, *IEEE Trans. Microwave Theory Tech.*, Vol. MTT-32, No. 9, pp. 983–990, Sept. 1984.

J.44 Cohn, S.B.: *Characteristic impedance of the shielded-strip transmission line*, *IRE Trans. Microwave Theory Tech.*, Vol. MTT-2, pp. 52–57, July 1954.

J.45 McQuiddy, D.N.; Wassel, J.W.; LaGrange, J.B.; Wisseman, W.R.: *Monolithic microwave integrated circuits: An historical perspective*, *IEEE Trans. Microwave Theory Tech.*, Vol. 32, No. 9, pp. 997–1008, 1984.

J.46 Petersen, K.E.: *Micro-mechanical membrane switches on Silicon*, *IBM J. Res. Dev.*, Vol. 23, No. 4, pp. 376–385, July 1979.

J.47 Yao, J.; Chang, M.F.: *A surface micro-machined miniature switch for telecommunication application*

with single freq. from DC up to 4 GHz, Proc. Transducer'95, pp. 384–387, June 1995.

J.48 Goldsmith, C.; Lin, T.H.; Powers, B.; Wu, W.R.; Norvel1, B.: *Micro-mechanical membrane switches for microwave application*, IEEE Microwave Theory Tech. Symp., MTT-S Digest, pp. 91–94, May 1995.

J.49 Rodriguez, A.R.; Wallace, A.B.: *Ceramic capacitor and method of making it*, Patent US 3004197, issued 10/10/1961.

J.50 Hajian, A.; Müftüoglu, D.; Konegger, T.; Schneider, M.; Schmid, U.: *On the porosification of LTCC substrates with sodium hydroxide*, *Compos. Part B: Eng.*, Vol. 157, pp. 14–23, 2019.

J.51 Veselago, V.: *The electrodynamics of substances with simultaneously negative values of ε and μ*, *Soviet Physics Uspekhi*, Vol. 10, No. 4, pp. 509–514, Jan., Feb. 1968.

J.52 Pendry, J.B.; Holden, A.J.; Stewart, W.J.; Youngs, I.: *Extremely low-frequency plasmons in metallic mesostructures*, *Phys. Rev. Lett.*, Vol. 76, No. 25, pp. 4773–4776, June 1996.

J.53 Pendry, J.B.; Holden, A.J.; Robbins, D.J.; Stewart, W.J.: *Magnetism from conductors and enhanced nonlinear phenomena*, *IEEE Trans. Microwave Theory Tech.*, Vol. 47, No. 11, pp. 2075–2084, Nov. 1999.

J.54 Shelby, R.A.; Smith, D.R.; Schultz, S.: *Experimental verification of a negative index of refraction*, *Science*, Vol. 292, No. 5514, pp. 77–79, April 2001.

J.55 Smith, D.R.; Padilla, W.J.; Vier, D.C.; Nemat-Nasser, S. C.; Schultz, S.: *Composite medium with simultaneously negative permeability and permittivity*, *Phys. Rev. Lett.*, Vol. 84, No. 18, pp. 4184–4187, May 2000.

J.56 Assaudourion, F.; Rimai, E.: *Simplified theory of microstrip transmission systems*, *Proc. IRE*, Vol. 40, pp. 1651–1657, Dec. 1952.

J.57 Cohn, S.B.: *Characteristic impedance of the shielded-strip transmission line*, *IRE Trans. Microwave Theory Tech.*, Vol. MTT-2, pp. 52–57, July 1954.

J.58 Cohn, S.B.: *Problems in strip transmission lines*, *IEEE Trans. Microwave Theory Tech.*, Vol. MTT-3, No. 2, pp. 119–126, March 1955.

J.59 Cohn, S.B.: *Shielded coupled-strip transmission line*, *IRE Trans. Microwave Theory Tech.*, Vol. MTT-3, pp. 29–38, Oct. 1955.

J.60 Cohn, S.B.: *Characteristic impedances of broadside-coupled strip transmission lines*, *IRE Trans. Microwave Theory Tech.*, Vol. MTT-8, pp. 633–637, Nov. 1960.

J.61 Wheeler, H.A.: *Transmission-line properties of parallel wide strips by a conformal-mapping approximation*, *IEEE Trans. Microwave Theory Tech.*, Vol. MTT-12, pp. 280–289, May 1964.

J.62 Wheeler, H.A.: *Transmission-line properties of parallel strips separated by a dielectric sheet*, *IEEE Trans. Microwave Theory Tech.*, Vol. MTT-13, pp. 172–185, March 1965.

J.63 Wheeler, H.A.: *Transmission-line properties of a strip on a dielectric sheet on a plane*, *IEEE Trans. Microwave Theory Tech.*, Vol. MTT-25, pp. 631–647, Aug. 1977.

J.64 Wheeler, H.A.: *Transmission line properties of a stripline between parallel planes*, *IEEE Trans. Microwave Theory Tech.*, Vol. MTT-26, pp. 866–876, Nov. 1978.

J.65 Cohn, S.B.: *Slotline on a dielectric substrate*, *IEEE Trans. Microwave Theory Tech.*, Vol. MTT-17, pp. 768–778, Oct. 1969.

J.66 Wen, C.P.: *Coplanar waveguide: a surface strip transmission line suitable for nonreciprocal gyromagnetic device application*, *IEEE Trans. Microwave Theory Tech.*, Vol. MTT-17, pp. 1087–1090, Dec. 1969.

J.67 Meier, P.J.: *Two new integrated-circuit media with special advantages at millimeter-wave lengths*, IEEE MTT-S Int. Microwave Symp. Dig., pp. 221–223, 1972.

J.68 Yamashita, E.; Mitra, R.: *Variational method for analysis of microstrip lines*, *IEEE Trans. Microwave Theory Tech.*, Vol. MTT-16, No. 4, pp. 251–256, April 1968.

J.69 Yamashita, E.: *Variational method for analysis of microstrip – like transmission lines*, *IEEE Trans. Microwave Theory Tech.*, Vol. MTT-16, No. 8, pp. 529–535, Aug. 1968.

J.70 Itoh, T.; Herbert, A.S.: *A generalized spectral domain analysis for coupled suspended microstrip lines with tuning septum*, *IEEE Trans. Microwave Theory Tech.*, Vol. MTT-26, No. 10, pp. 820–826, Oct. 1978.

J.71 Itoh, T.: *A generalized spectral domain analysis for multiconductor printed lines and its application to tunable suspended microstrips*, *IEEE Trans. Microwave Theory Tech.*, Vol. MTT-26, No. 12, pp. 983–987, Dec. 1978.

J.72 Itoh, T.; Mittra, R.: *Spectral-domain approach for calculating the dispersion characteristics of microstrip lines*, *IEEE Trans. Microwave Theory Tech.*, Vol. MTT-21, pp. 496–499, July 1973.

J.73 Itoh, T.; Mittra, R.: *Dispersion characteristics of slot lines*, *Electron. Lett.*, Vol. 7, pp. 364–365, 1971.

J.74 Itoh, T.: *Spectral-domain immittance approach for dispersion characteristics of generalized printed transmission lines*, *IEEE Trans. Microwave Theory Tech.*, Vol. MTT-28, pp. 733–736, 1980.

J.75 Jansen, R.H.: *High-speed computation of single and coupled microstrip parameters including dispersion, high-order modes, loss and finite strip thickness*, *IEEE Trans. Microwave Theory Tech.*, Vol. MTT-26, pp. 75–82, 1978.

2

Waves on Transmission Lines – I

(*Basic Equations, Multisection Transmission Lines*)

Introduction

The two-wire transmission line is a useful medium for the propagation of the voltage and current waves. It is also useful in the modeling of planar transmission lines. The EM-wave propagating on multilayered planar transmission lines could also be analyzed with the help of the multisection transmission lines. The primary purpose of this chapter is to review in detail the wave propagation on a transmission line without and with sources. Several other important topics such as the characterization of a line section, nature of wave velocities, dispersion, and reactively loaded lines are further discussed in chapter 3.

Objectives

- *To formulate Kelvin–Heaviside transmission line equations.*
- *To obtain the solution of the wave equation.*
- *To compute the power flow on a transmission line.*
- *To use Thevenin's theorem on a transmission line section to obtain its transfer function.*
- *To consider the wave propagation on a multi-section transmission line with the voltage and current sources.*
- *To understand the nature of the wave propagation on a nonuniform transmission line.*

2.1 Uniform Transmission Lines

This section presents the basic understanding of wave propagation on a uniform transmission line. The *Kelvin–Heaviside transmission line equations* are formulated using the *lumped circuit elements model* of the uniform transmission line.

The voltage and current wave equations are obtained and solved for a terminated line section. The phenomenon of the standing wave is discussed. The *Thevenin theorem* of the transmission line network is discussed and the transfer function of a line section is obtained.

2.1.1 Wave Motion

The wave motion could be treated as the transfer of oscillation from one location to another location. A harmonic oscillation is described either by a sine or by a cosine function. A periodic oscillation has a fixed period. An oscillation repeats itself after the periodic time (T). In general, an oscillation, i.e. an oscillatory motion can have any shape such as square, triangular, and so on. However, with the help of the Fourier series, such periodic oscillations can be decomposed to the harmonic functions. Likewise, wave motion can also acquire an arbitrary shape. The arbitrary periodic shape of a wave can be decomposed into the harmonic waves.

Figure (2.1) shows the instantaneous amplitude v(t) of the wave generated by an oscillating quantity, such as an oscillating ball (particle) at the location A. It has an angular frequency of oscillation ω radian/sec and maximum amplitude $V_{max.}$ The ball is attached to a spring and immersed in a water tank. It generates a wave motion at the surface of the water. The water wave travels with velocity v_p and causes another *delayed oscillation,* at the location B, in a similar ball attached to a spring. *Through the mechanism of wave motion, the oscillation is transferred from the location A to the location B separated by distance x.* Likewise, the oscillating quantity could be a charge, electric field, magnetic field, or voltage obtained from an oscillator connected to a cable.

The equation of the harmonic oscillation at location A is described by the cosine function,

$$v_a(t) = V_{max} \cos \omega t. \tag{2.1.1}$$

The equation of harmonic oscillation that appears at location B after a delayed time t' is

$$v_b(t) = V_{max} \cos \omega(t - t'). \tag{2.1.2}$$

The wave motion, created by the oscillation at the location A, travels with velocity v_p. The time delay in

Introduction to Modern Planar Transmission Lines: Physical, Analytical, and Circuit Models Approach, First Edition. Anand K. Verma.

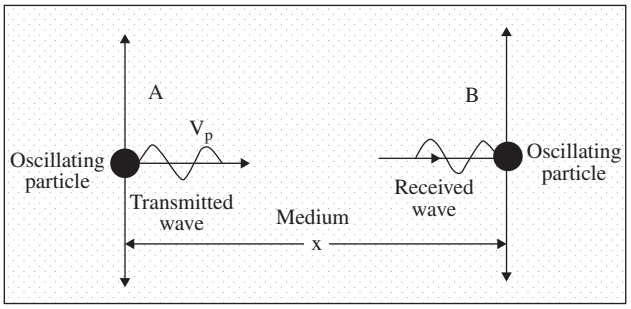

Figure 2.1 Delayed oscillation as a wave motion-initial oscillation v(t) at location A, and delayed oscillation $v(t - x/v_p)$ at location B. The waves propagate from the locations A to B.

setting up the oscillation at the location B is $t' = x/v_p$. So the equation of oscillation at the location B is

$$v_b(t) = V_{max} \cos \omega\left(t - x/v_p\right). \tag{2.1.3}$$

Equation (2.1.3) describes the propagating wave through the medium between locations A and B. It is called the *wave equation*. The *phase constant* β of the propagating wave is defined as $\beta = \omega/v_p$. On dropping the subscript "b," equation (2.1.3) is rewritten in the usual form,

$$v(t, x) = V_{max} \cos(\omega t - \beta x). \tag{2.1.4}$$

In equation (2.1.4), the *lagging phase* $\phi = \beta x$ is caused by the delay in oscillation at the receiving end. The medium supporting the wave motion is assumed to be lossless. The wave variable v(t, x) is a doubly periodic function of both time and space coordinates as shown in Fig (2.2a and b), respectively.

The *temporal period,* i.e. time-period T is related to the angular frequency ω as follows:

$$T = \frac{2\pi}{\omega} = \frac{1}{f}, \tag{2.1.5}$$

where f is the frequency in Hz (Hertz), i.e. the number of cycles per sec. The wavelength (λ) describes the *spatial period*, i.e. space periodicity. It is related to the *phase-shift constant (or phase constant)*, i.e. the propagation constant β, as follows:

$$\lambda = \frac{2\pi}{\beta}. \tag{2.1.6}$$

The wave motion or velocity of a *monochromatic wave* (the wave of a single frequency) is the motion of its *wavefront*. For the 3D wave motion in an isotropic space, the wavefront is a surface of the constant phase. In the case of the 1D wave motion, the wavefront is a line, whereas, for the 2D wave motion on an isotropic surface, the wavefront is a circle.

Figure (2.3) shows the peak point P at the wavefront of the ID wave. The motion of a constant phase surface is known as its *phase velocity* v_p. Thus, the peak point P at

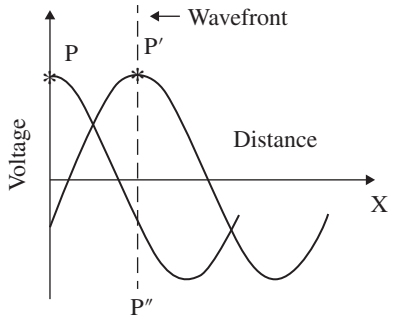

Figure 2.3 Wave motion as a motion of constant phase surface. It is shown as the moving point P.

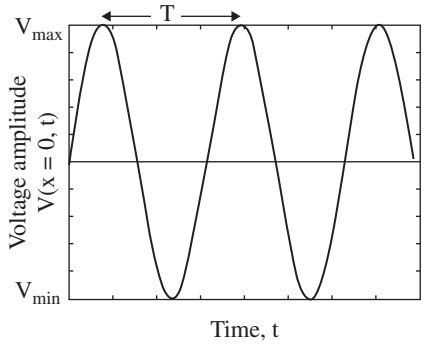

(a) Harmonic variation of the wave with respect to time, at the location x = 0.

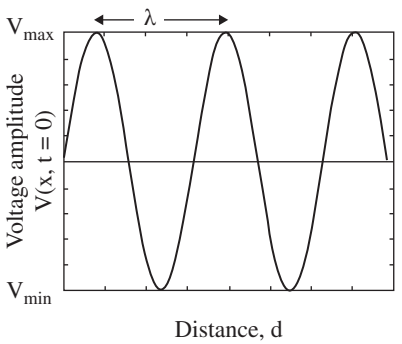

(b) Harmonic variation of the wave with respect to the distance, at time t = 0.

Figure 2.2 Double periodic variations of wave motion.

the wavefront has moved to a new location P′ in such a way that phase of the propagating wave remains constant, i.e. $\omega t - \beta x = \text{constant}$. On differentiating the constant phase with respect to time t, the expression for the phase velocity is obtained:

$$v_p = \frac{dx}{dt} = \frac{\omega}{\beta}. \tag{2.1.7}$$

In a *nondispersive* medium, the phase velocity of a wave is independent of frequency, i.e. the waves of all frequencies travel at the same velocity. Figure (2.4) shows the nondispersive wave motion on the $(\omega - \beta)$ diagram. It is a *linear graph*. The slope of the point Q on the dispersion diagram subtends an angle θ at the origin that corresponds to the *phase velocity* of a propagating wave,

$$v_p = \tan\theta = \frac{\omega}{\beta}. \tag{2.1.8}$$

Thus, for a frequency-independent nondispersive wave, the phase constant is a linear function of angular frequency.

$$\beta = \text{Constant} \times \omega. \tag{2.1.9}$$

The dispersive nature of the 1D wave motion is further discussed in sections (3.3) and (3.4) of the chapter 3. The phase velocity in a dispersive medium is usually frequency-dependent. It is known as the *temporal dispersion*. In some cases, the phase velocity could also depend on wavevector (β, or k). It is known as *spatial dispersion*. The spatial dispersion is discussed in the subsection (21.1.1) of the chapter 21. The dispersion diagrams of the wave propagation in the isotropic and anisotropic media are further discussed in the section (4.7) of the chapter 4, and also in the section (5.2) of chapter 5.

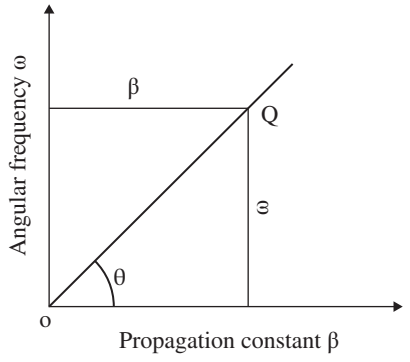

Figure 2.4 The ω-β dispersion diagram of nondispersive wave.

The one-dimensional (1D) wave travels both in the forward and in the backward directions. It can have any arbitrary shape. In general, the 1D wave propagation can be described by the following *wave function*, known as the *general wave equation*:

$$\psi(t, x) = \psi\left(t \mp \frac{x}{v_p}\right). \tag{2.1.10}$$

On taking the second-order partial derivative of the wave function $\psi(t, x)$ with respect to space-time coordinate x and t, the 1D second-order partial differential equation (PDE) of the wave equation is obtained. Similarly, wave functions $\psi(t, x, y)$ and $\psi(t, x, y, z)$ are solutions of two-dimensional (2D) and three-dimensional (3D) wave equations supported by the surface and free space medium, respectively. These PDEs are summarized below:

$$\frac{\partial^2\psi}{\partial x^2} = \frac{1}{v_p^2}\frac{\partial^2\psi}{\partial t^2} \quad (a), \quad \frac{\partial^2\psi}{\partial x^2} + \frac{\partial^2\psi}{\partial y^2} = \frac{1}{v_p^2}\frac{\partial^2\psi}{\partial t^2} \quad (b)$$
$$\frac{\partial^2\psi}{\partial x^2} + \frac{\partial^2\psi}{\partial y^2} + \frac{\partial^2\psi}{\partial z^2} = \frac{1}{v_p^2}\frac{\partial^2\psi}{\partial t^2} \quad (c), \Rightarrow \nabla^2\psi = \frac{1}{v_p^2}\frac{\partial^2\psi}{\partial t^2} \quad (d). \tag{2.1.11}$$

The dispersion diagram of the 2D wave propagation over the (x, y) surface is obtained by revolving the slant line of Fig (2.4) around the ω-axis with propagation constants β_x, β_y in the *x*- and *y*-direction. It is discussed in subsection (4.7.4) of chapter 4.

2.1.2 Circuit Model of Transmission Line

A physical transmission line, supporting the voltage/current wave, can be modeled by the lumped R, L, C, G components, i.e. the resistance, inductance, capacitance, and conductance per unit length (*p.u.l.*), respectively. The two-conductor transmission line can acquire many physical forms. A few of these forms are shown in Fig (2.5). The lines as shown in Fig (2.5a–c) support the wave propagation in the **t**ransverse **e**lectro-**m**agnetic mode, i.e. in the *TEM-mode; while Fig (2.5c) shows the quasi-TEM mode-supporting microstrip*. For TEM mode wave propagation, the electric field and magnetic field are normal to each other and also normal to the direction of wave propagation. For the TEM mode, there is no field component along the direction of propagation. However, the quasi-TEM mode also has component of weak fields along the longitudinal direction of wave propagation. The quasi-TEM mode is a *hybrid mode* discussed in the subsection (7.1.4) of chapter 7.

All TEM mode supporting transmission lines can be represented by a parallel two-wire transmission line

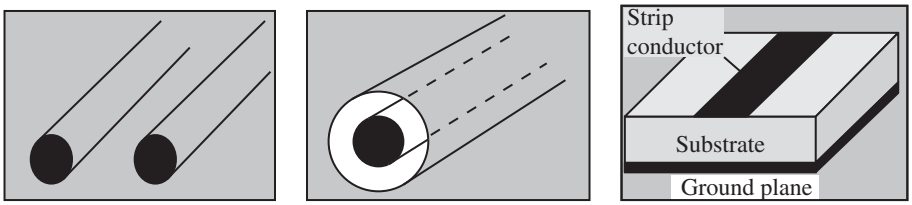

(a) Two-wire line. (b) Co-axial line. (c) Microstrip line.

Figure 2.5 Cross-section of a few two-conductor transmission lines.

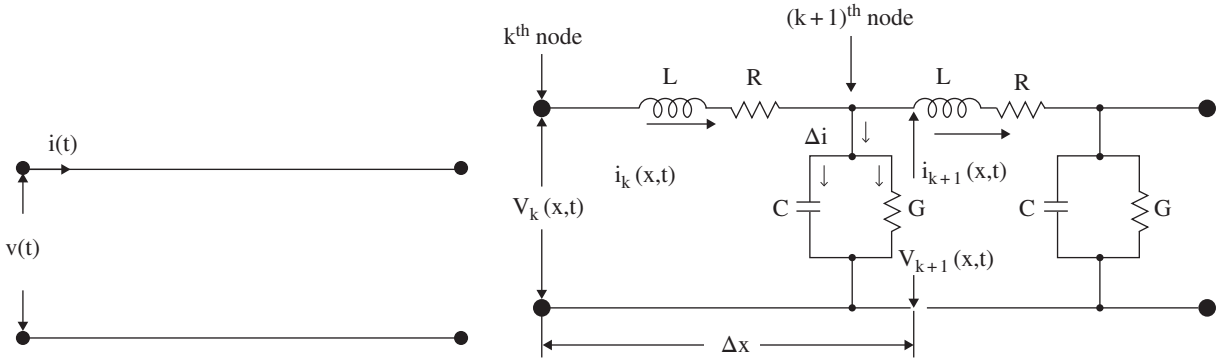

(a) Physical two-wire transmission line. (b) Equivalent circuit of the two-wire transmission line.

Figure 2.6 RLCG lumped circuit model of a transmission line.

shown in Fig (2.6a). A transmission line is a 1D wave supporting structure. Its cross-sectional dimension is much less than $\lambda/4$; otherwise, its TEM nature is changed. The longitudinal dimension can have any value, from a fraction of a wavelength to several wavelengths. The mode theory of the electromagnetic (EM) wave propagation is further discussed in chapter 7.

A two-conductor transmission line, or any other line supporting the TEM mode, is modeled as a chain of discrete passive RLCG components. As a matter of fact, by cascading several sections of discrete L-network of the series L and shunt C elements, or even discrete L-network of the series C and shunt L elements, an *artificial transmission line* can also be constructed. The artificial transmission line is discussed in section (3.4) of chapter 3, and also in the chapters 19 and 22. It plays a very important role in modern microwave planar technology. The behavior of a transmission line is determined in terms of the resistor (R), inductor (L), capacitor (C), and conductance (G); all line elements are in per unit length, i.e. *p.u.l.* Kelvin introduced the modeling of the telegraph cable laid in the ocean using the *RC circuit model*. Heaviside further introduced L and G components in the circuit model to improve the modeling of the lossy transmission line [B.1, B.2, J.1, J.2]. Kelvin RC-circuit model of the transmission line leads to the diffusion equation, not to the wave equation. Whereas using the RLGC circuit model, Heaviside finally obtained the wave equation for the voltage/current on a transmission line. Using the RLCG circuit model, shown in Fig (2.6b), the voltage, and current equations are obtained for the transmission line. The set of the coupled voltage and current equations are normally called the *telegrapher's equations;* as it was originally developed for the telegraph cables. However, the set of coupled transmission line equations can be called the *Kelvin–Heaviside transmission line equations* to recognize their contributions.

The Resistance of a Line

The electrical loss in a transmission line, known as the *conductor loss*, is due to the finite conductivity of the line. It is modeled as the resistance R *p.u.l.* It is also influenced by the skin effect phenomena at a higher frequency. The instantaneous current $i(t)$ flowing through a lumped resistance R^{lum} is related to the instantaneous voltage drop $v(t)$ by Ohm's law:

$$v(t) = R^{lum} i(t). \tag{2.1.12}$$

The Inductance of a Line

The current flowing in a conductor creates the magnetic field around itself. So the magnetic energy stored in the space around the transmission line, i.e. the time-varying current supporting line section, is modeled by a series inductor L *p.u.l.* The inductance of a line is not lumped at one point, i.e. it is not confined at one point. It is distributed over the whole length of a line. The instantaneous voltage across a lumped inductor L^{lum} is related to the current flowing through it by

$$v(t) = L^{lum}\frac{di(t)}{dt}. \tag{2.1.13}$$

The Capacitance of a Line

In a two-conductor transmission line, the conductors separated by a dielectric medium form a distributed system of capacitance. The electric field energy stored in a line is modeled by the shunt capacitance C *p.u.l.* The instantaneous shunt current through a lumped capacitor C^{lum} is related to the instantaneous voltage across it by

$$i_{sh}(t) = C^{lum}\frac{dv(t)}{dt}. \tag{2.1.14}$$

The Conductance of a Line

If the medium between two conductors of the transmission line is not a perfect dielectric, i.e. if it has finite conductivity, then a part of the line current shunts through the medium causing the *dielectric loss*. The dielectric loss of the line is modeled by shunt conductance G *p.u.l.* The instantaneous shunt current is related to the instantaneous voltage across a lumped conductance by

$$i_{sh}(t) = G^{lum}v(t). \tag{2.1.15}$$

Figure (2.6a) shows a physical transmission line that supports the TEM mode wave propagation. Figure (2.6b) shows that this line could be modeled as a chain of the lumped RLCG structure. More numbers of RLCG sections per wavelength are needed to model a transmission line. The RLCG model is the modeling of a transmission line by the lossy series inductor and lossy shunt capacitor. The transmission line supports the wave propagation from power AC to RF and above. Likewise, the corresponding lumped components model of a transmission line also supports such waves. The transmission line structure behaves like a low-pass filter.

2.1.3 Kelvin–Heaviside Transmission Line Equations in Time Domain

Figure (2.6b) shows the *lumped element equivalent circuit model* of a section Δx of the transmission line. The primary line constants R, L, C, G on the per unit length (*p.u.l.*) basis are related to the lumped circuit elements as $R^{lum} = R\Delta x$, $L^{lum} = L\Delta x$, $C^{lum} = C\Delta x$, and $G^{lum} = G\Delta x$. Figure (2.6b) shows the *voltage loop equation* and the *current node equation* for a small line section Δx. These are written as follows:

The Loop Equation

Differential voltage change across line length Δx = Voltage drop across inductor + Voltage drop across resistance

$$v_k - v_{k+1} = \Delta v = -(L\Delta x)\frac{\partial i}{\partial t} - (R\Delta x)i. \tag{2.1.16}$$

The instantaneous line voltage v(t) and the instantaneous line current i(t) are functions of the space–time variables x and t. In the limiting case of $\Delta x \to 0$, equation (2.1.16) is written as

$$\frac{\partial v}{\partial x} = -\left(Ri + L\frac{\partial i}{\partial t}\right). \tag{2.1.17}$$

The Node Equation

Differential shunt current at the node = Current through conductance + Current through capacitor

$$i_k - i_{k+1} = \Delta i = -(G\Delta x)v - (C\Delta x)\frac{\partial v}{\partial t}. \tag{2.1.18}$$

In the limiting case, $\Delta x \to 0$; and the above equation is written as

$$\frac{\partial i}{\partial x} = -\left(Gv + C\frac{\partial v}{\partial t}\right). \tag{2.1.19}$$

The pair of coupled voltage and current transmission line equations in the time-domain summarized below is known as "*the time domain telegrapher's equations*":

$$\frac{\partial v}{\partial x} = -\left(Ri + L\frac{\partial i}{\partial t}\right) \quad (a), \quad \frac{\partial i}{\partial x} = -\left(Gv + C\frac{\partial v}{\partial t}\right) \quad (b). \tag{2.1.20}$$

The above pair of equations can also be called the *Kelvin–Heaviside transmission line equations*. The coupled Kelvin–Heaviside transmission line equations relate the voltage and current on a transmission line through the line parameters, RLCG. These parameters

are known as the *primary constants* of a line. The RLCG parameters depend on the physical configuration of a line, i.e. on its physical shapes, dimensions, and the electrical properties of the medium. They could be frequency-dependent parameters also. For simple transmission lines such as a pair of wires and coaxial lines, the closed-form formulas are available to compute them. However, these parameters could also be obtained through measurements. The empirical expressions for the RLCG parameters of a *microstrip line* are also available [J.3]. The transmission line equations are the complementary parts of Maxwell's field equations that relate the time-varying electric and magnetic fields in a physical medium through the primary constants of a medium-conductivity (σ), permittivity (ε) and permeability (μ). It is discussed in chapter 4. The transmission line equations can be obtained from Maxwell's equations. It is discussed in section (7.3) of chapter 7.

The voltage and current coupled variables of equation (2.1.20) can be separated. The separation of the variables leads to the wave equations for the voltage and current waves on a transmission line. On differentiating equation (2.1.20a) with respect to the variable x, the *voltage wave equation* is obtained:

$$\frac{\partial^2 v}{\partial x^2} = -\left[R\frac{\partial i}{\partial x} + L\frac{\partial}{\partial x}\left(\frac{\partial i}{\partial t}\right)\right] = -\left[R\frac{\partial i}{\partial x} + L\frac{\partial}{\partial t}\left(\frac{\partial i}{\partial x}\right)\right]. \tag{2.1.21}$$

On substituting $\frac{\partial i}{\partial x}$ from equation (2.1.20b) in equation (2.1.21), the voltage wave equation is

$$\frac{\partial^2 v}{\partial x^2} = \left[RGv + (RC + LG)\frac{\partial v}{\partial t} + LC\frac{\partial^2 v}{\partial t^2}\right]. \tag{2.1.22}$$

The above partial differential equation describes the time-domain voltage wave on a lossy transmission line. Likewise, an equation could be written to describe the current wave on a transmission line:

$$\frac{\partial^2 i}{\partial x^2} = \left[RGi + (RC + LG)\frac{\partial i}{\partial t} + LC\frac{\partial^2 i}{\partial t^2}\right]. \tag{2.1.23}$$

A lossless transmission line has, R = G = 0. The voltage and current waves on a lossless line are given by the following 1D PDEs:

$$\frac{\partial^2 v}{\partial x^2} = LC\frac{\partial^2 v}{\partial t^2}. \tag{2.1.24}$$

$$\frac{\partial^2 i}{\partial x^2} = LC\frac{\partial^2 i}{\partial t^2}. \tag{2.1.25}$$

On comparing the above equations with equation (2.1.11a), the velocity of propagation, for both the current and voltage waves, is

$$v_p = \frac{1}{\sqrt{LC}}. \tag{2.1.26}$$

It is like the velocity of propagation of an electromagnetic wave in a dielectric medium obtained from Maxwell's equations, where the primary constant of the line L and C are replaced by the medium constants permeability μ and permittivity ε. The EM-wave is discussed in chapter 4.

2.1.4 Kelvin–Heaviside Transmission Line Equations in Frequency-Domain

The time-harmonic instantaneous voltage in the frequency domain, i.e. in the phasor form, is written as

$$v(t) = V_{max}\cos(\omega t + \phi) = \mathrm{Re}\left(\tilde{V}e^{j\omega t}\right). \tag{2.1.27}$$

where "Re" stands for the real part of the voltage phasor $\tilde{V}$. The voltage phasor $\tilde{V}$ is given by the following expression:

$$\tilde{V} = \tilde{V}_{max}e^{j\phi}. \tag{2.1.28}$$

The phasor is nothing but a polar form of a complex quantity. Likewise, the instantaneous current in the phasor form is

$$i(t) = I_{max}\cos(\omega t + \varphi) = \mathrm{Re}\left(\tilde{I}e^{j\omega t}\right), \tag{2.1.29}$$

where current phasor is

$$\tilde{I} = \tilde{I}_{max}e^{j\varphi}. \tag{2.1.30}$$

The phasor is either a constant or a function of only the space variable. It is not a function of time *t*. The phasor is shown with a tilde (~) sign in this chapter. However, in the subsequent chapters, the tilde (~) sign is dropped. The phasor is used at a single frequency. Using the phasor notation, the voltage across R, L, and the current through C, G; given by equations (2.1.12)–(2.1.15) in the time domain, can be rewritten in the frequency-domain:

$$\begin{aligned} &\tilde{V} = R\tilde{I} \quad (a), \quad \tilde{V} = j\omega L\tilde{I} \quad (b) \\ &\tilde{I} = j\omega C\tilde{V} \quad (c), \quad \tilde{I} = G\tilde{V} \quad (d). \end{aligned} \tag{2.1.31}$$

In the above equations, the time derivative $\partial/\partial t$ is replaced by jω converting the expression from the time-domain to frequency-domain. Following the conversion process, the time-domain coupled voltage-current

transmission line equation (2.1.20), is rewritten in the frequency-domain:

$$\begin{aligned} \frac{d\widetilde{V}}{dx} &= -(R + j\omega L)\widetilde{I} \qquad (a) \\ \frac{d\widetilde{I}}{dx} &= -(G + j\omega C)\widetilde{V} \qquad (b). \end{aligned} \tag{2.1.32}$$

On separation of the voltage and current variables, the following voltage and current wave equations are obtained in the frequency-domain:

$$\begin{aligned} \frac{d^2\widetilde{V}}{dx^2} &= (R + j\omega L)(G + j\omega C)\widetilde{V} \quad (a) \\ \frac{d^2\widetilde{I}}{dx^2} &= (R + j\omega L)(G + j\omega C)\widetilde{I} \quad (b). \end{aligned} \tag{2.1.33}$$

It is noted that the second-order partial differential wave equations in the time-domain are converted to the second-order ordinary differential equations in the frequency-domain. The factors at the right-hand side of the above equations help to define a *secondary parameter* γ, known as the *complex propagation constant* of a transmission line:

$$\gamma = [(R + j\omega L)(G + j\omega C)]^{\frac{1}{2}}, \tag{2.1.34}$$

where $\gamma = \alpha + j\beta$. The real part α(Np/m) of the complex propagation constant γ is called the *attenuation constant* and the imaginary part β (rad/sec) is the *propagation constant* of a lossy transmission line. The parameter β is also known as the *phase-shift constant or phase constant*. On separating the real and imaginary parts of the above equation, the following expressions are obtained:

$$\begin{aligned} \alpha &= \mathrm{Re}\,[\gamma] \\ &= \left\{ \frac{RG - \omega^2 LC + \sqrt{(RG - \omega^2 LC)^2 + \omega^2 (LG + RC)^2}}{2} \right\}^{\frac{1}{2}}. \end{aligned} \tag{2.1.35}$$

$$\begin{aligned} \beta &= \mathrm{Im}[\gamma] \\ &= \left\{ \frac{\omega^2 LC - RG + \sqrt{(RG - \omega^2 LC)^2 + \omega^2 (LG + RC)^2}}{2} \right\}^{\frac{1}{2}}. \end{aligned} \tag{2.1.36}$$

The attenuation constant α, and propagation constant β are given in terms of the primary line constants, R, L, C, G. Normally α and β are frequency-dependent. Thus, the phase velocity of both the current and voltage waves, given by $v_p = \omega/\beta$ is frequency-dependent. This kind of transmission line is known as the *dispersive transmission line*. A complex wave traveling on a lossy dispersive line gets distorted as each component of the complex wave travels with different phase velocity.

Using the complex propagation constant, the wave equation (2.1.33a and b) are rewritten as

$$\begin{aligned} \frac{d^2\widetilde{V}}{dx^2} - \gamma^2\widetilde{V} &= 0 \qquad (a) \\ \frac{d^2\widetilde{I}}{dx^2} - \gamma^2\widetilde{I} &= 0 \qquad (b). \end{aligned} \tag{2.1.37}$$

The above homogeneous wave equations on a transmission line could be treated as a *boundary value problem* to get the voltage and current at any location on the line. If a transmission line is infinitely long and excited from one end, then the voltage and current waves on the line always move in the forward direction without any reflection. At any location on the line, the voltage and current are related by another secondary parameter called "*the characteristic impedance*" of a transmission line:

$$\frac{\widetilde{V}}{\widetilde{I}} = Z_0. \tag{2.1.38}$$

The characteristic impedance of a transmission line could be viewed as a mechanism that explains the wave propagation on a line. It recasts the *Huygens' Principle* of the secondary wave formation in terms of the characteristic impedance. The characteristic impedance could be called the *Huygens' load*. It is an unusual load impedance with a special property. It absorbs power from the source and itself becomes a secondary source for the further transmission of power in the form of wave motion. In this manner, the wave on a transmission line moves; as the characteristic impedance, i.e. Huygens' load, acts both as a load and also as a source of the wave motion. The process is similar to the Huygens' secondary source for the wavefront propagation. The concept of the Huygens' load is further extended to engineer the *Huygens' metasurface* with unique characteristics to control the reflected and transmitted (refracted) EM-waves. It is discussed in subsection (22.5.2) of chapter 22.

The characteristic impedance, i.e. *Huygens'* load of a lossy line is a complex quantity. Its real part does not dissipate energy like the real part of a normal complex load. The imaginary part of Huygens's load indicates the presence of losses in a transmission line, whereas in the case of a normal complex load its imaginary part shows the storage of the reactive energy. For a lossless transmission line, Huygens' load is a real quantity $\sqrt{L/C}$ that is non-dissipative. Huygens adopted the secondary source

model to explain the propagation of the light wave in the space [B.3, B.4]. The expression for the characteristic impedance of a line is obtained from equation (2.1.32).

$$Z_0^2 = \frac{\Delta\widetilde{V}}{\widetilde{I}} \times \frac{\widetilde{V}}{\Delta\widetilde{I}} = \frac{R + j\omega L}{G + j\omega C}, \Rightarrow Z_0 = \sqrt{\frac{R + j\omega L}{G + j\omega C}}. \tag{2.1.39}$$

In general, the characteristic impedance of a lossy transmission line is a complex quantity. However, for a lossless line, the lossy elements are zero, i.e. $R = G = 0$. It leads to the following expressions:

$$\alpha = 0 \quad (a), \quad \beta = \omega\sqrt{LC} \quad (b), \quad Z_0 = \sqrt{\frac{L}{C}} \quad (c). \tag{2.1.40}$$

There is no attenuation in the propagating wave on a lossless line. If the line inductance L and the line capacitance C are frequency-independent, the transmission line is nondispersive. The characteristic impedance is a real quantity. The line parameters such as the attenuation constant (α), propagation constant (β), and characteristic impedance (Z_0) are known as the *secondary parameters* of a transmission line. These secondary parameters are finally expressed in terms of the physical geometry and the electrical characteristics of material medium of a line. A microwave circuit designer is more interested in these secondary parameters as compared to the primary line constants, RLCG, of a transmission line. The secondary parameters are more conveniently measured and numerically computed for a large class of the transmission line structures. For any practical transmission line, the losses are always present on a line.

2.1.5 Characteristic of Lossy Transmission Line

A transmission line, such as a coaxial cable, a flat cable, used in the computer, or a feeder to TV receiver, is embedded in a lossy dielectric medium. The loss in a dielectric medium is known as the *dielectric loss* of a transmission line. Of course, when the line is in the air medium, the dielectric loss could be neglected. Likewise, there is another kind of loss, known as the *conductor loss,* on a transmission line. It is due to the finite conductivity of the conducting wires or the strip conductors forming a line. All open transmission lines tend to radiate some power, leading to *radiation loss*. In the case of a planar transmission line, there are also other mechanisms of losses. However, this section considers only the conductor and the dielectric losses of a line and their effect on the propagation characteristics of the line.

Characteristic Impedance

The characteristic impedance Z_0 of a uniform lossy transmission line is given by equation (2.1.39). In the limiting case, $\omega \to 0$, i.e. at a lower frequency, it is reduced to a real quantity that is dominated by the lossy elements of a line:

$$Z_0 = \sqrt{\frac{R}{G}}. \tag{2.1.41}$$

The characteristic impedance Z_0 at very high frequency, i.e. for $\omega \to \infty$, is also reduced to a real quantity. However, now it is dominated by the lossless reactive elements:

$$Z_0 = \sqrt{\frac{L}{C}}. \tag{2.1.42}$$

At higher frequency, we have $\omega L >> R$ and $\omega C >> G$. Therefore, the R and G are normally ignored for the computation of characteristic impedance of a low-loss microwave transmission line. In the intermediate frequency range, the characteristic impedance of a line is a complex quantity. Its *imaginary part indicates the presence of the loss* in a line. Equation (2.1.42) is also applicable to a lossless line.

The characteristic impedance of transmission line in the lossless dielectric medium, or a moderately lossy medium where G could be neglected, is obtained in equation (2.1.43). However, the conductor loss is present on the line:

$$Z_0 = \left[\frac{R + j\omega L}{G + j\omega C}\right]^{\frac{1}{2}} = \left[\frac{L}{C}\left(1 + \frac{R}{j\omega L}\right)\right]^{\frac{1}{2}} \approx \sqrt{\frac{L}{C}}\left(1 - j\frac{R}{2\omega L}\right). \tag{2.1.43}$$

The measured or computed complex characteristic impedance of a line, over a certain frequency range, with a negative imaginary part, indicates that the loss in the line is mainly due to the conductor loss [J.4].

The alternative case of a lossy line, with $G \neq 0$, $R = 0$, could be also considered. In this case, the conductor loss is ignored; however, the dielectric loss is dominant. The characteristic impedance of such line is approximated as follows:

$$Z_0 = \left[\frac{j\omega L}{G + j\omega C}\right]^{\frac{1}{2}} \approx \sqrt{\frac{L}{C}}\left(1 + j\frac{G}{2\omega C}\right). \tag{2.1.44}$$

If the imaginary part of the characteristic impedance of a line is positive over some frequency range, then the dielectric loss dominates the loss in the line. However, if both R and G are moderately present, with $\omega L >> R$ and $\omega C >> G$, the real and imaginary parts of

the characteristic impedance could be approximated by using the binomial expansion as follows:

$$(1 \pm x)^{\frac{1}{2}} \approx 1 \pm \frac{x}{2} - \frac{x^2}{8}. \tag{2.1.45}$$

$$Z_0 = \sqrt{\frac{L}{C}}\left[\left(1 - j\frac{R}{\omega L}\right)\left(1 + j\frac{G}{\omega C}\right)\right]^{\frac{1}{2}}. \tag{2.1.46}$$

$$\Rightarrow Z_0 = \sqrt{\frac{L}{C}}\left[\left(1 + \frac{R^2}{8\omega^2 L^2} + \frac{G^2}{8\omega^2 C^2} + \frac{RG}{4\omega^2 LC}\right) + j\left(\frac{G}{2\omega C} - \frac{R}{2\omega L}\right)\right]. \tag{2.1.47}$$

In the above expression, ω^3 and ω^4 terms are neglected. If we neglect ω^2 terms and also take $G = 0$ or $R = 0$, equation (2.1.47) reduces to either equation (2.1.43) or equation (2.1.44), respectively. It is also possible that with the change of frequency, the imaginary part of characteristic impedance changes from a positive to a negative value indicating that the dominant loss can change from the dielectric loss to the conductor loss. For such cases, R and G are usually frequency-dependent [J.4]. Over a band of frequencies, the imaginary part of the characteristic impedance could be zero leading to

$$\frac{R}{L} = \frac{G}{C}. \tag{2.1.48}$$

It is well known as *Heaviside's condition*. On meeting it, a lossy line becomes dispersion-less and the propagation constant β becomes a linear function of frequency, while the attenuation constant becomes frequency-independent. Following the above equation (2.1.48), a lossy line could be made dispersionless by the inductive loading [B.5, B.6].

Propagation Constant

The propagation constant γ of a uniform lossy transmission line is given by equation (2.1.34). It could be approximated under the low-loss condition. Its real and imaginary parts are separated to get the frequently used approximate expressions for the attenuation and phase constants of a line:

$$\gamma = j\omega\sqrt{LC}\left[\left(1 - j\frac{R}{\omega L}\right)\left(1 - j\frac{G}{\omega C}\right)\right]^{\frac{1}{2}}$$

$$\Rightarrow \gamma \approx j\omega\sqrt{LC}\left[\left(1 - j\frac{R}{2\omega L} + \frac{R^2}{8\omega^2 L^2}\right)\left(1 - j\frac{G}{2\omega C} + \frac{G^2}{8\omega^2 C^2}\right)\right]. \tag{2.1.49}$$

On neglecting ω^2, ω^3, and ω^4 terms, the real part of the propagation constant γ provides the attenuation constant, whereas the imaginary part gives the propagation constant:

$$\alpha \approx \frac{R}{2\sqrt{L/C}} + \frac{G\sqrt{L/C}}{2} = \frac{R}{2Z_0} + \frac{GZ_0}{2} \quad (a)$$

$$\beta \approx \omega\sqrt{LC} \quad (b). \tag{2.1.50}$$

The *first term* of the above equation (2.1.50a) shows the conductor loss of a line, while the *second term* shows its dielectric loss. If R and G are frequency-independent, the attenuation in a line would be frequency-independent under $\omega L >> R$ and $\omega C >> G$ conditions. However, usually, R is frequency-dependent due to the skin effect. In some cases, G could also be frequency-dependent [B.7].

The dispersive phase constant β is obtained from the imaginary part of equation (2.1.49):

$$\beta \approx \omega\sqrt{LC}\left[\left(1 - \frac{RG}{4\omega^2 LC} + \frac{R^2}{8\omega^2 L^2} + \frac{G^2}{8\omega^2 C^2}\right)\right]. \tag{2.1.51}$$

On neglecting the second-order term, β becomes a linear function of frequency and the line is dispersionless. In that case, its phase velocity is also independent of frequency. *A lossy line is dispersive. However, it also becomes dispersionless under the Heaviside's condition – (2.1.48).* A transmission line, such as a microstrip in the inhomogeneous medium, can have dispersion even without losses.

2.1.6 Wave Equation with Source

In the above discussion, the development of the voltage and current wave equations has ignored the voltage or current source. However, a voltage or current source is always required to launch the voltage and current waves on a line. Therefore, it is appropriate to develop the transmission line equation with a source [B.8]. The consideration of a voltage/current source is important to solve the electromagnetic field problems of the layered medium planar lines, discussed in chapters 14 and 16.

Shunt Current Source

Figure (2.7) shows the lumped element model of a transmission line section of length Δx with a shunt current source $\widetilde{I}_s \Delta x$ located at $x = x_0$. It is expressed through Dirac's delta function as $\widetilde{I}_s \Delta x \delta(x - x_0)$. The lumped line constants R, L, C, G are given for *p.u.l.*

The loop and node equations are written below to develop the Kelvin–Heaviside transmission line equations with a current source:

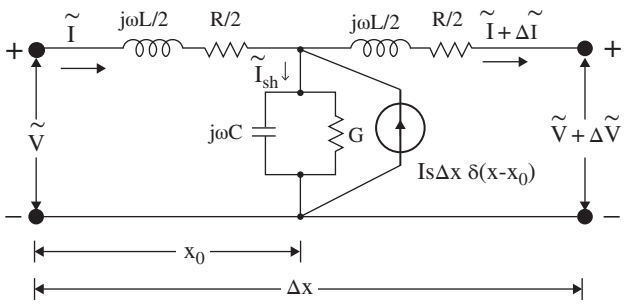

Figure 2.7 Equivalent lumped circuit of a transmission line with a shunt current source.

The Loop Equation

$$\tilde{V} - [(R + j\omega L)\Delta x/2]\tilde{I} - [(R + j\omega L)\Delta x/2]\left(\tilde{I} + \Delta\tilde{I}\right) - \left(\tilde{V} + \Delta\tilde{V}\right) = 0$$

$$\Rightarrow -\Delta\tilde{V} - [(R + j\omega L)\Delta x]\tilde{I} - \left[(R + j\omega L)\Delta x\Delta\tilde{I}/2\right] = 0,$$

By taking $\Delta x\Delta\tilde{I}/2 \approx 0$

$$\Rightarrow \frac{\Delta\tilde{V}}{\Delta x} = -[(R + j\omega L)]\tilde{I}$$

The Node Equation

$$\tilde{I} + \tilde{I}_s\Delta x\delta(x - x_0) - \left(\tilde{I} + \Delta\tilde{I}\right) - \tilde{I}_{sh} = 0$$

$$\Rightarrow \tilde{I} + \tilde{I}_s\Delta x\delta(x - x_0) - \left(\tilde{I} + \Delta\tilde{I}\right) - [(G + j\omega C)\Delta x]\left[\tilde{V} - \tilde{I}(R + j\omega L)\Delta x/2\right] = 0$$

$$\Rightarrow \frac{\Delta\tilde{I}}{\Delta x} = -(G + j\omega C)\left[\tilde{V} - \tilde{I}(R + j\omega L)\Delta x/2\right] + \tilde{I}_s\delta(x - x_0)$$

For $\Delta x \to 0$, the above equations are reduced to

$$\frac{d\tilde{V}}{dx} = -(R + j\omega L)\tilde{I} \quad (a)$$

$$\frac{d\tilde{I}}{dx} = -(G + j\omega C)\tilde{V} + \tilde{I}_s\delta(x - x_0) \quad (b). \tag{2.1.52}$$

The above equations are rewritten below in term of the characteristic impedance (Z_0) and propagation constant (γ) of a transmission line:

$$\frac{d\tilde{V}}{dx} = -\gamma Z_0\tilde{I} \quad (a), \qquad \frac{d\tilde{I}}{dx} = -\frac{\gamma}{Z_0}\tilde{V} + \tilde{I}_s\delta(x - x_0) \quad (b). \tag{2.1.53}$$

On solving the above equations for the voltage, the following inhomogeneous voltage wave equation, with a current source, is obtained:

$$\frac{d^2\tilde{V}}{dx^2} - \gamma^2\tilde{V} = -\gamma Z_0\tilde{I}_s\delta(x - x_0). \tag{2.1.54}$$

Away from the location of the current source, i.e. for $x \neq x_0$, equation (2.1.54) reduces to the homogeneous equation (2.1.37a). The wave equation for the current wave, with a shunt current source, could also be rewritten.

2.1.7 Solution of Voltage and Current-Wave Equation

The voltage and current wave equations in the phasor form are given in equation (2.1.37). The solution of a wave equation is written either in terms of the hyperbolic functions or in terms of the exponential functions. The first form is suitable for a line terminated in an arbitrary load. A section of the line transforms the load impedance into the input impedance at any location on the line. The impedance transformation takes place due to the standing wave formation. The *hyperbolic form* of the solution also provides the voltage and current distributions along the line. The *exponential form* of the solution demonstrates the traveling waves on a line, both in the forward and in the backward directions. A combination of the forward-moving and the backward-moving waves produces the *standing wave* on a transmission line.

The Hyperbolic Form of a Solution

Figure (2.8a) shows a section of the transmission line having a length ℓ. It is fed by a voltage source, $\tilde{V}_g$ with Z_g internal impedance. The general solutions for the line voltage $\tilde{V}(x)$ and line current $\tilde{I}(x)$ of the wave equation (2.1.37) are

$$\tilde{V}(x) = A_1\cosh(\gamma x) + B_1\sinh(\gamma x) \quad (a)$$

$$\tilde{I}(x) = A_2\cosh(\gamma x) + B_2\sinh(\gamma x) \quad (b). \tag{2.1.55}$$

At any section on the line, its characteristic impedance Z_0 relates the line voltage $\tilde{V}(x)$ and line current $\tilde{I}(x)$. So the constants A_2, B_2 are related to the constants A_1 and B_1. In Fig (2.8a), the point P on the line is located at a *distance x from the source end*, i.e. at a *distance* $d = (\ell - x)$ *from the load end*. The load is located at $d = 0$, and the source is located at $d = -\ell$. The $\tilde{V}_s$, and $\tilde{I}_s$ are the input voltage and the input current at the port-aa, i.e at $x = 0$. At $x = \ell$, i.e. at the port-bb, $\tilde{V}_R$ and $\tilde{I}_R$ are the load end voltage and current, respectively.

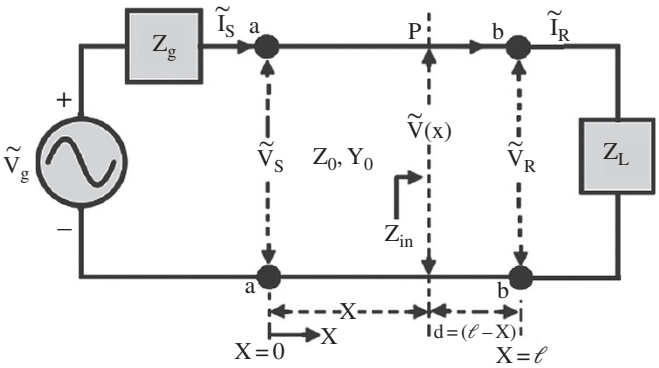

(a) Finite length transmission line with a voltage source and a load termination.

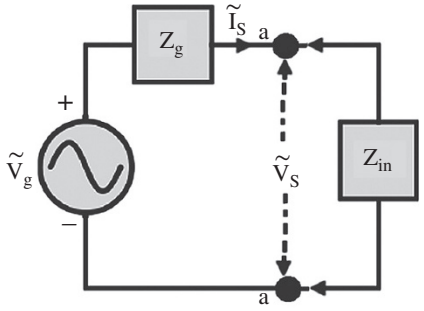

(b) Input equivalent circuit at plane a-a.

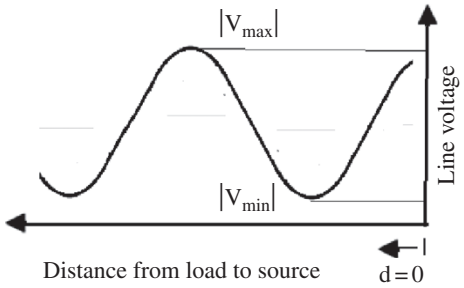

(c) A standing wave on the line.

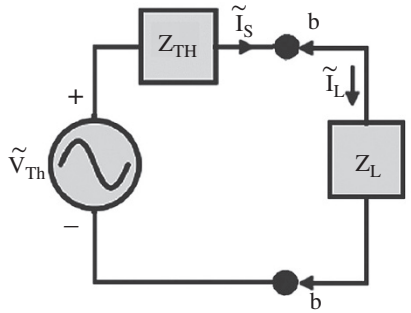

(d) Output Thevenin equivalent circuit at plane b-b.

Figure 2.8 Transmission line circuit. The distance x is measured from the source end; whereas the distance d is measured from the load.

The ideal voltage generator $\widetilde{V}_g$ has the internal impedance, $Z_g = 0$, i.e. $\widetilde{V}_S = \widetilde{V}_g$. The phasor form of the line current, from equations (2.1.32b) and (2.1.55a), is written below:

$$\widetilde{I}(x) = -(G + j\omega C)\int [A_1 \cosh(\gamma x) + B_1 \sinh(\gamma x)]dx$$
$$\Rightarrow \widetilde{I}(x) = -\frac{1}{Z_0}[A_1 \sinh(\gamma x) + B_1 \cosh(\gamma x)]. \tag{2.1.56}$$

On comparing the coefficients of sinh(γx) and cosh (γx), of equations (2.1.55b) and (2.1.56), two constants A_2 and B_2 are determined:

$$B_2 = -\frac{A_1}{Z_0}, \quad A_2 = -\frac{B_1}{Z_0}. \tag{2.1.57}$$

The phasor line voltage and line current are written as follows:

$$\widetilde{V}(x) = A_1 \cosh(\gamma x) + B_1 \sinh(\gamma x) \quad \text{(a)}$$
$$\widetilde{I}(x) = -\frac{1}{Z_0}[A_1 \sinh(\gamma x) + B_1 \cosh(\gamma x)] \quad \text{(b)}. \tag{2.1.58}$$

The constants A_1 and B_1 are determined by using the boundary conditions at input x = 0 and output x = ℓ.

- At x = 0, the line input voltage is $\widetilde{V}_S$, giving the value of A_1:

$$\widetilde{V}(x = 0) = A_1 = \widetilde{V}_S. \tag{2.1.59}$$

At the receiving end, x = ℓ, the load end voltage and current are

$$\widetilde{V}(x = \ell) = \widetilde{V}_R = \widetilde{V}_S \cosh(\gamma\ell) + B_1 \sinh(\gamma\ell) \quad \text{(a)}$$
$$\widetilde{I}(x = \ell) = \widetilde{I}_R = -\frac{1}{Z_0}\left[\widetilde{V}_S \sinh(\gamma\ell) + B_1 \cosh(\gamma\ell)\right] \quad \text{(b)}. \tag{2.1.60}$$

- At x = ℓ, i.e. at the receiving end, the voltage across load Z_L is

$$\widetilde{V}_R = Z_L \widetilde{I}_R. \tag{2.1.61}$$

The constant B_1 is evaluated on substituting $\widetilde{V}_R$ and $\widetilde{I}_R$, from equation (2.1.60), in the above equation:

$$B_1 = -\frac{\widetilde{V}_S[Z_0 \cosh(\gamma\ell) + Z_L \sinh(\gamma\ell)]}{Z_L \cosh(\gamma\ell) + Z_0 \sinh(\gamma\ell)}. \tag{2.1.62}$$

On substituting constants A_1 and B_1 in equation (2.1.58a), the expression for the line voltage at location P, from the source or load end, is

$$\widetilde{V}(x) = V_S\left[\frac{Z_L\cosh[\gamma(\ell-x)] + Z_0\sinh[\gamma(\ell-x)]}{Z_L\cosh(\gamma\ell) + Z_0\sinh(\gamma\ell)}\right] \quad (a)$$

$$\Rightarrow\widetilde{V}(d) = V_S\left[\frac{Z_L\cosh(\gamma d) + Z_0\sinh(\gamma d)}{Z_L\cosh(\gamma\ell) + Z_0\sinh(\gamma\ell)}\right] \quad (b). \tag{2.1.63}$$

Similarly, the line current at the location P is obtained as follows:

$$\widetilde{I}(x) = \frac{V_S}{Z_0}\left[\frac{Z_L\sinh[\gamma(\ell-x)] + Z_0\cosh[\gamma(\ell-x)]}{Z_L\cosh(\gamma\ell) + Z_0\sinh(\gamma\ell)}\right] \quad (a)$$

$$\Rightarrow\widetilde{I}(d) = \frac{V_S}{Z_0}\left[\frac{Z_L\sinh(\gamma d) + Z_0\cosh(\gamma d)}{Z_L\cosh(\gamma\ell) + Z_0\sinh(\gamma\ell)}\right] \quad (b). \tag{2.1.64}$$

At any location P on the line, the load impedance is transformed as input impedance by the line length $d = (\ell - x)$:

$$Z_{in}(x) = \frac{\widetilde{V}(x)}{\widetilde{I}(x)} = Z_0\left[\frac{Z_L + Z_0\tanh[\gamma(\ell-x)]}{Z_0 + Z_L\tanh[\gamma(\ell-x)]}\right] \quad (a)$$

$$\Rightarrow Z_{in}(d) = \frac{\widetilde{V}(d)}{\widetilde{I}(d)} = Z_0\left[\frac{Z_L + Z_0\tanh(\gamma d)}{Z_0 + Z_L\tanh(\gamma d)}\right] \quad (b)$$

$$\text{for } \alpha = 0,\ Z_{in}(d) = Z_0\left[\frac{Z_L + jZ_0\tan(\beta d)}{Z_0 + jZ_L\tan(\beta d)}\right] \quad (c). \tag{2.1.65}$$

Equations (2.1.65a,b) take care of the losses in a line through the complex propagation constant, $\gamma = \alpha + j\beta$. However, for a lossless line $\alpha = 0$, $\gamma = j\beta$ and the hyperbolic functions are replaced by the trigonometric functions shown in equation (2.1.65c). It shows the impedance transformation characteristics of $d = \lambda/4$ transmission line section.

Equations (2.1.63) and (2.1.64) could be further written in terms of the generator voltage $\widetilde{V}_g$ for the case, $Z_g \neq 0$. Figure (2.8b) shows that at the source end $x = 0$, the load appears as the input impedance Z_{in}. The sending end voltage is obtained as follows:

$\widetilde{V}_s = \widetilde{V}_g - Z_g\widetilde{I}_s$ where $\widetilde{I}_s = \frac{V_g}{Z_g + Z_{in}}$, and

$$Z_{in}(x=0) = Z_0\left[\frac{Z_L + Z_0\tanh\gamma\ell}{Z_0 + Z_L\tanh\gamma\ell}\right].$$

$$\widetilde{V}_s = \widetilde{V}_g - \widetilde{V}_g\frac{Z_g}{Z_{in} + Z_g} = \widetilde{V}_g\frac{Z_{in}}{Z_{in} + Z_g}$$

$$\Rightarrow \widetilde{V}_s = \widetilde{V}_g\left[\frac{Z_oZ_L + Z_0^2\tanh\gamma\ell}{(Z_0Z_L + Z_oZ_g) + (Z_0^2 + Z_LZ_g)\tanh\gamma\ell}\right]. \tag{2.1.66}$$

The line voltage, in terms of $\widetilde{V}_g$, Z_g, and Z_L, is obtained on substituting equation (2.1.66) in equation (2.1.63):

$$\widetilde{V}(x) = V_g\left[\frac{Z_0[Z_L\cosh\gamma(\ell-x) + Z_0\sinh\gamma(\ell-x)]}{(Z_0Z_L + Z_0Z_g)\cosh\gamma\ell + (Z_0^2 + Z_LZ_g)\sinh\gamma\ell}\right]. \tag{2.1.67}$$

Likewise, from equations (2.1.64) and (2.1.66), an expression for the line current is obtained:

$$\widetilde{I}(x) = V_g\left[\frac{[Z_L\sinh\gamma(\ell-x) + Z_0\cosh\gamma(\ell-x)]}{(Z_0Z_L + Z_0Z_g)\cosh\gamma\ell + (Z_0^2 + Z_LZ_g)\sinh\gamma\ell}\right]. \tag{2.1.68}$$

The above equations could be reduced to the following equations for a lossless line, i.e. for $\alpha = 0$, $\gamma = j\beta$, $\cosh(j\beta) = \cos\beta$ and $\sinh(j\beta) = j\sin\beta$:

$$\widetilde{V}(x) = V_g\left[\frac{Z_0[Z_L\cos\beta(\ell-x) + jZ_0\sin\beta(\ell-x)]}{(Z_0Z_L + Z_0Z_g)\cos\beta\ell + j(Z_0^2 + Z_LZ_g)\sin\beta\ell}\right]. \tag{2.1.69}$$

$$\widetilde{I}(x) = V_g\left[\frac{[Z_0\cos\beta(\ell-x) + jZ_L\sin\beta(\ell-x)]}{(Z_0Z_L + Z_0Z_g)\cos\beta\ell + j(Z_0^2 + Z_LZ_g)\sin\beta\ell}\right]. \tag{2.1.70}$$

Equation (2.1.65c), for the input impedance, could be obtained from the above two equations. The sending end voltage and current are obtained at the input port – aa, $x = 0$:

$$\widetilde{V}_s = \widetilde{V}(x=0) = V_g\left[\frac{Z_0[Z_L\cos\beta\ell + jZ_0\sin\beta\ell]}{(Z_0Z_L + Z_0Z_g)\cos\beta\ell + j(Z_0^2 + Z_LZ_g)\sin\beta\ell}\right]. \tag{2.1.71}$$

$$\widetilde{I}_s = \widetilde{I}(x=0) = V_g\left[\frac{[Z_0\cos\beta\ell + jZ_L\sin\beta\ell]}{(Z_0Z_L + Z_0Z_g)\cos\beta\ell + j(Z_0^2 + Z_LZ_g)\sin\beta\ell}\right]. \tag{2.1.72}$$

Likewise, the expressions for the voltage and current at the output port – bb, i.e. at the receiving end for $x = \ell$, are obtained:

$$\widetilde{V}_R = \widetilde{V}(x=\ell) = \widetilde{V}_g\left[\frac{Z_0Z_L}{(Z_0Z_L + Z_0Z_g)\cos\beta\ell + j(Z_0^2 + Z_LZ_g)\sin\beta\ell}\right]. \tag{2.1.73}$$

$$\widetilde{I}_R = \widetilde{I}(x = \ell) = \widetilde{V}_g \left[\frac{Z_0}{(Z_0 Z_L + Z_0 Z_g)\cos\beta\ell + j(Z_0^2 + Z_L Z_g)\sin\beta\ell} \right]. \quad (2.1.74)$$

Two special cases of the load termination, i.e. the short-circuited load and the open-circuited load, are discussed below. The voltage and current distributions on a transmission line for both the cases are also obtained.

Short-Circuited Receiving End

For the short-circuited load $Z_L = 0$, the line voltage at the load end is zero $\widetilde{V}(x = \ell) = 0$. However, the voltage on the line is not zero. Equations (2.1.63) and (2.1.64) provide the voltage and current distributions on a short-circuited line:

$$\widetilde{V}(x) = \widetilde{V}_S \frac{\sinh\gamma(\ell - x)}{\sinh\gamma\ell} \quad (a)$$

$$\widetilde{I}(x) = \frac{\widetilde{V}_S}{Z_0} \frac{\cosh\gamma(\ell - x)}{\sinh\gamma\ell} \quad (b). \quad (2.1.75)$$

The input impedance at any distance $(\ell - x)$ from the source end is

$$Z_{in}(x) = Z_0 \tanh\gamma(\ell - x) \quad (a)$$

$$Z_{in}(d) = Z_0 \tanh\gamma d \quad (b)$$

$$\text{for } \alpha = 0, Z_{in}(d) = jZ_0 \tan\beta d \quad (c). \quad (2.1.76)$$

At the load end, the voltage is zero. However, the line current is not infinite like the lumped element circuit with a short-circuited termination at output. A short-circuited transmission line draws only a finite current from the source. *The $\ell < \lambda/4$ short-circuited line section behaves as an inductive element*. The electrical nature of the line section can be controlled by changing its electrical length [B.9–B.15].

Open-Circuited Receiving End

The load impedance is $Z_L \to \infty$ for an open-circuited transmission line and the load current $\widetilde{I}(x = \ell) = 0$. Again, equations (2.1.63) and (2.1.64) provide the voltage and current distributions on an open-circuited transmission line. The voltage and current waves and the input impedance at location P from the load end can be computed for the open-circuited load as follows:

$$\widetilde{V}(x) = \widetilde{V}_S \frac{\cosh\gamma(\ell - x)}{\cosh\gamma\ell} \quad (a)$$

$$\widetilde{I}(x) = \frac{\widetilde{V}_S}{Z_0} \frac{\sinh\gamma(\ell - x)}{\cosh\gamma\ell} \quad (b). \quad (2.1.77)$$

$$Z_{in}(x) = Z_0 \coth\gamma(\ell - x) \quad (a)$$

$$\Rightarrow Z_{in}(d) = Z_0 \coth\gamma d \quad (b)$$

$$\text{for } \alpha = 0, Z_{in}(d) = -jZ_0 \cot\beta d \quad (c). \quad (2.1.78)$$

The $\ell < \lambda/4$ open-circuited line section behaves as a capacitive element. The electrical nature of the line section can be controlled by changing its electrical length.

Matched and Mismatched Termination

The input impedance at any location on a line is $Z_{in}(x) = Z_0$ if it is matched terminated in its characteristic impedance, i.e. $Z_L = Z_0$. Normally, the characteristics impedance of a microwave line is a real quantity. The line terminated in Z_0 does not create any reflected wave on a transmission line. However, for the mismatched termination $Z_L \neq Z_0$, there is a reflected wave on a transmission line, traveling from the load end to the source end.

Exponential Form of Solution

The wave nature of the line voltage and line current becomes more obvious from the exponential form of solutions of the wave equations. The solution of wave equation (2.1.37), for the phasor line voltage and line current, can also be written in the exponential form:

$$\widetilde{V}(x) = V^+ e^{-\gamma x} + V^- e^{\gamma x} \quad (a)$$

$$\widetilde{I}(x) = \frac{1}{Z_0}(V^+ e^{-\gamma x} - V^- e^{\gamma x}) \quad (b). \quad (2.1.79)$$

The distance x is measured from the source end. The time-dependent harmonic form of the voltage wave is $v(x,t) = \text{Re}\left[\widetilde{V}(x)\exp(j\omega t)\right]$. Finally, it is written as follows:

$$v(x,t) = \underbrace{V^+ e^{-\alpha x}\cos(\omega t - \beta x)}_{\text{Forward traveling wave}} + \underbrace{V^- e^{\alpha x}\cos(\omega t + \beta x)}_{\text{Backward traveling wave}}. \quad (2.1.80)$$

For an outgoing wave on a lossy line, the wave amplitude decays and its phase lags; whether the distance is measured from source end or load end. It is accounted for by the proper sign of distance x. The amplitude of a wave is exponentially decaying due to the line losses. It is expressed by the attenuation constant α (Np/m).

The expression of the traveling current wave on a line could be written as follows:

$$i(x,t) = \frac{1}{Z_0}[V^+ e^{-\alpha x}\cos(\omega t - \beta x) - V^- e^{\alpha x}\cos(\omega t + \beta x)].$$

↓ Forward traveling wave ↓ Backward traveling wave

(2.1.81)

If the source at $x = 0$ is connected to a line of infinite extent, there is no reflection from the load end, as the wave will never reach to the load end to get reflected. Therefore, for the forward traveling voltage and current waves on an infinite line, $V^- = 0$ and the above solutions of the wave equations are written as follows:

$$\widetilde{V}(x) = V^+ e^{-\gamma x} \quad (a)$$

$$\widetilde{I}(x) = \frac{V^+ e^{-\gamma x}}{Z_0} \quad (b)$$

$$v(x,t) = V^+ e^{-\alpha x}\cos(\omega t - \beta x) \quad (c)$$

$$i(x,t) = \frac{V^+}{Z_0} e^{-\alpha x}\cos(\omega t - \beta x) \quad (d).$$

(2.1.82)

The input impedance of an infinite line at any location x is $Z_{in}(x) = Z_0$. Thus, *a finite line terminated in its characteristic impedance, i.e. $Z_L = Z_0$ behaves as an infinite extent transmission line without any reflection*. The characteristic impedance shows a specific feature of a line that is determined by the geometry and physical medium of the line. Once a finite extent line is terminated in any other load impedance, i.e. $Z_L \neq Z_0$, the voltage and current waves are reflected from the load. The wave reflection is expressed by *the reflection coefficient*, $\Gamma(x)$. The reflection coefficient is a complex quantity and its phase changes over the length of a line. However, its magnitude remains constant over the length of a lossless line. The interference of the forward-moving and backward-moving reflected waves produces the *standing wave* with maxima and minima of the voltage and current on a line. Figure (2.8c) shows the voltage standing wave. The position and magnitude of the voltage maxima V_{max} and voltage minima V_{min} are measurable quantities. Their positions are measured from the load end. The *reflection coefficient*, and also the *voltage standing wave ratio*, VSWR, i.e. S, is defined using the V_{max} and V_{min}. The VSWR could be measured with a VSWR meter. Therefore, the reflection on a transmission line is expressed by both the reflection coefficient and the VSWR. The reflection at the input terminal of a line is also expressed as the *return-loss*, $RL = -20\log_{10}|\Gamma_{in}|$. The wave behavior in terms of the reflection parameter is an important quantity in the design of circuits and components in the microwave and RF engineering.

At the load end, the total line voltage is a sum of the forward and reflected waves, and it is equal to the voltage drop V_R across the load impedance Z_L. It is shown in Fig (2.8a). To simplify expressions for the line voltage and current, the origin is shifted from the source end to the load end. In that case, expressions for both the line voltage and line current, given by equation (2.1.79), have to be modified for the new distance variable $x < 0$. Now the source and load are located at $x = -\ell$ and at $x = 0$, respectively. For the origin at the load end, the reflected wave $V^- e^{(\omega t + \gamma x)}$ appears as the "forward-traveling wave" from load to the source, whereas the wave incident at the load $V^+ e^{(\omega t - \gamma x)}$ appears as the "backward-traveling" wave. The voltage drop across the load is

$$\widetilde{V}_R = Z_L \widetilde{I}_R. \quad (2.1.83)$$

Keeping in view that the origin of the distance ($x = 0$) is at the load, the line voltage and current at the load end are written, from equation (2.1.79), as follows:

$$\widetilde{V}_R = \widetilde{V}(x=0) = V^+ + V^- \quad (a)$$

$$\widetilde{I}_R = \widetilde{I}(x=0) = \frac{1}{Z_0}(V^+ - V^-) \quad (b). \quad (2.1.84)$$

The *voltage reflection coefficient* at the load end is defined as follows:

$$\Gamma_L = \frac{\text{Amplitude of reflected voltage}}{\text{Amplitude of forward(incident)voltage}} = \frac{V^-}{V^+}.$$

(2.1.85)

The expression to compute the reflection coefficient at the load end is obtained from the above equations (2.1.83) – (2.1.85): equations:

$$1 + \Gamma_L = \frac{Z_L}{Z_0}(1 - \Gamma_L) \quad (a)$$

$$\Rightarrow \Gamma_L = \frac{Z_L - Z_0}{Z_L + Z_0} \quad (b). \quad (2.1.86)$$

The mismatch of a load impedance Z_L with the characteristic impedance Z_0 of a line is the cause of the reflection at the load end. For the condition $Z_L = Z_0$, the matched load terminated line avoids the reflection on a line, as $\Gamma_L = 0$. At any distance x, the reflection coefficient is a complex quantity with both the magnitude and phase expressed as follows:

$$\Gamma(x) = |\Gamma(x)|e^{j\phi} = \Gamma_r(x) + j\Gamma_i(x) \quad (a)$$

$$|\Gamma(x)| = \sqrt{(\Gamma_r(x))^2 + (\Gamma_i(x))^2}$$

$$\phi = \tan^{-1}(\Gamma_i(x)/\Gamma_r(x)) \quad (b). \quad (2.1.87)$$

A lossless line has $|\Gamma(x)| = |\Gamma_L|$, i.e. on a lossless line magnitude of the reflection is the same at all locations

on a line. However, the lagging phase ϕ changes with distance. It has 180° periodicity, i.e. for an inductive load, the range of phase is $0 < \phi < \pi$, and a capacitive load has the phase in the range $-\pi < \phi < 0$. Using equation (2.1.79), the line voltage and line current are written in term of the load reflection coefficient:

$$\widetilde{V}(x) = V^+ e^{-\gamma x}\left[1 + \Gamma_L e^{2\gamma x}\right] \quad (a)$$

$$\widetilde{I}(x) = \frac{V^+ e^{-\gamma x}}{Z_0}\left[1 - \Gamma_L e^{2\gamma x}\right] \quad (b). \quad (2.1.88)$$

For a lossless transmission line, the above equations are written as follows:

$$\widetilde{V}(x) = |V^+|\left[1 + |\Gamma_L| e^{j(\phi + 2\beta x)}\right] \quad (a)$$

$$\widetilde{I}(x) = \frac{|V^+|}{Z_0}\left[1 - |\Gamma_L| e^{j(\phi + 2\beta x)}\right] \quad (b). \quad (2.1.89)$$

In the above equations, the origin is at the load end, i.e. $x < 0$. The maxima and minima of the voltage and current waves along the line occur due to the phase variation along the line. The voltage maximum occurs at $e^{j(\phi + 2\beta x)} = +1$. In this case, both the forward and reflected waves are in-phase. The voltage minimum occurs at $e^{j(\phi + 2\beta x)} = -1$. In this case, both the forward and reflected waves are out of phase. Finally, the maxima and minima of the voltage on a line are given as follows:

$$\widetilde{V}_{max}(x) = |V^+|[1 + |\Gamma_L|] \quad (a)$$

$$\widetilde{V}_{min}(x) = |V^+|[1 - |\Gamma_L|] \quad (b). \quad (2.1.90)$$

The reflection coefficient $\Gamma(x)$ at any location x from the load end is related to the reflection coefficient at the load Γ_L by

$$\text{For a lossy line}: \quad \Gamma(x) = \Gamma_L e^{2\gamma x} \quad (a)$$

$$\text{for a lossless line}: \quad \Gamma(x) = \Gamma_L e^{j2\beta x} \quad (b). \quad (2.1.91)$$

The measurable quantity *voltage standing wave ratio* (VSWR) is defined as follows:

$$S = VSWR = \frac{\widetilde{V}_{max}(x)}{\widetilde{V}_{min}(x)} = \frac{1 + |\Gamma(x)|}{1 - |\Gamma(x)|}. \quad (2.1.92)$$

For a lossless line, the VSWR is constant along the length of a line. Likewise, the current standing wave ratio is also defined.

The wave reflection also takes place at the sending end when the source impedance Z_g is not matched to the characteristic impedance of a line. The reflection coefficient at $x = -\ell$, i.e. at the generator (source) end is defined as $\Gamma(x = -\ell) = \Gamma_g$. The voltage and current at the generator end are obtained from equation (2.1.88),

$$\widetilde{V}_s(x) = \widetilde{V}(x = -\ell) = V^+ e^{+\gamma l}\left[1 + \Gamma_L e^{-2\gamma\ell}\right] \quad (a)$$

$$\widetilde{I}_s(x) = \widetilde{I}(x = -\ell) = \frac{V^+ e^{+\gamma l}}{Z_0}\left[1 - \Gamma_L e^{-2\gamma\ell}\right] \quad (b). \quad (2.1.93)$$

The amplitude factor V^+ is determined by the reflections at both the source and load ends.

Figure (2.8b) shows that the port voltage $\widetilde{V}_s$ and the line current $\widetilde{I}_s$, at the input port – aa, are related to the source voltage $\widetilde{V}_g$ and its internal impedance Z_g by

$$\widetilde{I}_s = \frac{\widetilde{V}_g - \widetilde{V}_s}{Z_g}. \quad (2.1.94)$$

On substitution of equation (2.1.93) in (2.1.94), the voltage wave amplitude V^+ is obtained as follows:

$$V^+\left\{(Z_g + Z_0)e^{+\gamma l} - (Z_g - Z_0)e^{-\gamma l}\Gamma_L\right\} = Z_0\widetilde{V}_g. \quad (2.1.95)$$

However, the reflection coefficient at the source end is

$$\Gamma_g = \frac{Z_g - Z_0}{Z_g + Z_0}. \quad (2.1.96)$$

Therefore, the amplitude of the voltage wave launched by the source is

$$V^+ = \widetilde{V}_g \frac{Z_0 e^{-\gamma\ell}}{(Z_g + Z_0)\left[1 - \Gamma_g\Gamma_L e^{-2\gamma\ell}\right]}. \quad (2.1.97)$$

Equation (2.1.88a and b) give the voltage and current waves on a transmission line with the amplitude factor V^+. The amplitude factor V^+ is given by equation (2.1.97).

2.1.8 Application of Thevenin's Theorem to Transmission Line

Thevenin's theorem is a very popular concept used in the analysis of the low-frequency lumped element circuits. It is equally applicable to a transmission line network. At the output end of the line, the input source voltage $\widetilde{V}_g$ and the line section are replaced by the equivalent Thevenin's voltage, $\widetilde{V}_{TH}(x = 0)$ with internal impedance, i.e. the Thevenin's impedance Z_{TH} [B.12]. Figure (2.8d) shows it. The distance is measured from the load end. *Thevenin's voltage* is an open-circuit voltage at the load end. In the case of the open-circuited load, $Z_L \to \infty$, equation (2.1.86) provides a reflection coefficient $\Gamma_L = 1$. Thevenin's voltage is obtained from equations (2.1.88a) and (2.1.97):

$$\widetilde{V}_{TH}(x=0)=\frac{2\widetilde{V}_g Z_o e^{-\gamma\ell}}{(Z_g+Z_o)\left[1-\Gamma_g e^{-2\gamma\ell}\right]}. \quad (2.1.98)$$

On replacing Γ_g from equation (2.1.96), Thevenin's voltage is

$$\widetilde{V}_{TH}(x=0)=\frac{\widetilde{V}_g Z_o}{\left[\,Z_o\cosh(\gamma\ell)+Z_g\sinh(\gamma\ell)\right]}. \quad (2.1.99)$$

Thevenin's impedance Z_{TH} is obtained from equation (2.1.88b) by computing *Norton current*, i.e. the short-circuit current at $x=0$. Under the short-circuited load condition at $x=0$, $\Gamma_L=-1$, and the Norton current is

$$\widetilde{I}_N(x=0)=\frac{2\widetilde{V}_g e^{-\gamma\ell}}{(Z_g+Z_o)\left[1+\Gamma_g e^{-2\gamma\ell}\right]}. \quad (2.1.100)$$

Thevenin's impedance is obtained as follows:

$$Z_{TH}=\frac{\widetilde{V}_{TH}}{\widetilde{I}_N},\ \Rightarrow Z_{TH}=Z_0\frac{1+\Gamma_g e^{-2\gamma\ell}}{1-\Gamma_g e^{-2\gamma\ell}}. \quad (2.1.101)$$

Transfer Function

The transmission line section could be treated as a circuit element. Its transfer function is obtained either with respect to the source voltage V_g or with respect to the input voltage V_s at the port- aa, as shown in Fig (2.8a). The load current is obtained from Fig (2.8d):

$$\widetilde{I}_L=\frac{\widetilde{V}_{TH}}{(Z_{TH}+Z_L)}. \quad (2.1.102)$$

The voltage across the load is

$$\widetilde{V}_R=Z_L\widetilde{I}_L=\frac{2Z_0Z_L\widetilde{V}_g}{(Z_{TH}+Z_L)(Z_g+Z_0)}\left[\frac{e^{-\gamma\ell}}{1-\Gamma_g e^{-2\gamma\ell}}\right]. \quad (2.1.103)$$

The transfer function of a transmission line with respect to the source voltage $\widetilde{V}_g$ is

$$H(\omega)=\frac{\widetilde{V}_R}{\widetilde{V}_g}=\frac{2Z_0Z_L}{(Z_{TH}+Z_L)(Z_g+Z_0)}\left[\frac{e^{-\gamma\ell}}{1-\Gamma_g e^{-2\gamma\ell}}\right]. \quad (2.1.104)$$

For a lossless transmission line connected to a matched source and a matched load, i.e. $\gamma\ell=j\beta\ell$, $Z_g=Z_0$, $Z_{TH}=Z_0$, $Z_L=Z_0$, $\Gamma_g=0$ the transfer function is

$$H(\omega)=\frac{e^{-\gamma\ell}}{2}. \quad (2.1.105)$$

However, if the transfer function is defined by the ratio of the input voltage $\widetilde{V}_s$ at the port – aa to the output voltage $\widetilde{V}_R$, $H(\omega)=e^{-\gamma\ell}$. It is obtained from equation (2.1.104) for $Z_g=0$.

2.1.9 Power Relation on Transmission Line

The average power over a time-period T in any time-harmonic periodic signal is [J.5, B.10]

$$P_{av}=\frac{1}{T}\int_0^T v(t)\cdot i(t)dt. \quad (2.1.106)$$

where the time-harmonic instantaneous voltage and current waveforms are

$$v(t)=V_0\cos(\omega t+\phi) \quad (a)$$
$$i(t)=I_0\cos(\omega t+\phi') \quad (b). \quad (2.1.107)$$

The voltage and current in the phasor form are written as follows:

$$\widetilde{V}=V_0e^{j\phi} \quad (a), \quad \widetilde{I}=I_0e^{j\phi'} \quad (b). \quad (2.1.108)$$

A complex number $X=a+jb$ has its complex conjugate, $X^*=a-jb$. Thus, the real (Re) and imaginary (Im) parts of a complex number are written as follows:

$$Re(X)=\frac{1}{2}(X+X^*) \quad (a)$$
$$Im(X)=\frac{1}{2}(X-X^*) \quad (b). \quad (2.1.109)$$

On using the above property, the instantaneous voltage and current are written as follows:

$$v(t)=\frac{1}{2}\left(\widetilde{V}e^{j\omega t}+\widetilde{V}^*e^{-j\omega t}\right) \quad (a)$$
$$i(t)=\frac{1}{2}\left(\widetilde{I}e^{j\omega t}+\widetilde{I}^*e^{-j\omega t}\right) \quad (b). \quad (2.1.110)$$

The average power in phasor form is obtained from equations (2.1.106) and (2.1.110),

$$P_{av}=\frac{1}{2}\,Re\left[\widetilde{V}\widetilde{I}^*\right]. \quad (2.1.111)$$

It can be expressed in the usual AC form,

$$P_{av}=\frac{1}{2}\,Re\left[V_0e^{j\phi}\cdot I_0^*e^{-j\phi'}\right]=\frac{1}{2}V_0I_0^*\cos(\phi-\phi'). \quad (2.1.112)$$

Available Power from Generator

Figure (2.9a) shows that the maximum available power from a source is computed by directly connecting the load to it. The average power supplied to the load is

$$P_{av} = \frac{1}{2}\,\mathrm{Re}\left[V_L \cdot I^*\right] = \frac{1}{2}\,\mathrm{Re}\left[|I|^2 Z_L\right] = \frac{1}{2}|I|^2 R_L. \tag{2.1.113}$$

The load current is

$$I = \frac{\tilde{V}_g}{Z_g + Z_L} = \frac{\tilde{V}_g}{(R_g + R_L) + j(X_g + X_L)}$$

$$\Rightarrow |I|^2 = \frac{\left|\tilde{V}_g\right|^2}{(R_g + R_L)^2 + (X_g + X_L)^2}.$$

Therefore, the average power supplied to the load is

$$P_{av} = \frac{1}{2}\left[\frac{\left|\tilde{V}_g\right|^2 R_L}{(R_g + R_L)^2 + (X_g + X_L)^2}\right]. \tag{2.1.114}$$

Under the *conjugate matching*, $X_L = -X_g$ and $R_L = R_g$, the average power supplied to load is maximum:

$$P_{av} = \frac{1}{8}\frac{\left|\tilde{V}_g\right|^2}{R_g}. \tag{2.1.115}$$

This is the maximum power available from a generator under the matching condition and delivered to a load R_L. At this stage, the maximum power delivered to a load is computed in the absence of the transmission line. For a matched terminated lossless line, the maximum available power from the source is delivered to the load. It is examined below.

The voltage and current waves on a line under no reflection case are

$$\tilde{V}(x) = \tilde{V}_S e^{-j\beta x} \quad (a), \quad \tilde{I}(x) = \frac{\tilde{V}_S e^{-j\beta x}}{Z_0} \quad (b). \tag{2.1.116}$$

The average power on the line is

$$P_{av} = \frac{1}{2}\,\mathrm{Re}\left[\tilde{V}(x)\tilde{I}^*(x)\right] = \frac{1}{2}\,\mathrm{Re}\left[\tilde{V}_S e^{-j\beta x}\frac{\tilde{V}_S^*}{Z_0}e^{j\beta x}\right] = \frac{\left|\tilde{V}_S\right|^2}{2Z_0}. \tag{2.1.117}$$

On a lossless line, the average power is independent of the distance x from a source. Physically it makes a sense, as the same amount of power flows at any location on the line. Under the matched load termination, $Z_L = Z_0$, the input impedance at the source end is Z_0 itself. It is shown in Fig (2.9b). The sending end voltage at the input port – aa of a transmission line is

$$\left|\tilde{V}_S\right| = \left|\frac{\tilde{V}_g Z_0}{Z_g + Z_0}\right|. \tag{2.1.118}$$

The maximum power is transferred from a generator to the transmission line under the matching condition, $R_g = Z_0$. The maximum available power from the generator to feed the line is given by equation (2.1.115). It is identical to the power determined from equation (2.1.117), as $\tilde{V}_s = \tilde{V}_g/2$.

If the line is not terminated in its characteristic impedance, then a reflection takes place at the load end. The reflected wave travels from the load toward the generator given by

$$\tilde{V}(x) = V^- e^{+j\beta x} \quad (a), \quad \tilde{I}(x) = -\frac{V^- e^{+j\beta x}}{Z_0} \quad (b). \tag{2.1.119}$$

The average power in the reflected wave is

$$P_{av} = \frac{1}{2}\,\mathrm{Re}\left[\tilde{V}(x)\tilde{I}^*(x)\right] = -\frac{|V^-|^2}{2Z_0}. \tag{2.1.120}$$

However, at the load end amplitude of the reflected voltage wave is $V^- = \Gamma_L V^+$; where $V^+ = \tilde{V}_s$. Therefore, the average reflected power on the line is

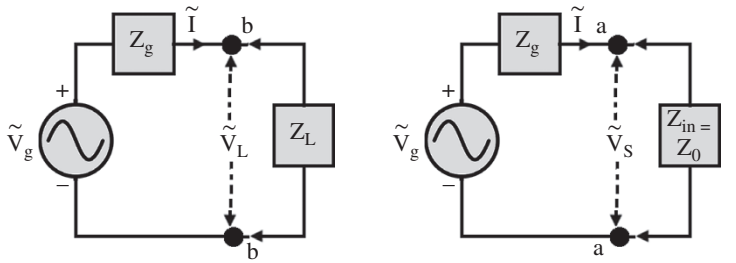

(a) Load directly connected to a source. (b) Line terminated in a matched load.

Figure 2.9 Load connections to a source.

$$P_{av} = -\frac{|\Gamma_L|^2 |V^+|^2}{2Z_0} = -\frac{|\Gamma_L|^2 \tilde{V}_s^2}{2Z_0}. \qquad (2.1.121)$$

The negative sign (−) shows that the reflected power travels from the load toward the source. Finally, under the mismatched load, the power delivered to the load is obtained from equations (2.1.117) and (2.1.121)

$$P_L = \frac{\tilde{V}_S^2}{2Z_0}\left(1 - |\Gamma_L|^2\right). \qquad (2.1.122)$$

For a lossless line, the power balance is written as follows:

$$P_{in} = \frac{1}{2Z_0}\left|\tilde{V}_s\right|^2\left[1 - |\Gamma_L|^2\right] = P_{out}. \qquad (2.1.123)$$

$$\downarrow \quad \downarrow$$

Incident power Reflected power

In equation (2.1.123), input power P_{in} at the input port – aa of the line enters into the line. It is supplied by a source. The output power P_{out} is the power supplied to the load.

2.2 Multisection Transmission Lines and Source Excitation

This section extends the solution of the voltage wave equation to the multisection transmission line [B.8, B.16]. Next, the voltage responses are obtained for the shunt connected current source, and also the series-connected voltage source, at any location on a line. This treatment is used in chapters 14 and 16 for the *spectral domain analysis* of the multilayer planar transmission lines.

2.2.1 Multisection Transmission Lines

Figure (2.10a) shows a multisection transmission line, consisting of the N number of line sections. Each line section has different lengths (d_1, d_2,...,d_N), different

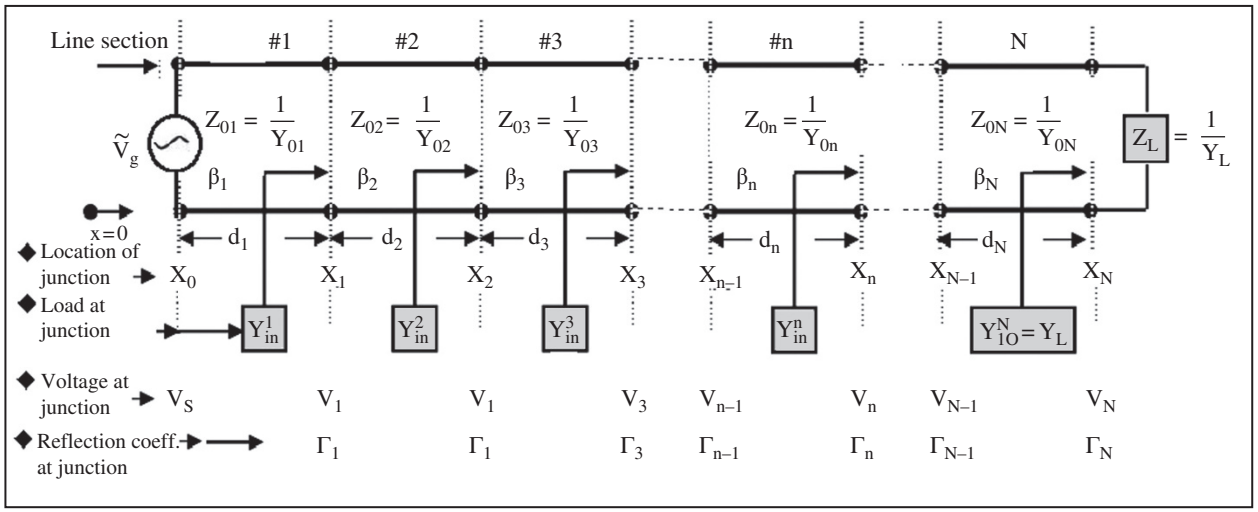

(a) Analysis of multi-section line structure.

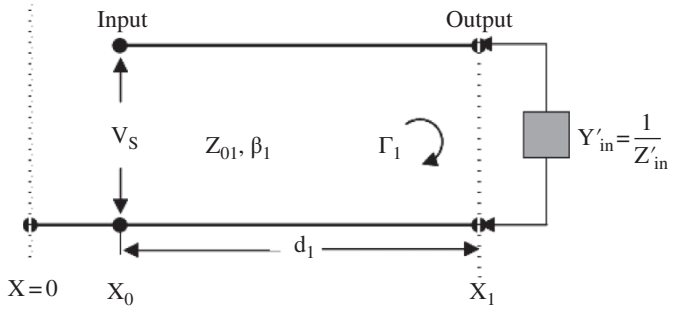

(b) Isolated first line section.

Figure 2.10 The multisection transmission line.

characteristic impedances (Z_{01}, Z_{02},...,Z_{0N}), or different characteristic admittances (Y_{01}, Y_{02},...,Y_{0N}) and different propagation constants (β_1, β_2, ..., β_N). At each junction of two dissimilar lines, the voltage wave reflection occurs with the reflection coefficient $\Gamma_1, \Gamma_2, ..., \Gamma_N$. At each junction, the input admittance of all succeeding line sections appears as a load. The input admittances at junctions (x_1, x_2, ..., x_N) are $\left(Y_{in}^1, Y_{in}^2, ..., Y_{in}^N\right)$. The distances of the junctions are measured from the origin that is located on the left-hand side. The input terminals of line sections 1,2,..., $N-1$ are located at the junctions (x_0, x_1, x_2,...,x_N). The voltage source V_s is located at the input of the first line section. The last line section is terminated in the load $Z_L = 1/Y_L$.

The objective is to find the voltage at each junction of the multisection line. Further, the voltage distribution on each line section is determined due to the input voltage $\widetilde{V}_s$.

The solutions for the voltage and current wave equations involve four constants. The constants of the current wave are related to two constants of the voltage wave through the characteristic impedance of a line. Out of two constants of the voltage wave, one is expressed in terms of the reflection coefficient at the load end; that itself is expressed by the characteristic impedance and the terminated load impedance. The reflection coefficient can also be expressed by the characteristic admittance and the terminated load admittance. The second constant is evaluated by the source condition at the input end. Figure (2.10b) shows the first isolated line section. The voltage and current waves, with respect to the origin at the load end x_1, on the line section ($x_0 \le x \le x_1$) are written from equation (2.1.88):

$$\widetilde{V}(x) = V^+\left[e^{-j\beta_1(x-x_1)} + \Gamma_1 e^{j\beta_1(x-x_1)}\right] \quad (a)$$

$$\widetilde{I}(x) = \frac{V^+}{Z_{01}}\left[e^{-j\beta_1(x-x_1)} - \Gamma_1 e^{j(x-x_1)}\right], (x_0 \le x \le x_1) \quad (b). \tag{2.2.1}$$

The reflection coefficient Γ_1 at the load end, i.e. at $x = x_1$ is given by

$$\Gamma_1 = \frac{Z_{in}^1 - Z_{01}}{Z_{in}^1 + Z_{01}} = \frac{Y_{01} - Y_{in}^1}{Y_{01} + Y_{in}^1}. \tag{2.2.2}$$

The load at the $x = x_1$ end is formed by the cascaded line sections after location $x = x_1$. The voltage amplitude V^+ is evaluated by the boundary condition at the input, $x = x_0$, of the first line section. At $x = x_0$, shown in Fig (2.10b), the source voltage $\widetilde{V}(x_0)$ is $\widetilde{V}_s$ and V^+ is evaluated as follows:

$$\widetilde{V}(x_0) = \widetilde{V}_S = V^+\left[e^{-j\beta_1(x_0-x_1)} + \Gamma_1 e^{j\beta_1(x_0-x_1)}\right]$$

$$\Rightarrow V^+ = \frac{\widetilde{V}_S}{e^{-j\beta_1(x_0-x_1)} + \Gamma_1 e^{j\beta_1(x_0-x_1)}}. \tag{2.2.3}$$

The voltage wave on the transmission line section #1 is

$$\widetilde{V}_1(x) = \frac{\widetilde{V}_S\left[e^{-j\beta_1(x-x_1)} + \Gamma_1 e^{j\beta_1(x-x_1)}\right]}{e^{-j\beta_1(x_0-x_1)} + \Gamma_1 e^{j\beta_1(x_0-x_1)}}. \tag{2.2.4}$$

The above expression is valid over the range $x_0 \le x \le x_1$. The voltage at the output of the line section #1 ($x = x_1$), that is at the junction of line #1 and line #2, is

$$\widetilde{V}_1(x_1) = \frac{\widetilde{V}_S[1+\Gamma_1]}{e^{-j\beta_1(x_0-x_1)} + \Gamma_1 e^{j\beta_1(x_0-x_1)}} = \frac{\widetilde{V}_S[1+\Gamma_1]}{e^{+j\beta_1 d_1} + \Gamma_1 e^{-j\beta_1 d_1}}, \tag{2.2.5}$$

where $d_1 = x_1 - x_0$ is the length of the line section #1. The above voltage is input to the line section #2. Equations (2.2.4) and (2.2.5) apply to any line section and at any junction. The voltage $\widetilde{V}_{n-1}(x_{n-1})$ is treated as the input voltage of the n^{th} line section. It is the same as the output voltage of the $(n-1)^{th}$ line section. The line length d_1 and reflection coefficient Γ_1 are replaced by d_n and Γ_n, respectively. The cascaded line sections to the right-hand side of any junction act as a load at the junction and the reflection coefficient at the junction is

At load end of the line section#1 :

$$\Gamma_1 = \frac{Y_{01} - Y_{in}^1}{Y_{01} + Y_{in}^1} \quad (a)$$

At load end of the line section#n :

$$\Gamma_n = \frac{Y_{0n} - Y_{in}^n}{Y_{0n} + Y_{in}^n} \quad (b)$$

Length of the line section#n :

$$d_n = x_n - x_{n-1}, \quad (n = 1, 2, ...N) \quad (c). \tag{2.2.6}$$

Equation (2.2.4) is applied to Fig (2.10a) to compute the voltage distribution on any line section. The voltage on line section #2 is

$$\widetilde{V}_2(x) = \frac{\widetilde{V}_1\left[e^{-j\beta_2(x-x_2)} + \Gamma_2 e^{j\beta_2(x-x_2)}\right]}{e^{-j\beta_2(x_1-x_2)} + \Gamma_2 e^{j\beta_2(x_1-x_2)}}, x_1 \le x \le x_2. \tag{2.2.7}$$

The voltage at the output of the line section #2, i.e. the junction voltage of the line sections #2 and # 3 at $x = x_2$, is obtained from the above equation:

$$\widetilde{V}_2(x_2) = \frac{\widetilde{V}_1[1+\Gamma_2]}{e^{+j\beta_2 d_2} + \Gamma_2 e^{-j\beta_2 d_2}}. \tag{2.2.8}$$

Using equation (2.2.5) and above equations, the voltage distribution on the line section #2, and also the junction voltage at $x = x_2$, are obtained:

$$\widetilde{V}_2(x) = \frac{\widetilde{V}_S[1+\Gamma_1]}{e^{+j\beta_1 d_1} + \Gamma_1 e^{-j\beta_1 d_1}} \left\{ \frac{e^{-j\beta_2(x-x_2)} + \Gamma_2 e^{j\beta_2(x-x_2)}}{e^{+j\beta_2 d_2} + \Gamma_2 e^{-j\beta_2 d_2}} \right\}. \tag{2.2.9}$$

$$\widetilde{V}_2(x_2) = \frac{\widetilde{V}_S[1+\Gamma_1]}{e^{+j\beta_1 d_1} + \Gamma_1 e^{-j\beta_1 d_1}} \left\{ \frac{1+\Gamma_2}{e^{+j\beta_2 d_2} + \Gamma_2 e^{-j\beta_2 d_2}} \right\}. \tag{2.2.10}$$

Finally, the voltage distribution on the n^{th} line section and the voltage at the n^{th} line junction can be written as follows:

$$\widetilde{V}_n(x) = \left[\prod_{n=1}^{N} \left\{ \frac{V_S(1+\Gamma_{n-1})}{e^{j\beta_{n-1}d_{n-1}} + \Gamma_{n-1} e^{-j\beta_{n-1}d_{n-1}}} \right\} \right] \left\{ \frac{e^{-j\beta_n(x-x_n)} + \Gamma_n e^{j\beta_n(x-x_n)}}{e^{+j\beta_n d_n} + \Gamma_n e^{-j\beta_n d_n}} \right\} \tag{2.2.11}$$

$$\widetilde{V}_n(x_n) = \left[\prod_{n=1}^{N} \left\{ \frac{V_S(1+\Gamma_n)}{e^{jd_n\beta_n} + \Gamma_n e^{-jd_n\beta_n}} \right\} \right]. \tag{2.2.12}$$

2.2.2 Location of Sources

The shunt voltage $\widetilde{V}_s$ could be located at any junction and the voltage distribution is computed on any line section due to it. However, it is also interesting to consider a *shunt current source* and a *series voltage source* located anywhere on a multisection transmission line. Both kinds of sources create the voltage wave on a line.

Current Source at the Junction of Finite Length Line and Infinite Length Line

Figure (2.11a) shows a transmission line circuit with a current source I_S located at $x = 0$ that is the junction of two lines of different electrical characteristics. The open-circuited line #1, with length $x = -d_1$, is located at the left-hand side of the current source. Its characteristics impedance/admittance is (Z_{01}/Y_{01}) and its propagation constant is β_1. The infinite length line #2, with

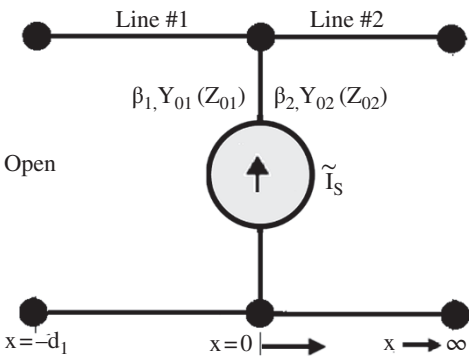

(a) Transmission line circuit with a shunt current source.

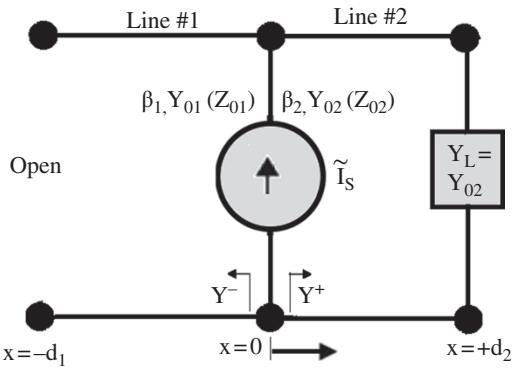

(b) Equivalent circuit.

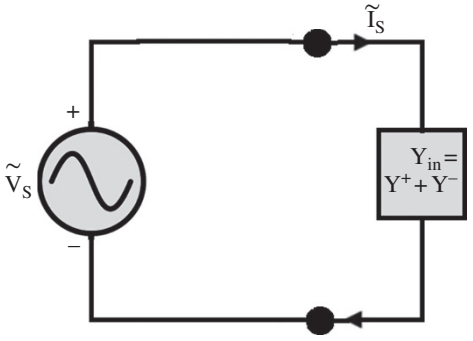

(c) Replacement of shunt current source by the equivalent voltage source.

Figure 2.11 A shunt current source at the junction of two-line sections.

characteristics impedance/admittance (Z_{02}/Y_{02}) and the propagation constant β_2, is located at the right-hand side of the current source. It can be replaced by a load admittance $Y_L = Y_{02}$ at a distance $x = d_2$, shown in Fig (2.11b). The objective is to find out the voltage waves on both the lines as excited by the current source.

The current source I_S can be replaced by an equivalent voltage source V_s, shown in Fig (2.11c), at $x = 0$:

$$\widetilde{V}_S = \frac{I_S}{Y_{in}} = \frac{I_S}{Y^- + Y^+}, \tag{2.2.13}$$

where Y_{in} is the total load admittance at the plane containing the current source I_S. Y^- and Y^+ are left-hand and right-hand side admittances at $x = 0$ given by

$$\begin{aligned} Y^- &= Y_{01}\tanh(\gamma_1 d_1) \\ &= jY_{01}\tan\beta_1 d_1 (\text{For a losslessline}), \quad Y^+ = Y_{02}. \end{aligned} \tag{2.2.14}$$

The general solution of a voltage wave is given by equation (2.1.79a). The constants V^+ and V^- are evaluated for the left-hand side of a lossless transmission line. At $x = 0$, $V(x = 0) = V_s$. On using this boundary condition in equation (2.1.79a): $V_S = V^+ + V^-$. At $x = -d_1$ the line is open-circuited with $I(x = -d_1) = 0$. On using this boundary condition in equation (2.1.79b): $V^+ e^{j\beta_1 d_1} - V^- e^{-j\beta_1 d_1} = 0$. The constants V^+ and V^-, from these two equations, are obtained as

$$V^+ = \frac{\widetilde{V}_S}{1 + e^{j2\beta_1 d_1}} \quad (a), \quad V^- = V^+ e^{j2\beta_1 d_1} \quad (b). \tag{2.2.15}$$

The voltage wave on the left-hand line #1 is obtained by substituting equation (2.2.15) in equation (2.1.79a):

$$\widetilde{V}(x) = \frac{\widetilde{V}_S}{\cos(\beta_1 d_1)}\cos[\beta_1(x + d_1)], \quad -d_1 \le x \le 0. \tag{2.2.16}$$

The line at the right-hand side of the current source is an infinite length line that supports a traveling wave without any reflection. Therefore, at $x = 0$, $V^- = 0$ and $V^+ = V_S$. The voltage wave on line #2 at the right-hand side is

$$\widetilde{V}(x) = \widetilde{V}_S e^{-j\beta_2 x}, \quad x \ge 0. \tag{2.2.17}$$

The method can be easily extended to a multisection line structure. For this purpose, the left-hand and right-hand side admittances Y^- and Y^+ are determined at the plane containing the current source.

Series Voltage Source

Figure (2.12a) shows the series-connected voltage source V_S at $x = 0$. The location $x = 0$ is a junction of two transmission lines – line #1 open-circuited finite-length line and line #2 infinite length line. The lines at the left-hand and right-hand sides of the voltage source can be replaced by the equivalent impedances Z^- and Z^+, respectively. It is shown in the equivalent circuit, Fig (2.12b). Again, the voltage waves on both lines, excited by a series voltage source, could be determined.

The voltages across loads Z^- (Z_1) and Z^+ (Z_2), shown in Fig (2.12b), are obtained as follows:

$$\begin{aligned} &\text{Line current}: \quad \widetilde{I} = \frac{\widetilde{V}_S}{Z^- + Z^+} && (a) \\ &\text{Voltage across } Z_1: \quad \widetilde{V}(x = 0^-) = -\frac{\widetilde{V}_S Z_1}{Z_1 + Z_2} && (b) \\ &\text{Voltage across } Z_2: \quad \widetilde{V}(x = 0^+) = \frac{\widetilde{V}_S Z_2}{Z_1 + Z_2} && (c). \end{aligned} \tag{2.2.18}$$

Line #1 is open-circuited and line #2 is of infinite extent. Therefore, their input impedances at $x = 0^-$ and $x = 0^+$ are

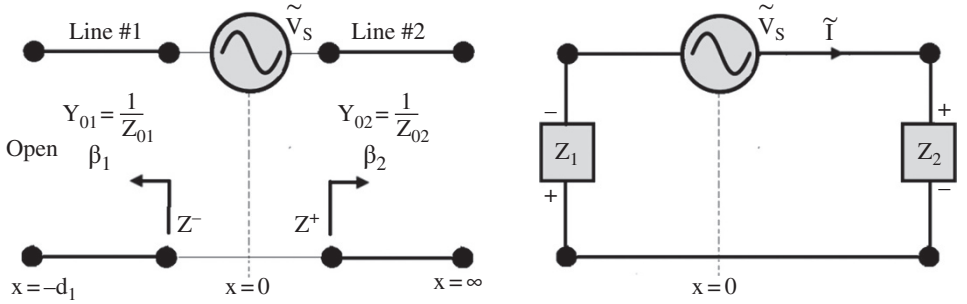

(a) Transmission line circuit with a series voltage source.

(b) Equivalent circuit.

Figure 2.12 A series voltage source at the junction of two-line sections.

$$Z_1 = -jZ_{01}\cot(\beta_1 d_1) \quad (a), \quad Z_2 = Z_{02} \quad (b). \tag{2.2.19}$$

The voltage at $x = 0^+$ from equations (2.2.18c) and (2.2.19) is

$$\widetilde{V}(x=0^+) = \widetilde{V}_S \frac{1}{Y_{02}} \times \frac{1}{\left[\frac{1}{jY_{01}\tan(\beta_1 d_1)} + \frac{1}{Y_{02}}\right]}$$
$$= \widetilde{V}_S \frac{jY_{01}\tan(\beta_1 d_1)}{Y_{02} + jY_{01}\tan(\beta_1 d_1)}. \tag{2.2.20}$$

For a lossy transmission line, the above equation could be written as follows:

$$\widetilde{V}(x=0^+) = \widetilde{V}_S \frac{Y_{01}\tanh(\gamma_1 d_1)}{Y_{02} + Y_{01}\tanh(\gamma_1 d_1)}. \tag{2.1.21}$$

The voltage wave on the infinite extent lossy line #2 is

$$\widetilde{V}(x) = \widetilde{V}(x=0^+)e^{-\gamma_2 x}$$
$$= \widetilde{V}_S \frac{Y_{01}\tanh(\gamma_1 d_1)}{Y_{02} + Y_{01}\tanh(\gamma_1 d_1)} e^{-\gamma_2 x}, \quad x \geq 0. \tag{2.2.22}$$

The voltage at $x = 0^-$ on the lossless line #1 is

$$\widetilde{V}(x=0^-) = -\widetilde{V}_S \frac{Y_{02}}{Y_{02} + jY_{01}\tan(\beta_1 d_1)}. \tag{2.2.23}$$

However, the voltage at $x = 0^-$ on a lossy line #1 is

$$\widetilde{V}(x=0^-) = -\widetilde{V}_S \frac{Y_{02}}{Y_{02} + Y_{01}\tanh(\gamma_1 d_1)}. \tag{2.2.24}$$

The voltage wave on the open-circuited lossless line #1 is obtained from equations (2.2.16) and (2.2.23):

$$\widetilde{V}(x) = \frac{V(x=0^-)}{\cos(\beta_1 d_1)}\cos[\beta_1(x+d_1)]$$
$$\Rightarrow \widetilde{V}(x) = -\widetilde{V}_S \frac{Y_{02}}{Y_{02} + jY_{01}\tan(\beta_1 d_1)}$$
$$\times \frac{\cos[\beta_1(x+d_1)]}{\cos(\beta_1 d_1)}, \quad -d_1 \leq x \leq 0. \tag{2.2.25}$$

2.3 Nonuniform Transmission Lines

The previous sections have presented the voltage and current waves on the uniform transmission line that has no change in the geometry along the direction of propagation. For a uniform line, the relative permittivity and relative permeability also do not change along the line. For such a uniform lossless or low-loss transmission line, the voltage and current waves travel at a definite velocity from low frequency to high frequency. The uniform transmission line behaves as a low-pass filter (LPF) section. The propagation constant for such a uniform transmission line is the same at any section of the line. The line also has a unique characteristic impedance that is independent of the location on a line. However, if the geometry of a transmission line or an electrical property of the medium of a line changes in the direction of propagation, such a line is no longer a uniform transmission line. It is a *nonuniform transmission line*. Its electrical properties, such as the RLCG primary constants, propagation constant, phase velocity, and characteristic impedance, become a function of the space coordinate along the direction of propagation. The characteristic impedance of a nonuniform transmission line changes from one end to another end; therefore, it finds application in the broadband impedance matching [B.9, B.10, B.12]. It is also used for the design of delay equalizers, filters, wave-shaping circuits, etc. [J.6–J.9]. It is an essential section of the on-chip measurement system [J.10]. *Unlike a uniform transmission line, it shows a cut-off phenomenon, i.e. the wave propagates on the line only above the cut-off frequency*. Below the cut-off frequency, the wave only attenuates with distance. Thus, the nonuniform transmission line behaves like a high-pass filter (HPF) section [J.11–J.13, B.17].

The present section obtains the wave equations for a nonuniform transmission line. However, like the uniform transmission lines, the nonuniform transmission lines do not have closed-form solutions for the voltage and current waves. The numerical methods have been used to determine the response of an arbitrarily shaped nonuniform transmission line [J.10, J.11]. However, this section discusses only the *exponential nonuniform transmission line* to understand its characteristics.

2.3.1 Wave Equation for Nonuniform Transmission Line

Figure (2.13) shows a nonuniform transmission line. The line parameters (primary line constants) R(x), L(x), C(x), G(x) are distance-dependent. It results in the distance-dependent characteristic impedance, $Z_0(x)$, and propagation constant, $\gamma(x)$. Using equation (2.1.20), the voltage and current equations for a nonuniform transmission line are written as follows:

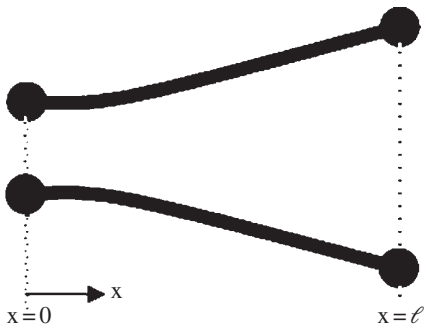

Figure 2.13 Nonuniform transmission line.

$$\frac{\partial v}{\partial x} = -\left(R(x)i + L(x)\frac{\partial i}{\partial t}\right) \quad (a)$$
$$\frac{\partial i}{\partial x} = -\left(G(x)v + C(x)\frac{\partial v}{\partial t}\right) \quad (b). \quad (2.3.1)$$

The following expressions are obtained on differentiating equation (2.3.1a) with x and equation (2.3.1b) with t:

$$\frac{\partial^2 v}{\partial x^2} = -\left(R(x)\frac{\partial i}{\partial x} + i\frac{\partial R(x)}{\partial x} + L(x)\frac{\partial^2 i}{\partial x \partial t} + \frac{\partial i}{\partial t}\frac{\partial L(x)}{\partial x}\right). \quad (2.3.2)$$

$$\frac{\partial^2 i}{\partial t \partial x} = -\left(G(x)\frac{\partial v}{\partial t} + C(x)\frac{\partial^2 v}{\partial t^2}\right). \quad (2.3.3)$$

On substituting equations (2.3.1b) and (2.3.3) in equation (2.3.2):

$$-\frac{\partial^2 v}{\partial x^2} = -R(x)\left(G(x)v + C(x)\frac{\partial v}{\partial t}\right) + i\frac{\partial R(x)}{\partial x} - L(x)\left(G(x)\frac{\partial v}{\partial t} + C(x)\frac{\partial^2 v}{\partial t^2}\right) + \frac{\partial i}{\partial t}\frac{\partial L(x)}{\partial x}. \quad (2.3.4)$$

This equation has both the voltage and current variables v(x, t) and i(x, t). However, most of the transmission lines are low-loss lines. Thus, using $R(x) \to 0$ $G(x) \to 0$ in equations (2.3.1a) and (2.3.4), the following *voltage wave equation* is obtained for a lossless nonuniform transmission line:

$$\frac{\partial^2 v}{\partial x^2} = L(x)C(x)\frac{\partial^2 v}{\partial t^2} + \left(\frac{1}{L(x)}\frac{\partial L(x)}{\partial x}\right)\frac{\partial v}{\partial x}. \quad (2.3.5)$$

Likewise, the *current wave equation* is obtained as,

$$\frac{\partial^2 i}{\partial x^2} = L(x)C(x)\frac{\partial^2 i}{\partial t^2} + \left(\frac{1}{C(x)}\frac{\partial C(x)}{\partial x}\right)\frac{\partial i}{\partial x}. \quad (2.3.6)$$

If L(x) and C(x) are not a function of x, then equations (2.3.5) and (2.3.6) reduce to the familiar wave equations (2.1.24) and (2.1.25) on a uniform transmission line.

For a lossy nonuniform transmission line, it is not possible to get separate voltage and current wave equations in the time domain. However, separate voltage and current wave equations can be obtained in the frequency domain by using the phasor form of voltage and current. The transmission line equations in the phasor form are

$$\frac{d\tilde{V}(x)}{dx} = -Z(x)\tilde{I}(x) \quad (a)$$
$$\frac{d\tilde{I}(x)}{dx} = -Y(x)\tilde{V}(x) \quad (b), \quad (2.3.7)$$

where the line series impedance and shunt admittance *p.u.l.* are given by

$$Z(x) = R(x) + j\omega L(x) \quad (a)$$
$$Y(x) = G(x) + j\omega C(x) \quad (b). \quad (2.3.8)$$

The following wave equations for the nonuniform transmission line are obtained:

$$\frac{d^2\tilde{V}(x)}{dx^2} - \left(\frac{1}{Z(x)}\frac{dZ(x)}{dx}\right)\frac{d\tilde{V}(x)}{dx} - Z(x)Y(x)\tilde{V}(x) = 0. \quad (2.3.9)$$

$$\frac{d^2\tilde{I}(x)}{dx^2} - \left(\frac{1}{Y(x)}\frac{dY(x)}{dx}\right)\frac{d\tilde{I}(x)}{dx} - Z(x)Y(x)\tilde{I}(x) = 0. \quad (2.3.10)$$

If Z(x) and Y(x) are not a function of x, the above wave equations reduce to wave equation (2.1.37a and b) for a uniform transmission line. For a lossless nonuniform line, the series impedance and shunt admittance per unit length are $Z(x) = j\omega L(x)$, $Y(x) = j\omega C(x)$. The voltage wave equation (2.3.9) could be written as

$$\frac{d^2\tilde{V}(x)}{dx^2} - \left[\frac{1}{L(x)}\frac{dL(x)}{dx}\right]\frac{d\tilde{V}(x)}{dx} + \left(\frac{\omega}{v_p(x)}\right)^2\tilde{V}(x) = 0, \quad (2.3.11)$$

where position-dependent *nominal* phase velocity of a nonuniform transmission line is given by

$$v_p = \frac{1}{\sqrt{L(x)C(x)}}. \quad (2.3.12)$$

It is difficult to get a general solution for the above wave equations. However, under the case of no reflection on a line, and the line with a small fractional change in L(x) and C(x) over a wavelength, Lewis and Wells, and Wohler [B.17, J.11] have given the following solution of wave equation (2.3.11):

$$\widetilde{V}(x) = \widetilde{V}(0)\left[\frac{Z_0(x)}{Z_0(0)}\right]^{\frac{1}{2}} \exp\left[-j\omega\int_0^x \frac{dx}{v_p(x)}\right]. \tag{2.3.13}$$

In this expression $Z_0(x)$ is the *nominal* characteristic impedance at any location x on the nonuniform transmission line, whereas characteristic impedance $Z_0(0)$ is the nominal characteristic impedance at $x = 0$. For a uniform line, the phase velocity $v_p(x)$ is constant and $Z_0(x) = Z_0(0)$, $\dfrac{dL(x)}{dx} = 0$. The wave equation (2.3.11) is reduced to the wave equation of a uniform transmission line. The solution (2.3.13) is also reduced to the standard solution, $\widetilde{V}(x) = \widetilde{V}(0)e^{-j\beta x}$.

Equation (2.3.13) shows that for increasing characteristic impedance $Z_0(x)$ along the line length, the voltage amplitude also increases as the square root of nominal characteristic impedance. Lewis and Wells [B.17] have also given an expression for the reflection coefficient of the nonuniform transmission line terminated in the load Z_L at $x = \ell$:

$$\Gamma(x) = \frac{\left[1 - \dfrac{1}{j2\omega}\dfrac{v_p(x=\ell)}{Z_0(x=\ell)}\left(\dfrac{dZ_0(x)}{dx}\right)_{x=\ell}\right]Z_L - Z_0(x=\ell)}{\left[1 + \dfrac{1}{j2\omega}\dfrac{v_p(x=\ell)}{Z_0(x=\ell)}\left(\dfrac{dZ_0(x)}{dx}\right)_{x=\ell}\right]Z_L + Z_0(x=\ell)}. \tag{2.3.14}$$

For a uniform transmission line $Z_0(x = \ell) = Z_0$, and equation (2.3.14) is reduced to the nominal reflection coefficient,

$$\Gamma_{nom}(x) = \frac{Z_L - Z_0(x=\ell)}{Z_L + Z_0(x=\ell)} = \frac{Z_L - Z_0}{Z_L + Z_0}. \tag{2.3.15}$$

At higher operating frequency ω, the reflection coefficient for any termination, given by equation (2.3.14), is also reduced to equation (2.3.15). However, reflection occurs at a lower frequency ω on a nonuniform transmission line, even if the nominal reflection coefficient $\Gamma_{nom}(x = \ell)$ zero, i.e. even if the line is matched at the load end. This behavior is different from that of a uniform transmission line.

2.3.2 Lossless Exponential Transmission Line

The general solution of the wave equation for a nonuniform transmission line is not available. However, the closed-form solution is obtained for an exponential transmission line [J.11, J.13]. This case demonstrates the properties of a nonuniform line. The following exponential variation is assumed for the line inductance and capacitance of a nonuniform transmission line:

$$L(x) = L_0 e^{2px}, \quad C(x) = C_0 e^{-2px}, \tag{2.3.16}$$

where L_0 and C_0 are primary line constants at $x = 0$ and p is a *parameter controlling the propagation characteristics*. The above choice of line inductance and capacitance maintains a constant phase velocity that is independent of the location along the line length. The characteristic impedance of a lossless exponential transmission line changes exponentially along the line length. Its propagation constant is also frequency-dependent. Therefore, *a lossless nonuniform line is dispersive*. The *nominal* characteristic impedance at any location x on the line is

$$Z_0(x) = \sqrt{\frac{L(x)}{C(x)}} = \sqrt{\frac{L_0}{C_0}}e^{2px} = Z_0(x=0)e^{2px}. \tag{2.3.17}$$

The parameter p, defined below, could be determined from the characteristic impedance at the input and output ends of the line:

$$p = \frac{1}{2\ell}\log_e\frac{Z_0(\ell)}{Z_0(x=0)}. \tag{2.3.18}$$

If the impedances at both ends of a line are fixed, changing the line length, ℓ, can change the parameter p. The parameter p also determines the propagation characteristics of a nonuniform transmission line. The series impedance and shunt admittance *p.u.l.* of the exponential line can be written as follows:

$$Z(x) = j\omega L_0 e^{2px} \quad (a), \quad Y(x) = j\omega C_0 e^{-2px} \quad (b). \tag{2.3.19}$$

In case of an exponential line, the voltage and current wave equations (2.3.9) and (2.3.10) reduce to

$$\frac{d^2\widetilde{V}(x)}{dx^2} - 2p\frac{d\widetilde{V}}{dx} + \omega^2 L_0 C_0 \widetilde{V}(x) = 0. \tag{2.3.20}$$

$$\frac{d^2\widetilde{I}(x)}{dx^2} + 2p\frac{d\widetilde{I}}{dx} + \omega^2 L_0 C_0 \widetilde{I}(x) = 0. \tag{2.3.21}$$

Let us assume the following exponential form of the solution for the above wave equations with separate propagation constants for the voltage and current waves:

$$\widetilde{V}(x) = \widetilde{V}_0 e^{-\gamma_1 x} \quad (a), \quad \widetilde{I}(x) = \widetilde{I}_0 e^{-\gamma_2 x} \quad (b). \tag{2.3.22}$$

The above differential equations provide the following characteristic equations:

$$\gamma_1^2 + 2p\gamma_1 + \omega^2 L_0 C_0 = 0 \quad (a)$$
$$\gamma_2^2 - 2p\gamma_2 + \omega^2 L_0 C_0 = 0 \quad (b). \tag{2.3.23}$$

On solving the above equations, the following expressions are obtained for the complex propagation constants:

$$\gamma_1 = \alpha_1 \pm j\beta_1 = -p \pm \sqrt{p^2 - \omega^2 L_0 C_0} \quad (a)$$
$$\gamma_2 = \alpha_2 \pm j\beta_2 = p \pm \sqrt{p^2 - \omega^2 L_0 C_0} \quad (b). \tag{2.3.24}$$

In the case of a uniform transmission line ($p = 0$), the propagation constants for the voltage and current waves are identical. The parameter p determines the attenuation constant, i.e. α of a nonuniform line. It is positive for the condition $Z_0(x = \ell) > Z_0(x = 0)$. Thus, there is an attenuation factor even for a lossless nonuniform line. The factor under the radical sign provides the propagation constant, i.e. the phase-shift constant β. At the cut-off frequency, $\omega = \omega_c$, β is zero. The cut-off frequency is given by

$$\omega_c = \frac{p}{\sqrt{L_0 C_0}}, \tag{2.3.25}$$

where phase velocity of the voltage and current waves on the line at $x = 0$ is

$$V_p(x = 0) = \frac{1}{\sqrt{L_0 C_0}}. \tag{2.3.26}$$

The complex propagation constants can be rewritten as follows:

$$\gamma_1 = \alpha_1 \pm j\beta_1 = -p \pm jp\sqrt{\left(\frac{\omega}{\omega_c}\right)^2 - 1} \quad (a)$$
$$\gamma_2 = \alpha_2 \pm j\beta_2 = p \pm jp\sqrt{\left(\frac{\omega}{\omega_c}\right)^2 - 1} \quad (b). \tag{2.3.27}$$

The propagation constants β_1 and β_2 are imaginary quantities for the signal below the cut-off frequency $\omega < \omega_c$. Under such conditions, no wave propagates on the nonuniform line. The initial signal only gets attenuated. It is called the *evanescent mode*. The wave propagation takes place only for $\omega > \omega_c$. Therefore, a nonuniform transmission line behaves like a high-pass filter (HPF). However, real parts of the complex propagation constants γ_1 and γ_2 are nonzero. For $p > 0$, the voltage wave gets attenuated while the current wave is increased in the positive direction of wave propagation. In the backward direction, the reflected voltage and current waves have opposite behavior. The attenuation in the signal is not due to any ohmic loss of a line. It is due to the continuous reflection of the wave as it progresses on the line. The opposite behavior of the voltage and current waves maintains the constant flow of power (P) at any location on a line:

$$P(x) = \frac{1}{2}\widetilde{V}(x)\widetilde{I}^*(x) = \frac{1}{2}V_0 I_0 e^{-(\gamma_1 + \gamma_2^*)x}, \tag{2.3.28}$$

where $\gamma_1 + \gamma_2^* = 0$. Unlike a lossless uniform transmission line, the phase velocity of the voltage and current waves on a lossless nonuniform transmission line is dispersive as given below:

$$v_p = \frac{\omega}{\beta} = \frac{\omega}{p\sqrt{\left(\frac{\omega}{\omega_c}\right)^2 - 1}}. \tag{2.3.29}$$

The phase velocity shows singularity at the cut-off frequency. After the cut-off frequency, i.e. for $\omega >> \omega_c$, it decreases, with an increase in frequency, to a value given by expression (2.3.26).

References

Books

B.1 Nahin Paul, J.: *Oliver Heaviside, Sage in Solitude: The Life, Work, and Times of an Electrical Genius of the Victorian Age*, IEEE Press, New York, 1988.

B.2 MacCluer, C.R.: *Boundary Value Problems and Fourier Expansions*, Dover Publications, Mineola, NY, 2004.

B.3 Sears, F.W.; Zemansky, M.W.: *University Physics*, Addition-Wesley, Boston, MA, 1973.

B.4 Huygens, C.: *Treatise on Light*, Macmillan, London, 1912.

B.5 Karakash, J.J.: *Transmission Lines and Filter Networks*, Macmillan, New York, 1950.

B.6 Johnson, W.C. *Transmission Lines and Networks*, McGraw-Hill, Inc., New York, 1950.

B.7 Mattick, R.E.: *Transmission Lines for Digital and Communication Networks*, IEEE Press, New York, 1995.

B.8 Weeks, W.L.: *Electromagnetic Theory for Engineering Applications*, John Wiley & Sons, New York, 1964.

B.9 Rizzi, P.A.: *Microwave Engineering- Passive Circuits*, Prentice-Hall International Edition, Englewood Cliff, NJ, 1988.

B.10 Pozar, D.M.: *Microwave Engineering*, 2nd Edition, John Wiley & Sons, Singapore, 1999.

B.11 Ramo, S.; Whinnery, J.R.; Van Duzer, T.: *Fields, and Waves in Communication Electronics*, 3rd Edition, John Wiley & Sons, Singapore, 1994.

B.12 Collin, R.E.: *Foundations for Microwave Engineering*, 2nd Edition, McGraw-Hill, Inc., New York, 1992.

B.13 Rao, N.N.: *Elements of Engineering Electromagnetics*, 3rd Edition, Prentice-Hall, Englewood Cliff, NJ, 1991.

B.14 Sadiku, M.N.O.: *Elements of Electromagnetics*, 3rd Edition, Oxford University Press, New York, 2001.

B.15 Cheng, D.K.: *Fields and Wave Electromagnetics*, 2nd Edition, Pearson Education, Singapore, 1089.

B.16 Bhattacharyya, A.K.: *Electromagnetic Fields in Multilayered Structures*, Artech House, Norwood, MA, 1994.

B.17 Lewis, I.A.D.; Wells, F.H.: *Millimicrosecond Pulse Techniques*, 2nd Edition, Pergamon Press, London, 1939.

Journals

J.1 Searle, G.F.C., et al. *The Heaviside Centenary Volume*, The Institution of Electrical Engineers, London, 1950.

J.2 Whittaker, E.T.: *Oliver Heaviside*, In *Electromagnetic Theory* Vol. 1, Oliver Heaviside, Reprint, Chelsea Publishing Company, New York, 1971.

J.3 Verma, A.K.; Nasimuddin: *Quasistatic RLCG parameters of lossy microstrip line for CAD application*, *Microwave Opt. Tech. Lett.*, Vol. 28, No. 3, pp. 209–212, Feb. 2001

J.4 Hasegawa, H.; Furukawa, M.; Yanai, H.: *Properties of microstrip line on Si-SiO2 system*, *IEEE Trans. Microwave Theory Tech.*, Vol. MTT-19, pp. 869–881, 1971.

J.5 Kurokawa, K.: *Power waves and the scattering matrix*, *IEEE Trans. Microwave Theory Tech.*, Vol. 13, No. 2, pp. 607–610, 1965.

J.6 Tang, C.C.H.: Delay equalization by tapered cutoff waveguides, *IEEE Trans. Microwave Theory Tech.*, Vol. 12, No. 6, pp. 608–615, Nov. 1964.

J.7 Roberts, P.P.; Town, G.E.: *Design of microwave filters by inverse scattering*, *IEEE Trans. Microwave Theory Tech.*, Vol. 7, pp. 39–743, April 1995.

J.8 Burkhart, S.C.; Wilcox R.B.: *Arbitrary pulse shape synthesis via nonuniform transmission lines*, *IEEE Trans. Microwave Theory Tech.*, Vol. 38, No. 10, pp.1514–1518, Oct. 1990.

J.9 Hayden, L.A.; Tripathi, V.K.: *Nonuniform coupled microstrip transversal filters for analog signal processing*, *IEEE Trans. Microwave Theory Tech.*, Vol. 39, No. 1, pp. 47–53, Jan. 1991.

J.10 Young, P.R.; McPherson, D.S.; Chrisostomidis, C.; Elgaid, K.; Thayne, I.G.; Lucyszyn, S.; Robertson I.D.: *Accurate non-uniform transmission line model and its application to the de-embedding of on-wafer measurements*, *IEEE Proc. Microwave Antennas Propag.*, Vol. 148, No. 1, pp. 153–156, June 2001.

J.11 Wohlers, M.R.: *Approximate analysis of lossless tapered transmission lines with arbitrary terminations*, *Proc. IRE*, Vol. 52, No. 11, 1365, Dec. 1964.

J.12 Khalaj-Amirhosseini, M.: *Analysis of periodic and aperiodic coupled nonuniform transmission lines using the Fourier series expansion*, *Prog. Electromagn. Res., PIER*, Vol. 65, pp. 15–26, 2006.

J.13 Ghose, R.N.: *Exponential transmission lines as resonators and transformers*, *IRE Trans. Microwave Theory Tech.*, Vol. 5, No. 3, pp. 213–217, July 1957.

3

Waves on Transmission Lines – II

(*Network Parameters, Wave Velocities, Loaded Lines*)

Introduction

The transmission line sections are used to develop various passive components. These are characterized by several kinds of matrix parameters. This chapter discusses the matrix parameters and their conversion among themselves. It also discusses various kinds of dispersion and wave propagation encountered on transmission lines. The transmission lines could be loaded by the reactive elements and resonating circuits to modify the nature of the wave propagation on the lines. Such loaded lines are important in modern planar microwave technology. Such loaded lines are introduced in this chapter. The primary purpose of this chapter is to review in detail the matrix description of lines and wave propagations on the dispersive transmission line that supports various kinds of wave phenomena.

Objectives

- *To review the matrix representations of the two-port networks using the [Z], [Y], and [ABCD] parameters.*
- *To discuss the basic properties and use of the scattering [S] parameters.*
- *To understand the process of de-embedding of true [S] parameters of a device.*
- *To understand the process of extraction of the propagation constant from the [S] parameters.*
- *To understand the phase and group velocities in a dispersive medium.*
- *To discuss the circuit modeling of the reactively loaded line supporting both the forward and backward waves.*

3.1 Matrix Description of Microwave Network

At low frequency, the circuit is described in terms of several kinds of matrices that relate the port voltages to the port currents. These matrices could be the *impedance matrix* [Z], *admittance matrix* [Y], and *hybrid matrix* [H]. The *transmission matrix* is defined as the [ABCD] matrix. It is useful in cascading of two or more networks or transmission line sections. At low radio frequency, the voltage and current are measurable parameters. Therefore, the matrix elements of a network and device could be experimentally determined.

Normally, the microwave passive components, circuits, and networks are constructed around the transmission lines supporting the TEM or the *quasi*-TEM mode. Sometimes, the lumped elements are also used. The waveguide sections supporting non-TEM mode are also used to develop components and circuits. As a matter of fact, the voltage and current can be uniquely defined only for the TEM mode supporting structures. However, for non-TEM line structures, only the *equivalent* voltage and current, based on the power equivalence principle, is defined [B.1, B.2].

The abovementioned parameters are discussed in this section, as these are important for the analysis of the line networks and the networks involving both the line sections and lumped circuit elements. The results of the analysis and measurement are also presented using these parameters. The reader can study these parameters in detail from any of the excellent textbooks [B.1, B.3–B.7]. One basic difference could be seen between the lumped elements based low-frequency circuits and the transmission line sections based on high-frequency circuits. The low-frequency circuits are the *oscillation type circuits*, whereas the high-frequency microwave circuits are the *wave type circuits*. In the case of the low-frequency oscillation type circuits, the port voltage and port current are described by a single voltage or current. In general at any port, for the high-frequency wave-type circuits, the port voltage is described by a sum of the incident and reflected voltages, also the port current is a sum of the incident and reflected currents. It is illustrated in the discussions on the evaluation of the parameters.

Introduction to Modern Planar Transmission Lines: Physical, Analytical, and Circuit Models Approach, First Edition. Anand K. Verma.

How to characterize the components, circuits, and network made of the transmission line sections and waveguide sections? At the microwave frequency, port voltage and port current are not the measurable quantities. However, from the analysis point of view, the networks can be characterized by the [Z], [Y], and [ABCD] parameters. But these are not the measurable parameters at microwave frequencies. A different kind of matrix parameter, called the *scattering or [S]-parameters*, is used for the practical characterization of the microwave network and the transmission line structures [J.1]. The [S] parameter is a measurable quantity. A *Scalar Network Analyzer* is used to measure the magnitude |S| of S-parameter of any microwave circuit and network. For the measurement of the complex [S] parameters, i.e. both the magnitude and phase response of a network, a *Vector Network Analyzer* (VNA) is used. The *Circuit Simulators* and the *EM-Simulators* (Electromagnetic field simulators) are also used to get the frequency-dependent [S] parameters response of the microwave circuits.

3.1.1 [Z] Parameters

The [Z] matrix defines the impedance parameter of a two-port or a multiport network. The matrix elements are evaluated by *open circuiting* the ports. Therefore, the [Z] parameters or the impedance parameters are also called the *open-circuit parameters*. The *port voltage* (V_N) and the *port current* (I_N) are the sums of the reflected and incident voltages and currents, respectively. The port current is an independent variable, whereas the port voltage is the dependent variable. Therefore, the port currents are the *excitation* sources creating the port voltages as the *response*. The response voltage is proportional to the excitation current and the proportionality constant has the dimension of impedance.

The impedance matrix could be obtained for a general linear two-port network, shown in Fig (3.1). The wave entering the port is the *incident voltage* (V_n^+) or the *incident current* (I_n^+) wave. The *reflected voltage* (V_n^-) and *reflected current* (I_n^-) waves are also present at the ports. The total port voltage (V_n) or current (I_n) is the sum of the incident and reflected voltage or current:

$$V_n = V_n^+ + V_n^- \text{ (a)}, I_n = I_n^+ - I_n^- \text{ (b)}; n = 1, 2. \tag{3.1.1}$$

In equation (3.1.1), n = 1, 2 is the port number, i.e. port-1, port-2. The power entering the network is taken as a positive quantity for the incident wave, so the power

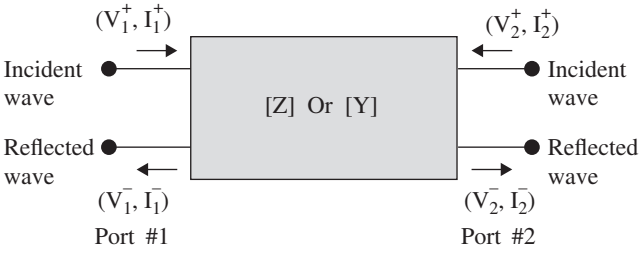

Figure 3.1 Two-port network to determine [Z] and [Y] parameters.

coming out of the network, i.e. the power of the reflected wave, is taken as a negative quantity. The reflected voltage (V_n^-) is positive. To maintain the negative direction of power flow, the reflected current wave (I_n^-) is taken as negative in the above equation. At each port, the current entering the port from outside is positive, whereas the current leaving the port is negative. For the linear networks, the voltage at any port is a combined response of the currents applied to all ports. On using the superposition of the voltage responses, the following set of equations is written:

$$\begin{aligned} V_1 &= Z_{11} I_1 + Z_{12} I_2 \\ V_2 &= Z_{21} I_1 + Z_{22} I_2. \end{aligned} \tag{3.1.2}$$

Equation (3.1.2) is written in a more compact matrix form:

$$[V] = [Z]\,[I], \tag{3.1.3}$$

where [V] and [I] are the column matrices. The two-port impedance matrix is

$$[Z] = \begin{bmatrix} Z_{11} & Z_{12} \\ Z_{21} & Z_{22} \end{bmatrix}. \tag{3.1.4}$$

The [Z] parameter can be easily extended to the N-port networks [B.1, B.3–B.5]. The Z-parameters are the *open-circuited parameters*. The coefficient of the matrix can be defined in terms of the open circuit condition at the ports:

$$Z_{ii} = \left.\frac{V_i}{I_i}\right|_{I_k = 0}, \quad i = 1, 2..., \text{and } k \neq i. \tag{3.1.5}$$

All the ports are open-circuited, except the i^{th} port at which the matrix element Z_{ii} is defined. For instance, in the case of a two-port network, Z_{11} is obtained when current I_1 is applied to port-1 and the voltage response is also obtained at the port-1, while keeping the port-2 open-circuited, i.e. $I_2 = 0$. The coefficient, Z_{11}, is known as the *self-impedance* of the network. These are the

diagonal elements of a [Z] matrix. The off-diagonal elements of a [Z] matrix are defined as follows:

$$Z_{ij} = \left.\frac{V_i}{I_j}\right|_{I_k = 0}, \quad k \neq j. \tag{3.1.6}$$

In this case, the current excitation is applied at the port-j and the voltage response is obtained at the port-i. All other ports are kept open-circuited allowing $I_k = 0$, except at the port-j. For instance, in the case of a two-port network to evaluate Z_{12}, the current source is applied at the port-2, and the voltage response is obtained at the port-1, while keeping the port-1 open-circuited. The coefficient Z_{12} is the *mutual impedance* that describes the coupling of port-2 with the port-1. A network can have $Z_{11} = Z_{22}$, i.e. both of the ports are electrically identical. Such a network is known as the *symmetrical* network. Furthermore, the voltage response of a network at the port-1 due to the current at the port-2 can be identical to the voltage response at the port-2, due to the current at the port-1. This kind of network is a *reciprocal* network. It has a $Z_{12} = Z_{21}$. If $Z_{12} = Z_{21} = 0$, the ports are *isolated* one.

Example 3.1
Figure (3.2) shows lumped elements T-network. Determine the [Z] parameter of the network.

Solution

For the port-2 open-circuited, $I_2 = 0$. The voltage at the port-1 is

$$V_1 = (Z_A + Z_C)I_1, \quad Z_{11} = \left.\frac{V_1}{I_1}\right|_{I_2 = 0} = Z_A + Z_C.$$

$$V_2 = I_1 Z_C, \qquad Z_{21} = \left.\frac{V_2}{I_1}\right|_{I_2 = 0} = Z_C.$$

Likewise, for the port-1 open-circuited, $I_1 = 0$, and the parameters are $Z_{22} = Z_B + Z_C$, $Z_{12} = Z_C$. The [Z] matrix description of a T-network is

$$[Z] = \begin{bmatrix} Z_A + Z_C & Z_C \\ Z_C & Z_B + Z_C \end{bmatrix}. \tag{3.1.7}$$

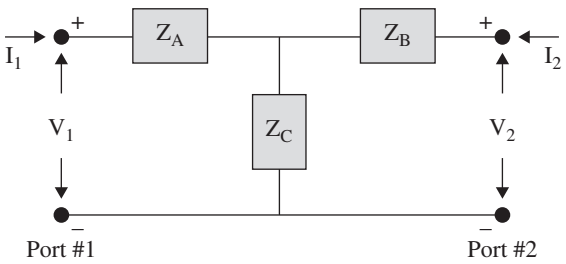

Figure 3.2 Lumped T-network.

The given circuit is asymmetrical. However, it is a reciprocal circuit. It becomes symmetrical for $Z_A = Z_B$.

Example 3.2
Determine the [Z]-parameter of a section of the transmission line of length ℓ shown in Fig (3.3).

Solution

Let the port-2 be open-circuited and an incident voltage $V^{inc} = V_1^+$ is applied at the port-1. The voltage wave reaches to the port-2 and reflects from there. It reaches the port-1 as the voltage wave $V_1^+ e^{-2\gamma\ell}$. The maximum of the voltage wave occurs at the port-2. The total port voltages are given below:

At the port-1: $V_1 = V_{inc} + V_{ref} = V_1^+ + V_1^+ e^{-2\gamma\ell}$.
At the port-2: $V_2 = V_{inc} + V_{ref} = 2V_1^+ e^{-\gamma\ell}$.
At the port-1: $I_1 = I_{inc} - I_{ref} = \frac{V_1^+}{Z_0} - \frac{V_1^+}{Z_0} e^{-2\gamma\ell}$.
At the port-2: $I_2 = 0$.

Thus, the [Z] parameters are obtained as follows:

$$Z_{11} = \left.\frac{V_1}{I_1}\right|_{I_2 = 0} = Z_0\left(\frac{1 + e^{-2\gamma\ell}}{1 - e^{-2\gamma\ell}}\right) = Z_0 \coth(\gamma\ell).$$

$$Z_{21} = \left.\frac{V_2}{I_1}\right|_{I_2 = 0} = Z_0\left(\frac{2e^{-\gamma\ell}}{1 - e^{-2\gamma\ell}}\right) = Z_0 \operatorname{cosech}(\gamma\ell).$$

The following [Z] matrix of a line section is obtained by keeping in view that the uniform transmission line is a symmetrical and reciprocal network:

$$[Z] = \begin{bmatrix} Z_0 \coth(\gamma\ell) & Z_o \operatorname{cosech}(\gamma\ell) \\ Z_0 \operatorname{cosech}(\gamma\ell) & Z_0 \coth(\gamma\ell) \end{bmatrix} \quad (a).$$

For the lossless transmission line, $\gamma = j\beta$, $\alpha = 0$ and [Z] is

$$[Z] = -\begin{bmatrix} jZ_0 \cot(\beta\ell) & jZ_o \operatorname{cosec}(\beta\ell) \\ jZ_0 \operatorname{cosec}(\beta\ell) & jZ_0 \cot(\beta\ell) \end{bmatrix} \quad (b). \tag{3.1.8}$$

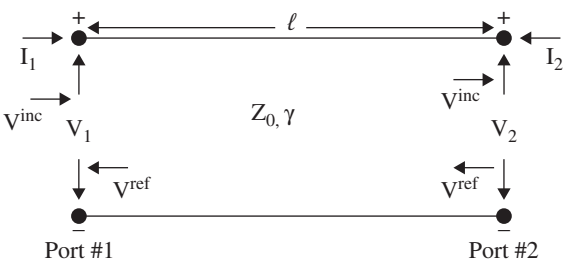

Figure 3.3 A transmission line section.

3.1.2 Admittance Matrix

To define the [Y] parameters, the voltage is taken as an independent variable and current as of the dependent one for a two-port network shown in Fig (3.1). In this case, the voltage is a source of *excitation,* and current at the port is the *response*. Thus, for a linear network, the total port current is a superposition of currents due to the voltages applied at both the ports:

$$\begin{aligned} I_1 &= Y_{11}V_1 + Y_{12}V_2 \\ I_2 &= Y_{21}V_1 + Y_{22}V_2 \end{aligned} \text{ (a)}, \Rightarrow \quad [I] = [Y][V] \text{ (b)}, \tag{3.1.9}$$

where [V] and [I] are the voltage and current column matrices. The admittance matrix of the two-port network is

$$[Y] = \begin{bmatrix} Y_{11} & Y_{12} \\ Y_{21} & Y_{22} \end{bmatrix}. \tag{3.1.10}$$

The Y-parameters are defined as the *short-circuited parameters*. For the short-circuited port-2, $V_2 = 0$, and Y_{11} and Y_{21} are defined from equation (3.1.9):

$$Y_{11} = \left.\frac{I_1}{V_1}\right|_{V_2 = 0}, \quad Y_{21} = \left.\frac{I_2}{V_1}\right|_{V_2 = 0}. \tag{3.1.11}$$

Likewise, for the short-circuited port-1, the Y-parameters are

$$Y_{22} = \left.\frac{I_2}{V_2}\right|_{V_1 = 0}, \quad Y_{12} = \left.\frac{I_1}{V_2}\right|_{V_1 = 0}. \tag{3.1.12}$$

The [Y] parameters are extended to a multiport network by defining its matrix elements as follows:

$$Y_{ii} = \left.\frac{I_i}{V_i}\right|_{V_k = 0}, \quad i = 1, 2..., \text{and } k \neq i. \tag{3.1.13}$$

Equation (3.1.13) shows that to get Y_{ii}, i.e. the diagonal elements of the [Y] matrix, all the ports are short-circuited, except the i^{th} port. The current is evaluated at the i^{th} port for the voltage applied at the i^{th} port itself. To get Y_{ij}, i.e. the off-diagonal elements of the [Y] matrix, the voltage is applied at the j^{th} port. Y_{ij} is the mutual admittance describing the coupling between the j^{th} port and the i^{th} port. The current at the i^{th} port is evaluated or measured, while all other ports are short-circuited. The admittance element Y_{ij} is evaluated as

$$Y_{ij} = \left.\frac{I_i}{V_j}\right|_{V_k = 0}, \quad i = 1, 2..., \text{and } k \neq j. \tag{3.1.14}$$

Example 3.3

Fig (3.2) shows the T-network. Determine the [Y] parameter of the network.

Solution

The loop equations for the circuit are written as

$$V_1 = (Z_A + Z_C)\, I_1 + Z_C\, I_2, V_2 = Z_C\, I_1 + (Z_B + Z_C)\, I_2.$$

For the short-circuited port-2, $V_2 = 0$: $I_2 = -\frac{Z_C}{(Z_B + Z_c)}\, I_1$.

From the above equations:

$$Y_{11} = \frac{I_1}{V_1} = \frac{Z_B + Z_C}{(Z_A + Z_C)(Z_B + Z_c) - Z_C^2}.$$
$$Y_{21} = \frac{I_2}{V_1} = -\frac{Z_C}{(Z_A + Z_C)(Z_B + Z_c) - Z_C^2}.$$

Likewise, the expressions for Y_{22} and Y_{12} could be computed by short-circuiting the port-1, $V_1 = 0$. Final [Y] matrix of the T-network is

$$[Y] = \frac{1}{\Delta Z}\begin{bmatrix} Z_B + Z_C & -Z_C \\ -Z_C & Z_A + Z_C \end{bmatrix}, \quad \text{where} \tag{3.1.15}$$
$$\Delta Z = (Z_A + Z_C)(Z_B + Z_C) - Z_C^2.$$

The above matrix is a reciprocal of the [Z] matrix, given in of length ℓ equation (3.1.7).

Example 3.4

Determine the [Y] parameter of a section of the transmission line of length ℓ shown in Fig (3.3).

Solution

The incident voltage $V^{inc} = V_1^+$ excites the port-1, and it reaches the port-2 as $V_1^+ e^{-\gamma\ell}$. The port-2 is short-circuited to determine the [Y] parameter. Under the short-circuit condition, the reflected voltage at the port-2 is $-V_1^+ e^{-\gamma\ell}$ such that the total voltage at the port-2 is zero. The reflected voltage at the port-1 is $-V_1^+ e^{-2\gamma\ell}$. The total voltage and the total current at the port-1 are

$$V_1 = V_{inc} + V_{ref}, \quad \Rightarrow \quad V_1 = V_1^+ - V_1^+ e^{-2\gamma\ell}.$$
$$I_1 = I_{inc} - I_{ref}, \quad \Rightarrow \quad I_1 = \frac{V_1^+}{Z_0} + \frac{V_1^+}{Z_0} e^{-2\gamma\ell}.$$

At the port-1, the incident current I_{inc} enters the port, so it is positive, whereas at the port-1, the reflected current I_{ref} leaves the port, so it is negative. At the port-2, the incident current I_{inc} enters the port-2 from the port-1 side and leaves the port-2, so it is negative, whereas at the port-2, the reflected current I_{ref} from the terminated load, enters the port-2, so it is positive. The total voltage and the total current at the port-2 are

$$V_2 = V_1^+ e^{-\gamma\ell} + \left(-V_1^+ e^{-\gamma\ell}\right) = 0, I_2 = -I_{inc} + I_{ref}$$
$$\Rightarrow I_2 = -\frac{V_1^+}{Z_0} e^{-\gamma\ell} + \left(-\frac{V_1^+}{Z_0} e^{-\gamma\ell}\right) = -\frac{2V_1^+}{Z_0} e^{-\gamma\ell}.$$
$$Y_{11} = \left.\frac{I_1}{V_1}\right|_{V_2=0} = \frac{1}{Z_0}\frac{1+e^{-2\gamma\ell}}{1-e^{-2\gamma\ell}} = Y_0 \coth(\gamma\ell).$$
$$Y_{21} = \left.\frac{I_2}{V_1}\right|_{V_2=0} = -\frac{2e^{-\gamma\ell}}{Z_0(1-e^{-2\gamma\ell})} = -Y_0 \operatorname{cosech}(\gamma\ell).$$

The line section is symmetrical and reciprocal giving the [Y] parameter:

for the lossy line section:

$$[Y] = \begin{bmatrix} Y_0 \coth(\gamma\ell) & -Y_o \operatorname{cosech}(\gamma\ell) \\ -Y_0 \operatorname{cosech}(\gamma\ell) & Y_0 \coth(\gamma\ell) \end{bmatrix} \quad (a)$$

and for the lossless line section:

$$[Y] = \begin{bmatrix} -jY_0 \cot(\beta\ell) & jY_o \operatorname{cosec}(\beta\ell) \\ jY_0 \operatorname{cosec}(\beta\ell) & -jY_0 \cot(\beta\ell) \end{bmatrix} \quad (b). \tag{3.1.16}$$

3.1.3 Transmission [ABCD] Parameter

On many occasions, two or more circuit elements or circuit blocks are interconnected in such a way that the output voltage and current of the first circuit block become the input to the next circuit block. To facilitate such combination or cascading, the circuit elements and blocks are characterized using the *transmission parameters*, i.e. the [ABCD] matrix, instead of [Z] or [Y] matrix. The great strength of the transmission parameter, i.e. the [ABCD] parameter, is due to its ability to provide [ABCD] matrix of the complete cascaded network, as a multiplication of the [ABCD] matrices of the individual circuit element or circuit block. The [ABCD] parameter, different from the T-matrix, is applicable to a two-port network only.

To obtain the transmission matrix description of a two-port network, the output voltage and current are treated as the independent variables. The following expressions relate to the input and output voltage and current of the two-port network shown in Fig (3.4):

$$\begin{aligned} V_1 &= A V_2 + B I_2 \\ I_1 &= C V_2 + D I_2. \end{aligned} \tag{3.1.17}$$

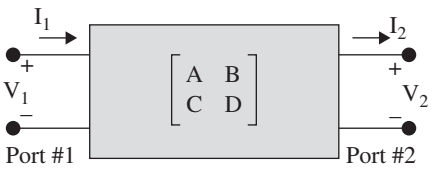

Figure 3.4 Two-port network for transmission parameter.

These expressions can be written in the matrix form,

$$\begin{bmatrix} V_1 \\ I_1 \end{bmatrix} = \begin{bmatrix} A & B \\ C & D \end{bmatrix} \begin{bmatrix} V_2 \\ I_2 \end{bmatrix}. \tag{3.1.18}$$

In the case of the [Z] and [Y] parameters, the positive current I_2 enters the port, while in the above network defining the [ABCD] parameter in Fig (3.4), *the output current I_2 leaving the port is taken as positive* [B.1, B.3]. It is an input to the next circuit block, as shown in Fig (3.5). However, like defining the [Z] and [Y] parameters, to define the [ABCD] parameter current, I_2 could be taken as the current entering the output port. In this case, I_2 in equation (3.1.18) is replaced by $(-I_2)$ [B.1, B.4].

The matrix elements A, B, C, D can be determined from the open and short circuit conditions at the output port. When the output is open-circuited, $I_2 = 0$. Equation (3.1.17) provides the parameter-A and C:

$$A = \left.\frac{V_1}{V_2}\right|_{I_2=0} \quad (a), \quad C = \left.\frac{I_1}{V_2}\right|_{I_2=0} \quad (b). \tag{3.1.19}$$

The parameter A is the *voltage ratio* that is a reciprocal of the voltage gain. The parameter C is the *trans-admittance* of a network. It relates the output voltage of a network to its input current source.

When the output is short-circuited, $V_2 = 0$. Equation (3.1.17) again provides the parameters-B and D:

$$B = \left.\frac{V_1}{I_2}\right|_{V_2=0}, \quad D = \left.\frac{I_1}{I_2}\right|_{V_2=0}. \tag{3.1.20}$$

The parameter B is the *trans-impedance* of a network. It provides the output current when the input of a network is excited by the voltage source. The parameter D is the *current ratio* giving a reciprocal of the current gain of a network.

Fig (3.5) demonstrates the usefulness of the transmission parameters to obtain an equivalent [ABCD] parameter of the cascaded networks. The [ABCD] parameters for the first and the second network are written as

$$\begin{bmatrix} V_1 \\ I_1 \end{bmatrix} = \begin{bmatrix} A_1 & B_1 \\ C_1 & D_1 \end{bmatrix} \begin{bmatrix} V_2 \\ I_2 \end{bmatrix}, \begin{bmatrix} V_3 \\ I_3 \end{bmatrix} = \begin{bmatrix} A_2 & B_2 \\ C_2 & D_2 \end{bmatrix} \begin{bmatrix} V_4 \\ I_4 \end{bmatrix}.$$

At the junction of two networks, $I_2 = I_3$ and $V_2 = V_3$. Therefore, from the above equations, the following expression is obtained:

$$\begin{bmatrix} V_1 \\ I_1 \end{bmatrix} = \begin{bmatrix} A_1 & B_1 \\ C_1 & D_1 \end{bmatrix} \begin{bmatrix} A_2 & B_2 \\ C_2 & D_2 \end{bmatrix} \begin{bmatrix} V_4 \\ I_4 \end{bmatrix}. \tag{3.1.21}$$

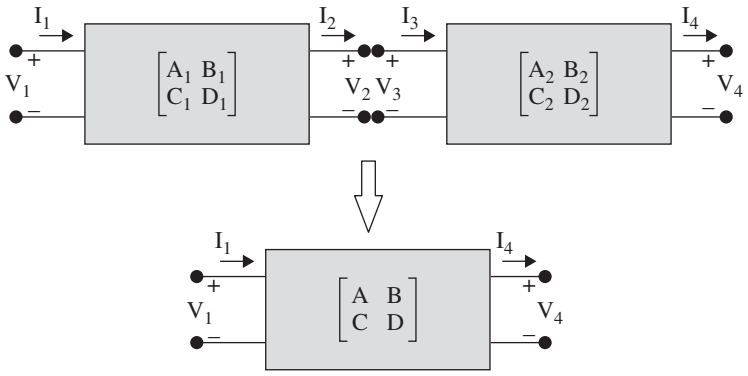

Figure 3.5 Cascading of two networks to get one equivalent network.

Finally, two cascaded networks can be replaced by one equivalent 2-port network having equivalent [ABCD] parameter. It is given by the following expression:

$$\begin{bmatrix} A & B \\ C & D \end{bmatrix} = \begin{bmatrix} A_1 & B_1 \\ C_1 & D_1 \end{bmatrix} \begin{bmatrix} A_2 & B_2 \\ C_2 & D_2 \end{bmatrix}. \tag{3.1.22}$$

Expression (3.1.22) can be extended to the cascading of N-networks by multiplying the individual matrix of each network.

Example 3.5

Determine the [ABCD] parameters of the series impedance as shown in Fig (3.6).

Solution

The output port is open-circuited, $I_2 = 0$. Therefore, equation (3.1.17) provides $V_1 = AV_2$ and $I_1 = CV_2$. For the port 2 of Fig (3.6) open-circuited, $I_2 = 0$, $V_1 = V_2$ and $I_2 = I_1 = 0$. On comparing these equations, the computed parameters are $A = 1$ and $C = 0$.

For the output port is short-circuited, $V_2 = 0$. Therefore, equation (3.1.17) helps to get, $V_1 = BI_2$ and $I_1 = DI_2$. Using Fig (3.6) shows, $V_2 = 0$, $V_1 = ZI_2$ and $I_1 = I_2$. The comparison of these equations provide $B = Z$ and $D = 1$.

Thus, the [ABCD] matrix of series impedance is written as

$$\begin{bmatrix} A & B \\ C & D \end{bmatrix} = \begin{bmatrix} 1 & Z \\ 0 & 1 \end{bmatrix}. \tag{3.1.23}$$

Example 3.6

Determine the [ABCD] parameters of a shunt admittance shown in Fig (3.7).

Solution

The output port-2 is open-circuited, $I_2 = 0$. Therefore, from matrix equation (3.1.17): $V_1 = AV_2$ and $I_1 = CV_2$.At the open-circuited output port 2: $I_2 = 0$, $V_1 = V_2$ and $I_1 = YV_2$. On comparing these equations: $A = 1$ and $C = Y$. At the short-circuited output port 2: $V_2 = 0, V_1 = BI_2$ and $I_1 = DI_2$.Using Fig (3.7), for $V_2 = 0$, $V_1 = 0$ and $I_1 = I_2$. On comparing these equations: $B = 0$ and $D = 1$. Finally, the [ABCD] matrix of shunt admittance can be written as

$$\begin{bmatrix} A & B \\ C & D \end{bmatrix} = \begin{bmatrix} 1 & 0 \\ Y & 1 \end{bmatrix}. \tag{3.1.24}$$

The [ABCD] matrix could be easily evaluated for the L, T, and π networks, shown in Fig (3.8). The [ABCD] matrix of each element is known and the complete circuit is a cascading of the elements.

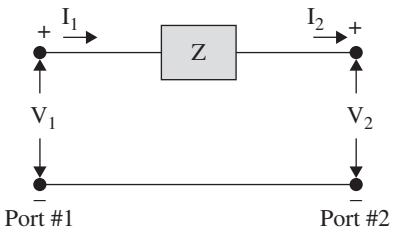

Figure 3.6 Series impedance.

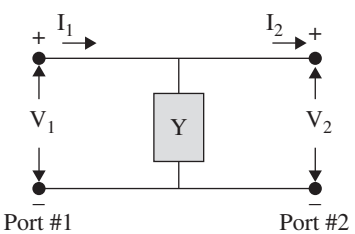

Figure 3.7 Shunt admittance.

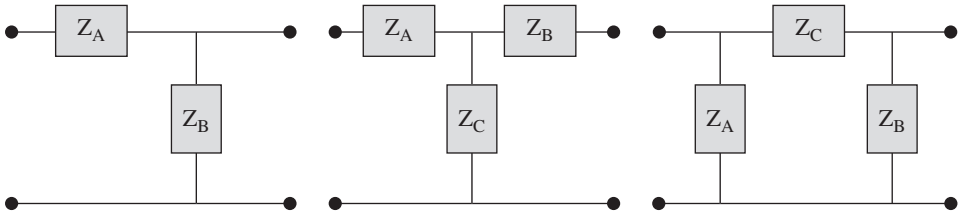

(a) L-Network. (b) T-Network. (c) π-Network.

Figure 3.8 Basic networks.

Example 3.7
Determine the [ABCD] parameters of a section of transmission line shown in Fig (3.3).

Solution

Equations (2.1.79) of chapter 2 provide the voltage and current waves on a transmission line:

$$V(x) = V^+ e^{-\gamma x} + V^- e^{\gamma x}, I(x) = \frac{V^+}{Z_0} e^{-\gamma x} - \frac{V^-}{Z_0} e^{\gamma x}.$$

The V^+ and V^- are the amplitudes of the forward and reflected waves, respectively. For convenience, the distance x is measured from the port-2. The voltage and current at the port-2 are

$$V(x = 0) = V_2 = V^+ + V^-, I(x = 0) = Z_0 I_2 = V^+ - V^-.$$

The amplitudes of the forward and reflected voltages in terms of the port voltage and port current are

$$V^+ = \frac{V_2 + Z_0 I_2}{2}, \quad V^- = \frac{V_2 - Z_0 I_2}{2}.$$

The voltage and current on a transmission line can be written as

$$V(x) = \left[\frac{e^{\gamma x} + e^{-\gamma x}}{2}\right] V_2 + \left[\frac{e^{-\gamma x} - e^{\gamma x}}{2}\right] Z_0 I_2.$$
$$I(x) = \frac{1}{Z_0}\left[\frac{e^{-\gamma x} - e^{\gamma x}}{2}\right] V_2 + \left[\frac{e^{-\gamma x} + e^{\gamma x}}{2}\right] I_2.$$

The voltage and current at the input port-1 are obtained for $x = -\ell$:

$$V(x = -\ell) = V_1 = \cosh(\gamma\ell) V_2 + Z_0 \sinh(\gamma\ell) I_2$$
$$I(x = -\ell) = I_1 = \frac{\sinh(\gamma\ell)}{Z_0} V_2 + \cosh(\gamma\ell) I_2.$$

Above equations can be written in the matrix form:

$$\begin{bmatrix} V_1 \\ I_1 \end{bmatrix} = \begin{bmatrix} \cosh(\gamma\ell) & Z_o \sinh(\gamma\ell) \\ Y_0 \sinh(\gamma\ell) & \cosh(\gamma\ell) \end{bmatrix} \begin{bmatrix} V_2 \\ I_2 \end{bmatrix}.$$

The [ABCD] parameters of the lossy and lossless transmission line sections are given by equation (3.1.25a) and equation (3.1.25b), respectively:

$$\begin{bmatrix} A & B \\ C & D \end{bmatrix} = \begin{bmatrix} \cosh(\gamma\ell) & Z_o \sinh(\gamma\ell) \\ Y_0 \sinh(\gamma\ell) & \cosh(\gamma\ell) \end{bmatrix} \quad \text{(a)}$$

$$\begin{bmatrix} A & B \\ C & D \end{bmatrix} = \begin{bmatrix} \cos(\beta\ell) & j Z_o \sin(\beta\ell) \\ j Y_0 \sin(\beta\ell) & \cos(\beta\ell) \end{bmatrix}; \ \alpha = 0, \gamma = j\beta \quad \text{(b)}. \tag{3.1.25}$$

The above example can be further extended to a network of several cascaded transmission line sections having different ℓ, Z_0, and γ. The overall [ABCD] parameter of the multisection transmission line can be obtained by a multiplication of the [ABCD] matrix of each line section. The line sections can be attached to the series and the shunt lumped elements. Even in such cases, one can find the overall [ABCD] parameter of a complete network. The input impedance, output impedance, Thevenin and Norton equivalent circuits, and power transfer relation, etc. of a complete circuit can be written in terms of the [ABCD] matrix. However, a detailed discussion of these aspects is out of the scope of this book. The reader can follow many available texts for this purpose [B.1, B.2–B.5, B.7, B.8].

3.1.4 Scattering [S] Parameters

The [Z], [Y], and [ABCD] matrix descriptions of any microwave network or component are based on the port voltage and port current relations. The evaluation of these parameters requires the short-circuiting and open-circuiting of the ports. At the microwave frequency, usually, it is difficult to measure the voltage and current. Similarly, the short-circuiting and open-circuiting of the ports may not be always possible at the microwave frequency. Thus, these parameters are normally not measurable quantities. However, these parameters are useful for the analysis of the microwave circuits built around the lumped and distributed circuit elements. At this stage, another kind of measurable parameters is needed to characterize the microwave circuits. At the microwave frequency, the power could be

measured, and also the forward and reflected power waves could be obtained. The frequency and phase of a microwave signal are also measurable quantities. The *scattering parameters*, also called the *S-parameters,* are defined for any two-port network, or even the multiport microwave network, in terms of the measurable incident and reflected power waves [J.1].

Basic Concept

A commonly used two-port network is suitable to develop the concept of the S-parameter. Even the S-parameters of a multiport network are measured as the two-port parameters, while other ports are terminated in the matched loads. Figure (3.9) shows the two-port network. It is to be characterized by the S-parameters. The port-1 and port-2 are terminated with the line sections of characteristic impedance Z_{01} and Z_{02}, respectively. However, most of the two-port networks have $Z_{01} = Z_{02} = Z_0$, i.e. the identical transmission line sections at both the ports. The *reference* impedance Z_0 is normally 50Ω. The incident voltage waves at both the ports-V_1^+ and V_2^+, enter the ports and the reflected voltage waves at both the ports-V_1^- and V_2^-, come out of the ports.

The forward power, i.e. the incident power entering the port-1, is

$$P_1^+ = \frac{V_1^{+2}}{Z_0}\ (a), \quad P_1^+ = \frac{V_{1\,max}^{+2}}{2Z_0}\ (b). \tag{3.1.26}$$

In equation (3.1.26b), $V_1^+ = V_{1\,max}^+/\sqrt{2}$ is the RMS voltage of the voltage wave. In general for the two-port or N-port network, the forward power entering the i^{th} port is written as

$$P_i^+ = \frac{V_i^{+2}}{Z_{0i}}, \quad i = 1, 2, ..., N. \tag{3.1.27}$$

The *incident power variable* a_i at the i^{th} port is defined in a way that the power entering the port is given by the square of the *power variable*:

$$P_i^+ = a_i^2. \tag{3.1.28}$$

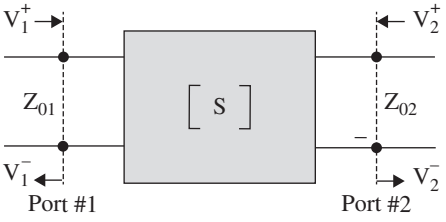

Figure 3.9 Two-port network for evaluation of S-parameter.

Using equations (3.1.27) and (3.1.28), the power variable a_i is written in terms of the forward RMS voltage V_i^+ at the i^{th} port

$$a_i = \frac{V_i^+}{\sqrt{Z_{0i}}}, \quad i = 1, 2, ..., N. \tag{3.1.29}$$

The forward voltage can also be written in term of the power variable as

$$V_i^+ = \sqrt{Z_{0i}}\, a_i. \tag{3.1.30}$$

The power variable a_i is simply a normalized forward voltage wave, incident on the i^{th} port. The normalization is done with respect to the square root of the characteristic impedance at the port. The forward power variable can also be viewed as the incident normalized current. The power entering the i^{th} port, in terms of the incident RMS current I_1^+, is given below:

$$P_i^+ = I_i^{+\,2} Z_{0i} = a_i^2 \Rightarrow a_i = I_i^+ \sqrt{Z_{0i}}, \quad i = 1, 2, ..., N. \tag{3.1.31}$$

The forward port current in terms of the forward power variable is

$$I_i^+ = \frac{a_i}{\sqrt{Z_{0i}}}, \quad i = 1, 2, ..., N. \tag{3.1.32}$$

The multiplication of the voltage and current of equations (3.1.30) and (3.1.32), again provides the forward power, $P_i^+ = V_i^+ I_i^+ = a_i^2$. Thus, the definitions of the power variable both as the *normalized voltage wave* and as *the normalized current wave* are consistent. However, one must be careful about the presence of the square root of the characteristic impedance in the numerator and denominator for two definitions.

Consider the reflected power wave at the i^{th} port with characteristic impedance Z_{0i}. Figure (3.10) shows that the i^{th} port is connected to a source with impedance Z_0. For the sake of clarity, the port is taken out of the

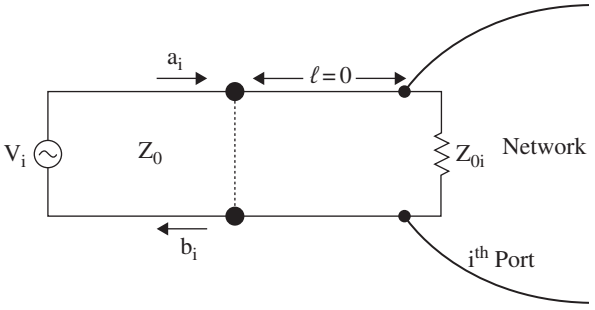

Figure 3.10 A section of the multiport network. Port is shown extended with length ℓ = 0.

network using an interconnect line of characteristic impedance Z_0 with zero length, $\ell = 0$. The total power available from the source does not enter the network. A part of it gets reflected. The reflected power in terms of the *reflected power variable* b_i is

$$P_i^- = b_i^2 = \frac{V_i^{-\,2}}{Z_{0i}}, \quad i = 1, 2, ..., N. \tag{3.1.33}$$

The reflected power variable is related to the reflected port voltage and the reflected port current as follows:

$$b_i = \frac{V_i^-}{\sqrt{Z_{0i}}}, \qquad \Rightarrow \quad V_i^- = \sqrt{Z_{0i}}\, b_i. \tag{3.1.34}$$

$$b_i = \sqrt{Z_{oi}}\, I_i^-, \qquad \Rightarrow \quad I_i^- = \frac{b_i}{\sqrt{Z_{0i}}}. \tag{3.1.35}$$

The power entering the i^{th} port is

$$P_{i,in} = P_i^+ - P_i^- = a_i^2 - b_i^2 = a_i\left(1 - |\Gamma_i|^2\right), \tag{3.1.36}$$

where the *reflection coefficient* at the i^{th} port is $\Gamma_i = b_i/a_i$. The *total port voltage* and the *total port current* in term of the power variables can be written as

$$\begin{aligned} V_i &= V_i^+ + V_i^- = \sqrt{Z_{0i}}(a_i + b_i) \quad (a) \\ I_i &= I_i^+ - I_i^- = \frac{1}{\sqrt{Z_{0i}}}(a_i - b_i) \qquad (b). \end{aligned} \tag{3.1.37}$$

The reflected port current I_i^- is negative, such that the reflected power $P_i^- = V_i^-\, I_i^-$ travels in the opposite direction, i.e. it travels away from the port. Using equation (3.1.37), the power variables can be written in terms of the total port voltage and the total port current:

$$\begin{aligned} a_i &= \frac{1}{2}\left(\frac{V_i}{\sqrt{Z_{0i}}} + I_i\sqrt{Z_{0i}}\right) \qquad (a) \\ b_i &= \frac{1}{2}\left(\frac{V_i}{\sqrt{Z_{0i}}} - I_i\sqrt{Z_{0i}}\right) \qquad (b). \end{aligned} \tag{3.1.38}$$

The definition of the power wave variables given by the equations (3.1.30), (3.1.32), (3.1.34), and (3.1.35) are valid for the special cases of the forward wave and reflected waves. The definition, given in equation (3.1.38), is valid for the general case. It is applicable at any port for any kind of termination. *The power-variables a_i and b_i are complex quantities*. The incident and reflected power are

$$P_i^+ = |a_i|^2 = a_i\, a_i^*, \quad P_i^- = |b_i|^2 = b_i\, b_i^*. \tag{3.1.39}$$

Scattering [S] Matrix

Figure (3.11) shows the N-port network. The power *entering* the i^{th} port is given in terms of the forward voltage wave V_i^+ or the forward power variable a_i and the power *leaving* the i^{th} port is given in terms of the reflected (backward) voltage wave V_i^- or the reflected (backward) power variable b_i. A part of the microwave power is reflected at the i^{th} port itself and remaining power entering the network comes out of all other ports as $(V_1^-, V_2^-, ..., V_N^-)$ or as $(b_1^-, b_2^-, ..., b_N^-)$. The outcoming power from any port is a linear combination of the transmitted power from all other ports. Using either the voltage variables or the power variables, the incident power and reflected power at various ports are correlated as follows:

$$\begin{bmatrix} V_1^- \\ V_2^- \\ .. \\ .. \\ V_N^- \end{bmatrix} = \begin{bmatrix} S_{11} & S_{12} & .. & S_{1N} \\ S_{21} & S_{22} & .. & S_{2N} \\ .. & .. & .. & .. \\ .. & .. & .. & .. \\ S_{N1} & S_{N2} & .. & S_{NN} \end{bmatrix} \begin{bmatrix} V_1^+ \\ V_2^+ \\ .. \\ .. \\ V_N^+ \end{bmatrix} \quad (a), \qquad \begin{bmatrix} b_1 \\ b_2 \\ .. \\ .. \\ b_N \end{bmatrix} = \begin{bmatrix} S_{11} & S_{12} & .. & S_{1N} \\ S_{21} & S_{22} & .. & S_{2N} \\ .. & .. & .. & .. \\ .. & .. & .. & .. \\ S_{N1} & S_{N2} & .. & S_{NN} \end{bmatrix} \begin{bmatrix} a_1 \\ a_2 \\ .. \\ .. \\ a_N \end{bmatrix} \quad (b). \tag{3.1.40}$$

Response — Network — Excitation — Response — Network — Excitation

The incident power at the port is treated as the *excitation*, and reflected/transmitted power at the port is considered as the *response*. The network is characterized by the S-parameters.

Therefore, the matrix elements S_{ij} relating the excitation (V_i^+ or a_i) to the response (V_i^- or b_i) are described as follows:

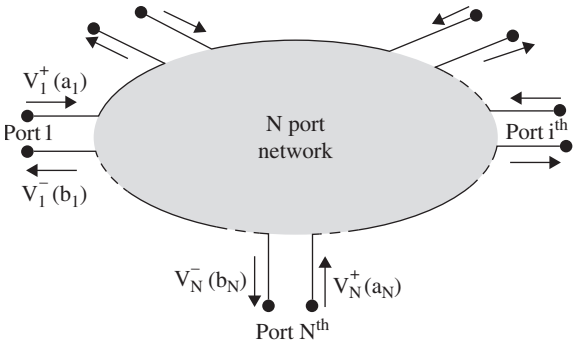

Figure 3.11 N-port network showing power variables (a_i, b_i) in terms of voltage variables (V_i^+, V_i^-).

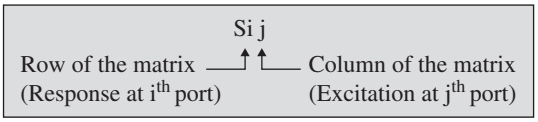

The S_{ij} is defined with the help of the matched termination. The matched termination also helps to measure the matrix elements S_{ij}.

Reflection Coefficient S_{ii}

Figure (3.12) shows that the i^{th} port of a multiport network is terminated in a load equal to the characteristic impedance of the port. The power wave b_i coming out of the port is incident on the load Z_L, whereas the incident power wave a_i is the reflected wave from the load. If a port is terminated in its characteristic impedance, i.e. $Z_L = Z_0$, then the reflection from the load at the port is zero, i.e. $a_i = 0$. Thus, for the excitation a_j applied at the j^{th} port, while all other ports are terminated in their characteristic impedances, the ports have $V_1^+ (a_1) = V_2^+ (a_2) = \cdots = V_i^+ (a_i) = 0, (i \neq j)$. However, the power b_j is reflected from the j^{th} port.

The reflection coefficient at the j^{th} port is obtained from equation (3.1.40):

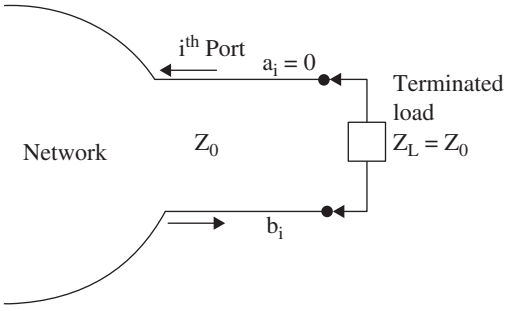

Figure 3.12 At the i^{th} port, the load is terminated in port characteristic impedance.

$$S_{ij} = \left.\frac{b_j}{a_j}\right|_{a_i = 0} = \left.\frac{V_j^-}{V_j^+}\right|_{V_i^+ = 0}, \quad i \neq j. \tag{3.1.41}$$

Therefore, S_{ij} is the reflection coefficient (Γ_j) at the j^{th} port, provided all other ports are terminated in their characteristic impedances. However, if other ports are not terminated in their characteristic impedances, then S_{jj} is not a measure of the true reflection coefficient of the network or a device at the j^{th} port. The true reflection coefficient at the j^{th} port, under the unmatched load condition, is more than S_{jj} that is defined under the matched load condition.

Transmission Coefficient S_{ij}

If the excitation source is connected only to the j^{th} port and the response is seen at the i^{th} port, while all other ports are terminated in their characteristic impedances, it leads to $V_1^+ = V_2^+ = \cdots = V_k^+ = 0$, i.e. $a_1 = a_2 = \cdots = a_k = 0, (k \neq j)$. It shows that the excitation is zero at all ports, except at the j^{th} port. The transmitted power, i.e. the scattered power, from the j^{th} port is available at all ports, i = 1, 2, ..., k. However, at the j^{th} port, a part of the incident power appears as the reflected power. The *transmission coefficient*, S_{ij} for the power transfer from the j^{th} port to the i^{th} port is defined as

$$S_{ij} = \left.\frac{b_i}{a_j}\right|_{a_k = 0, k \neq j} = \frac{V_i^-}{V_j^+}\left.\sqrt{\frac{Z_{0j}}{Z_{0i}}}\right|_{V_k^+ = 0, k \neq j} = \frac{I_i^-}{I_j^+}\left.\sqrt{\frac{Z_{0i}}{Z_{0j}}}\right|_{V_k^+ = 0, k \neq j}. \tag{3.1.42}$$

Normally, the network has identical port impedances and equal to the system impedance, i.e. $Z_{0i} = Z_{0j} = Z_0$. Equation (3.1.40) is written in compact form as

$$[V^-] = [S]\,[V^+], \quad \Rightarrow [b] = [S]\,[a]. \tag{3.1.43}$$

The elements of the [S] matrix are determined using equations (3.1.41) and (3.1.42).

Properties of [S] Matrix

Some important properties of the [S] matrix description of the network are summarized below, without going for the formal proof of these statements. Usually, elements of the [S] matrix are complex quantities. The detailed discussion is available in the well-known textbooks [B.1–B.5, B.7].

Reciprocity Property

The [S] matrix of a *reciprocal* network is a symmetric matrix, i.e. the transpose $[S]^T$ of the [S] matrix is equal to the [S] matrix itself:

$$[S] = [S]^T. \tag{3.1.44}$$

Unitary Property

The [S] matrix of a *lossless* network is a unitary one. However, if the network is not lossless, then it is not unitary. The definition of the unitary matrix provides the following relation for the given [S] matrix:

$$[S]^T [S]^* = [I], \tag{3.1.45}$$

where $[S]^T$ is the transpose of the [S] matrix, $[S]^*$ is a complex conjugate of the complex [S] matrix and [I] is the identity matrix. Thus, for a given 2-port [S] matrix, we have

$$[S] = \begin{bmatrix} S_{11} & S_{12} \\ S_{21} & S_{22} \end{bmatrix}, \quad [S]^* = \begin{bmatrix} S_{11}^* & S_{12}^* \\ S_{21}^* & S_{22}^* \end{bmatrix}, \quad [S]^T = \begin{bmatrix} S_{11} & S_{21} \\ S_{12} & S_{22} \end{bmatrix}.$$

On substituting these expressions in the unitary relation (3.1.45), the following result is obtained:

$$\begin{bmatrix} S_{11} & S_{21} \\ S_{12} & S_{22} \end{bmatrix} \begin{bmatrix} S_{11}^* & S_{12}^* \\ S_{21}^* & S_{22}^* \end{bmatrix} = \begin{bmatrix} 1 & 0 \\ 0 & 1 \end{bmatrix}$$
$$\Rightarrow \begin{bmatrix} S_{11}S_{11}^* + S_{21}S_{21}^* & S_{11}S_{12}^* + S_{21}S_{22}^* \\ S_{12}S_{11}^* + S_{22}S_{21}^* & S_{12}S_{12}^* + S_{22}S_{22}^* \end{bmatrix} = \begin{bmatrix} 1 & 0 \\ 0 & 1 \end{bmatrix}. \tag{3.1.46}$$

On equating each element of matrix equation (3.1.46), the following relations are obtained:

$$\begin{aligned} S_{11}S_{11}^* + S_{21}S_{21}^* &= 1 \\ S_{12}S_{12}^* + S_{22}S_{22}^* &= 1 \end{aligned} \text{ (a)}, \quad \begin{aligned} S_{11}S_{12}^* + S_{21}S_{22}^* &= 0 \\ S_{12}S_{11}^* + S_{22}S_{21}^* &= 0 \end{aligned} \text{ (b)}. \tag{3.1.47}$$

Equations (3.1.47) are generalized for the N-port network:

$$\sum_{i=1}^{N} \left(S_{ik}S_{ik}^*\right) = 1, \ k = 1, 2, ..., N. \tag{3.1.48}$$

$$\sum_{i=1}^{N} \left(S_{ik}S_{ij}^*\right) = 0, \ j \neq k \quad j, k = 1, 2, ..., N. \tag{3.1.49}$$

Equation (3.1.48) shows that both elements have identical columns, whereas in equation (3.1.49) column are not identical. The [S] matrix is formed by the column vector as follows:

$$[S] = \left[\vec{p}, \vec{q}\right], \text{where } \left[\vec{p}\right] = \begin{bmatrix} S_{11} \\ S_{21} \end{bmatrix} \text{ and } \left[\vec{q}\right] = \begin{bmatrix} S_{12} \\ S_{22} \end{bmatrix}. \tag{3.1.50}$$

Therefore, in the usual vector notation we have

$$\begin{aligned} \vec{p} &= \hat{i}\, S_{11} + \hat{j}\, S_{21} \\ \vec{q} &= \hat{i}\, S_{12} + \hat{j}\, S_{22}. \end{aligned} \tag{3.1.51}$$

Hence, for a lossless network the following statements, based on equations (3.1.48) and (3.1.49) are made:

- The dot product of any column vector with its complex conjugate is unity, $\vec{p} \cdot \vec{p}^{\,*} = 1$.
- The dot product of any column vector with the complex conjugate of any other column vector is zero, $\vec{p} \cdot \vec{q}^{\,*} = 0$.
- The [S] matrix forms an orthogonal set of the vectors.

The following expressions are written from equation (3.1.47):

$$|S_{11}|^2 + |S_{21}|^2 = 1 \text{ (a)}, \ |S_{12}|^2 + |S_{22}|^2 = 1 \text{ (b)}. \tag{3.1.52}$$

Equation (3.1.52) is the power balance equations for the lossless two-port networks. The unit input power fed to the port-1 is a sum of the reflected power ($|S_{11}|^2$) at the port-1 and the transmitted power $|S_{21}|^2$ to the port-2. In the case $|S_{11}|^2 + |S_{21}|^2$ is less than unity, some power is lost in the network through the mechanism of conductor, dielectric, and radiation losses. The lost power, i.e. the power dissipation in the network, is

$$P_d = 1 - \left(|S_{11}|^2 + |S_{21}|^2\right). \tag{3.1.53}$$

Phase Shift Property

The [S] parameter is a complex quantity. It has both magnitude and phase. Thus, the [S]-parameter is always defined with respect to a *reference plane*. In Fig (3.13) [S]-parameter of the N-port network is known at the location x = 0. It is determined at the new location, $x = -\ell_n$. Alternatively, once the [S] parameters are known at $x = -\ell_n$, these are determined at x = 0, i.e. at the port of the network. The location ℓ_n shows the length of the line connected to each port of an N-port network. Normally, it is the point of measurement of the [S] parameters of the network or device. The interconnecting transmission line is lossless and has propagation constant β_n. Thus, the electrical length of the connecting line is $\theta_n = \beta_n \ell_n$.

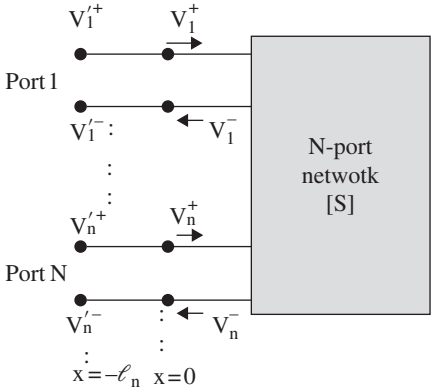

Figure 3.13 N-port network showing phase-shifting property.

For an N-port network, the incident wave at the n^{th} port, $x = -\ell_n$, after reflection from the port at $x = 0$, returns to $x = -\ell_n$. In the process, it travels the electrical length $2\theta_n$. Similarly, if the wave is incident at port #1, located at $x = -\ell_1$ and arrives at the port-2, located at $x = -\ell_2$; the electrical length traveled by the wave is $\theta_1 + \theta_2 = \beta_1\ell_1 + \beta_2\ell_2$, or $2\theta_1$, on the assumption that $\beta_1 = \beta_2$, and $\ell_1 = \ell_2$, i.e. the transmission lines connected at both the ports are identical. The measured or simulated scattering matrix $[S']$ at the location $x = -\ell_n$ is related to the [S] parameters of the network by the following expression

$$[S'] = [S]\left[e^{-j\,2\theta_n}\right]. \tag{3.1.54}$$

The [S]-parameter of the network is extracted from equation (3.1.54), as

$$[S] = \left[S'\right]\left[e^{+j\,2\theta_n}\right]. \tag{3.1.55}$$

For reducing the cascaded network to a single equivalent network, the [S] parameters cannot be cascaded like the [ABCD] parameters. The [ABCD] matrix is suitable for this purpose. However, it is not defined in terms of the power variables. Therefore, another suitable transmission matrix, called [T] *matrix* has been defined in terms of the power variables to cascade the microwave networks. The [S] matrix is easily converted to the [T] parameters [B.1, B.2–B.5, B.7, B.9].

The concept of the [S] matrix is used below to some simple, but useful circuits. These examples would help to appreciate the applications of the [S] parameters.

Example 3.8

Determine the S-parameters and return loss of a 2-port network with arbitrary termination shown in Fig (3.14).

Solution

The 2-port network (device) is connected to a source at the port-1 and a load Z_L at the port-2. The source has voltage V_g with internal impedance Z_g. The network scattering parameters-[S] are computed under the matched condition. The characteristic impedance of the connecting line between the port-1 and the source is Z_{01}, whereas the characteristic impedance of the connecting line between the port-2 and the load is Z_{02}. The lengths of the connecting lines are zero. The reflection and transmission coefficients are to be determined at the input and output terminals. This is a practical problem for the measurement and simulation of the 2-port network:

$$\begin{aligned} b_1 &= S_{11}a_1 + S_{12}\,a_2 \quad (a)\\ b_2 &= S_{21}a_1 + S_{22}\,a_2 \quad (b). \end{aligned} \tag{i}$$

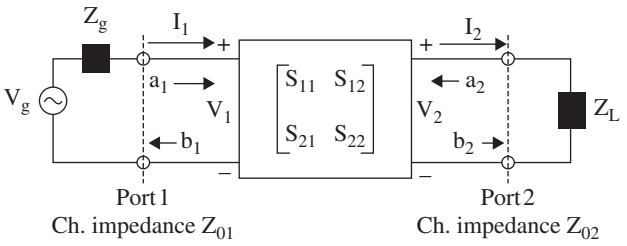

Figure 3.14 A two-port network with arbitrary termination.

Figure (3.14) shows that the power variable b_2 is the incident wave at the load Z_L and the power variable a_2 is the reflected wave from the load. Thus, the reflection coefficient at the load is

$$\Gamma_L = \frac{Z_L - Z_{02}}{Z_L + Z_{02}} = \frac{a_2}{b_2}\,. \tag{ii}$$

From above equations (i) and (ii):

$$\begin{aligned} b_1 &= S_{11}a_1 + S_{12}\,\Gamma_L b_2 \quad (a)\\ b_2 &= S_{21}a_1 + S_{22}\,\Gamma_L b_2\\ \Rightarrow b_2 &= \frac{S_{21}}{1 - S_{22}\Gamma_L}a_1 \quad (b). \end{aligned} \tag{iii}$$

On substituting b_2 from equation (b) in equation (a):

$$b_1 = \left[S_{11} + \frac{S_{12}S_{21}\Gamma_L}{1 - S_{22}\Gamma_L}\right]a_1. \tag{iv}$$

The input reflection coefficient at the port-1 is

$$\Gamma_{in} = \Gamma_1 = \frac{\text{Reflected wave from port} - 1}{\text{Incident wave at port} - 1} = \frac{b_1}{a_1}$$

$$\Rightarrow \quad \Gamma_1 = \left[S_{11} + \frac{S_{12}S_{21}\Gamma_L}{1 - S_{22}\Gamma_L}\right]. \tag{3.1.56}$$

The reflection coefficient Γ_1 is more than S_{11} of the network. The mismatch at the load degrades the return loss (RL) of the network. It is given by

$$RL = -20\log_{10}|\Gamma_1|. \tag{3.1.57}$$

For the port 2 open-circuited ($Z_L \to \infty$), the waves get reflected in-phase, i.e. $\Gamma_L = 1$, and for a short-circuited load ($Z_L = 0$) the total reflection is out of phase, i.e. $\Gamma_L = -1$. If the network is terminated in a matched load ($Z_L = Z_{02}$), the incident waves are absorbed with $\Gamma_L = 0$ and $\Gamma_1 = S_{11}$. Likewise, the source reflection coefficient Γ_g could be defined at the input port-1. Figure (3.14) again shows that b_1 is the incident wave on the internal impedance of the source Z_g and a_1 is the reflected wave from Z_g. Thus,

$$\Gamma_g = \frac{Z_g - Z_{01}}{Z_g + Z_{01}} = \frac{a_1}{b_1}\,. \tag{v}$$

The output reflection coefficient Γ_2 at the port-2 is obtained from equations (i) and (v):

$$\Gamma_2 = \frac{b_2}{a_2} = \left[S_{22} + \frac{S_{21}S_{12}\Gamma_g}{1 - S_{11}\Gamma_g}\right]. \tag{3.1.58}$$

Again under the matched condition ($Z_g = Z_{01}$) at the input port, $\Gamma_g = 0$. For most of the applications, 50 Ω system impedance is used, i.e. $Z_{01} = Z_{02} = Z_0 = 50\,\Omega$. For a 2-port lossless network, we have the following expressions:

$$S_{11}S_{11}^* + S_{21}S_{21}^* = 1\,(a),\ S_{12}S_{12}^* + S_{22}S_{22}^* = 1\,(b).$$

However, for a reciprocal network $S_{12} = S_{21}$. Thus, the above equations provide

$$|S_{11}| = |S_{22}| \quad (a), \quad |S_{12}| = \sqrt{1 - |S_{11}|^2} \qquad (b). \tag{3.1.59}$$

The network also follows $S_{11}S_{12}^* + S_{21}S_{22}^* = 0$. The S-parameters are complex quantities. The S-parameters are written in the phasor form: $S_{11} = |S_{11}|\,e^{j\theta_1}$, $S_{22} = |S_{22}|\,e^{j\theta_2}$ and $S_{12} = |S_{12}|\,e^{j\phi}$. From the above equation, the phase relation is obtained:

$$|S_{11}|\sqrt{1 - |S_{11}|^2}\left[e^{j(\theta_1 - \phi)} + e^{j(\phi - \theta_2)}\right] = 0 \qquad (a)$$

$$\Rightarrow\ \phi = \frac{\theta_1 + \theta_2}{2} + \frac{\pi}{2} \mp n\pi \qquad (b). \tag{3.1.60}$$

Therefore, once the complex S_{11} and S_{22} are measured, both the magnitude and phase of the S_{21} are determined. However, usually, both S_{11} and S_{21} are obtained from a VNA and also from the circuit simulator or EM-simulator. The magnitude of S_{21} provides the *insertion-loss* of the network and ϕ is the phase shift at the output of the network.

Example 3.9

Determine the S-parameters of the series impedance shown in Fig (3.15). Also, compute the attenuation and the phase shift offered by the series impedance.

Solution

To compute S_{11} that is the reflection coefficient of a network under the matched condition, the port-2 is terminated in Z_0. Thus, $Z_{in} = Z + Z_0$ and the reflection coefficient at port-1 is

$$S_{11} = \frac{Z_{in} - Z_0}{Z_{in} + Z_0} = \frac{Z}{Z + 2Z_0}. \tag{3.1.61}$$

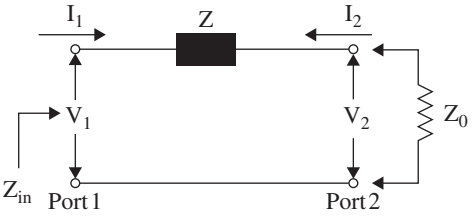

Figure 3.15 Network of series impedance.

Likewise, to compute S_{22}, the port-1 is terminated in Z_0. It gives $Z_{out} = Z + Z_0$ at the port-2. The S_{22} is

$$S_{22} = \frac{Z_{out} - Z_0}{Z_{out} + Z_0} = \frac{Z}{Z + 2Z_0}. \tag{3.1.62}$$

The total port voltage at the port-1 is a sum of the forward and reflected voltages:

$$V_1 = V_1^+ + V_1^- = (S_{11} + 1)V_1^+ \quad (i) \quad \left\{\text{Note: } S_{11} = \frac{V_1^-}{V_1^+}\right\}.$$

To compute S_{21}, i.e. the transmission coefficient from the port-1 to the port-2 under the matched termination, at first, the total port voltage at the port-2 is obtained:

$$V_2 = V_2^+ + V_2^- = V_2^- \qquad (ii)$$
$$\{\text{Note: } V_2^+ = 0 \text{ due to the matched termination.}\}$$

Therefore, from equations (i) and (ii):

$$S_{21} = \left.\frac{V_2^-}{V_1^+}\right|_{V_2^+ = 0} = \frac{V_2}{V_1}(S_{11} + 1) \qquad (iii)$$

However, the port voltage V_2 computed from the port current is

$$I_1 = \frac{V_1}{Z + Z_0} \text{ and } V_2 = Z_0 I_1 = \frac{Z_0 V_1}{Z + Z_0} \qquad (iv)$$

Finally, S_{21} is obtained from equations (iii), (iv) and (3.1.61):

$$S_{21} = \frac{V_2}{V_1}(S_{11} + 1) = \frac{Z_0}{Z + Z_0}\left(1 + \frac{Z}{Z + 2Z_0}\right) = \frac{2Z_0}{Z + 2Z_0}. \tag{3.1.63}$$

Equations (3.1.61) and (3.1.63) provide the following relation:

$$S_{11} + S_{21} = 1. \tag{3.1.64}$$

The [S] matrix of the series impedance is

$$[S] = \begin{bmatrix} S_{11} & 1 - S_{11} \\ 1 - S_{11} & S_{11} \end{bmatrix}. \tag{3.1.65}$$

The attenuation and phase shift of a signal, applied at the input port-1 of series impedance $Z = R + jX$, are computed below.

Using S_{21} from equation (3.1.63), the attenuation offered by the series impedance is

$$\alpha(\text{dB}) = 20\log_{10}\left|\frac{1}{S_{21}}\right| = 20\log_{10}\left|1 + \frac{R + jX}{2Z_0}\right|$$
$$\Rightarrow \alpha(\text{dB}) = 10\log\left[\left(1 + \frac{R}{2Z_0}\right)^2 + \left(\frac{X}{2Z_0}\right)^2\right]. \tag{3.1.66}$$

The lagging phase shift of the signal at the output port-2, due to the series element, is

$$\phi = -\tan^{-1}\left(\frac{X}{R + 2Z_0}\right). \tag{3.1.67}$$

Example 3.10

Determine the S-parameter of a shunt admittance shown in Fig (3.16). Also, compute the attenuation and the phase shift offered by the shunt admittance.

Solution

The shunt admittance is $Y = G + jB$. To compute S_{11}, the port-2 is terminated in Z_0 ($=1/Y_0$) giving $Y_{in} = Y + Y_0$. The reflection coefficient of the shunt admittance under matched termination is

$$S_{11} = \frac{Y_0 - Y_{in}}{Y_o + Y_{in}} = \frac{-Y}{2Y_0 + Y}. \tag{3.1.68}$$

Likewise, to compute S_{22} of the shunt admittance, the port-1 is terminated in Z_0:

$$S_{22} = \frac{-Y}{2Y_0 + Y}. \tag{3.1.69}$$

Following the previous case of the series impedance, the S_{21} is computed:

$S_{21} = \frac{V_2}{V_1}(S_{11} + 1)$. Fig (3.16) shows $V_1 = V_2$; therefore,

$$S_{21} = 1 + S_{11} = \frac{2}{2 + YZ_0}. \tag{3.1.70}$$

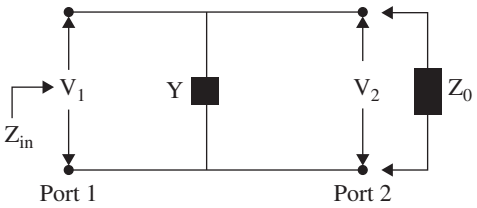

Figure 3.16 Network of shunt admittance.

The [S] matrix of the shunt admittance is

$$[S] = \begin{bmatrix} \frac{-YZ_0}{2 + YZ_0} & \frac{2}{2 + YZ_0} \\ \frac{2}{2 + YZ_0} & \frac{-YZ_0}{2 + YZ_0} \end{bmatrix}. \tag{3.1.71}$$

The attenuation of the input signal due to the shunt admittance is

$$\alpha(\text{dB}) = 20\log_{10}\left|\frac{1}{S_{21}}\right| = 20\log_{10}\left|1 + \frac{Y}{2Y_0}\right|$$
$$\Rightarrow \alpha(\text{dB}) = 10\log\left[\left(1 + \frac{G}{2Y_0}\right)^2 + \left(\frac{B}{2Y_0}\right)^2\right]. \tag{3.1.72}$$

The lagging phase shift of the signal at the output port-2, due to the shunt admittance, is

$$\phi = -\tan^{-1}\left(\frac{B}{G + 2Y_0}\right). \tag{3.1.73}$$

Example 3.11

Determine the S-parameters of a transmission line section, shown in Fig (3.17), with an arbitrary characteristic impedance.

Solution

The line has an arbitrary characteristic impedance nZ_0 and propagation constant β. The Z_0 is taken as the reference impedance to define the S-parameter. The reflection coefficient at the load end is

$$\Gamma_L(x = 0) = \frac{Z_0 - nZ_0}{Z_0 + nZ_0} = \frac{1 - n}{1 + n}. \tag{3.1.74}$$

Using equation (2.1.88) of chapter 2, the input impedance at the port-1 of the transmission line having characteristic impedance nZ_0 is

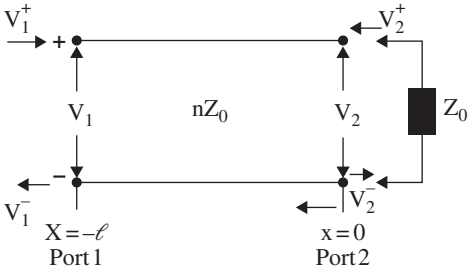

Figure 3.17 A transmission line circuit with an arbitrary characteristic impedance.

$$Z_{in} = nZ_0\left[\frac{1+\Gamma_L(x=0)\,e^{-j\,2\beta\ell}}{1-\Gamma_L(x=0)\,e^{-j\,2\beta\ell}}\right].\text{On substituting } \Gamma_L,$$

$$Z_{in} = nZ_0\left[\frac{(1+n)+(1-n)\,e^{-j\,2\beta\ell}}{(1+n)-(1-n)\,e^{-j\,2\beta\ell}}\right]. \tag{3.1.75}$$

Thus, the reflection coefficient at the port-1 is

$$S_{11} = \frac{Z_{in}-Z_0}{Z_{in}+Z_0} = \frac{(n^2-1)\left(1-e^{-j\,2\beta\ell}\right)}{(n+1)^2+(n-1)^2\,e^{-j\,2\beta\ell}}\,. \tag{3.1.76}$$

The transmission parameter S_{21} is computed in terms of S_{11}. If the amplitude of the forward traveling voltage wave on the transmission line is V_1^+, the total voltage on the transmission line is given by

$$V(x) = V_1^+\left[e^{-j\,\beta x} + \Gamma_L(x=0)e^{j\,\beta x}\right], \tag{3.1.77}$$

where x is measured from the load end, as shown in Fig (3.17). The input port-1 is located at $x = -\ell$. The voltage at the port-1 is

$$V_1 = V_1^+\left[e^{j\,\beta\ell} + \Gamma_L(x=0)e^{-j\,\beta\ell}\right]. \tag{3.1.78}$$

The port voltage V_1 is obtained as a sum of the incident and reflected voltages at the port-1:

$$V_1 = V_1^+ + V_1^- = V_1^+\,[1+S_{11}],\ \left\{S_{11} = V_1^-/V_1^+\right\}. \tag{3.1.79}$$

At the port-2, under the matched termination, $Z_L = nZ_0$ giving $V_2^+ = 0$ and $V_2 = V_2^-$. Equation (3.1.77) shows that the voltage at the port-2, i.e. at $x = 0$ is

$$V_2 = V_1^+\,[1+\Gamma_L(x=0)]. \tag{3.1.80}$$

Using equation (3.1.79), the transmission coefficient, S_{21} of the circuit shown in Fig (3.17) is obtained as

$$S_{21} = \frac{V_2^-}{V_1^+} = \frac{V_2}{V_1}(S_{11}+1)\,. \tag{3.1.81}$$

On substituting V_1 from equation (3.1.78) and V_2 from equation (3.1.80) in the above equation S_{21} is obtained:

$$\begin{aligned} S_{21} &= \frac{[1+\Gamma_L(x=0)]\,(1+S_{11})}{e^{j\,\beta\ell}+\Gamma_L(x=0)e^{-j\,\beta\ell}} \\ &= \frac{2(1+S_{11})}{(1+n)e^{j\,\beta\ell}+(1-n)e^{-j\,\beta\ell}}\,. \end{aligned} \tag{3.1.82}$$

The present line network is symmetrical and reciprocal. It has $S_{11} = S_{22}$ and $S_{21} = S_{12}$. The above expressions are checked for $n = 1$, i.e. for a transmission line of characteristic impedance Z_0. For this case, $S_{11} = S_{22} = 0$ and $S_{21} = S_{12} = e^{-j\,\beta\ell}$. These are expressions of the S-parameters for a line having characteristic impedance Z_0.

3.2 Conversion and Extraction of Parameters

Sometimes, the conversion of one kind of network parameter to another kind is needed for the analysis of a circuit. For instance, if several circuit blocks comprising of the lumped elements and the transmission line sections are cascaded, each circuit block could be expressed by its [ABCD] matrix. It helps to get an overall [ABCD] matrix of the cascaded network. However, the final [ABCD] matrix, describing the cascaded network is further converted to the [S] matrix. Similarly, the [S] matrix of each building block of the cascaded network has to be converted to the [ABCD] matrix to get the overall [ABCD] matrix of the cascaded network. Finally, the overall [ABCD] matrix is converted to the [S] matrix of the cascaded network. The S-parameters are measurable quantities. The performance of a network is measured in the [S] matrix using a *VNA*.

On several occasions, the S-parameters of a line section or a network are known either from the simulations or from the measurements. The S-parameters are used to get the characteristic impedance and the propagation constant of a line, or a network. However, the *true S-parameters* of a network are needed for this purpose. The true S-parameters are normally *embedded* in the measured or the simulated S-parameters at the ports of measurement, or the ports of simulation. The true S-parameters of a line or a network are extracted, i.e. de-embedded, from the measured, or simulated, S-parameters at the ports. This is known as the *de-embedding* process [B.10]. The EM-Simulators have provision to de-embed the true S-parameters from the S-parameters obtained at the measurement or simulation ports.

This section presents the conversion of matrix parameters, de-embedding of the S-parameters, and extraction of the propagation characteristics.

3.2.1 Relation Between Matrix Parameters

[Z] and [ABCD] Parameters

Figure (3.18) shows a network with its known [Z] parameters. It requires conversion to the [ABCD] parameters. The [ABCD] and [Z] parameters of the network are summarized below:

$$\begin{aligned} V_1 &= A\,V_2 + B\,I_2 \quad &(a)\\ I_1 &= C\,V_2 + D\,I_2 \quad &(b). \end{aligned} \tag{3.2.1}$$

$$\begin{aligned} V_1 &= Z_{11}I_1 - Z_{12}\,I_2 \quad &(a)\\ V_2 &= Z_{21}I_1 - Z_{22}\,I_2 \quad &(b). \end{aligned} \tag{3.2.2}$$

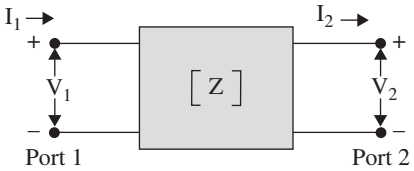

Figure 3.18 Network for Z-parameter.

The current (I_2) entering the port-2 is taken positively. However, the Z-parameter is defined in Fig (3.18) for the output current leaving the port. In this case, I_2 is negative. Equation (3.2.2) is rearranged to get the port voltage and current V_1 and I_1 at the port-1 in terms of the V_2 and I_2 at the port-2:

$$\begin{aligned} V_1 &= \frac{Z_{11}}{Z_{21}} V_2 + \left[\frac{Z_{11}\,Z_{22}}{Z_{21}} - Z_{12}\right] I_2 \qquad \text{(a)} \\ I_1 &= \frac{1}{Z_{21}} V_2 + \frac{Z_{22}}{Z_{21}} I_2 \qquad \text{(b)}. \end{aligned} \tag{3.2.3}$$

On comparing equations (3.2.1) and (3.2.3), the following conversion expressions are obtained:

$$A = \frac{Z_{11}}{Z_{21}}, \quad B = \left[\frac{Z_{11}\,Z_{22}}{Z_{21}} - Z_{12}\right], \quad C = \frac{1}{Z_{21}}, \quad D = \frac{Z_{22}}{Z_{21}}. \tag{3.2.4}$$

Likewise, the relations between [Y] and [ABCD] parameters are obtained:

$$\begin{aligned} A &= \frac{-Y_{22}}{Y_{21}}, & B &= \frac{-1}{Y_{21}} \\ C &= -\left[\frac{Y_{11}\,Y_{22}}{Y_{21}} - Y_{12}\right], & D &= \frac{-Y_{11}}{Y_{21}}. \end{aligned} \tag{3.2.5}$$

A complete set of the conversion table of parameters is available in textbooks [B.1, B.5, B.7].

[S] and [Z] Parameters

The N-port network, having normalized reference port impedance, $Z_{0n} = 1$, is considered. The port voltage and port current in terms of the incident and reflected voltage can be written as

$$V_n = V_n^+ + V_n^- \quad \text{(a)}, \quad I_n = I_n^+ - I_n^- = V_n^+ - V_n^- \quad \text{(b)}. \tag{3.2.6}$$

The above equations are written in the column matrix form:

$$[V] = [V^+] + [V^-] \quad \text{(a)}, \quad [I] = [V^+] - [V^-] \qquad \text{(b)}. \tag{3.2.7}$$

The port voltage is related to the port current through the [Z]-matrix:

$$\begin{aligned} &[V] = [Z]\ [I] \Rightarrow [V^+] + [V^-] = [Z]\,\{[V^+] - [V^-]\} \\ &\Rightarrow [V^-] = \left\{\frac{[Z] - [I]}{[Z] + [I]}\right\}[V^+], \end{aligned} \tag{3.2.8}$$

where [I] is a unit or identity matrix. Keeping in view the definition of the [S] matrix, the following relations, between the [S] matrix and [Z] matrix, are obtained:

$$[S] = \frac{[Z] - [I]}{[Z] + [I]} \quad \text{(a)}, \quad \Rightarrow [Z] = \frac{[I] + [S]}{[I] - [S]} \quad \text{(b)}. \tag{3.2.9}$$

Similarly, the following expressions, relating [S] and [Y]-parameters are obtained:

$$[S] = \frac{[I] - [Y]}{[I] + [Y]} \quad \text{(a)}, \quad \Rightarrow [Y] = \frac{[I] - [S]}{[I] + [S]} \quad \text{(b)}. \tag{3.2.10}$$

[ABCD] and [S] Parameters

Figure (3.19) shows a 2-port network. The known [ABCD] parameters of the network are to be converted to the [S] parameters. The voltage pair (V_1^+, V_2^+), and (V_1^-, V_2^-) are the incident voltage and reflected voltage at both port-1 and port-2. Figure (3.19) also shows the total port voltage (V_1, V_2) and total port current (I_1, I_2). The port currents, at both the ports, enter into the network. Therefore, the current I_2 is negative. The input port voltage and port current are related to the output port voltage and port current through the [ABCD] parameters as follows:

$$\begin{aligned} V_1 &= A\,V_2 + B\,(-I_2) \qquad \text{(a)} \\ I_1 &= C\,V_2 + D\,(-I_2) \qquad \text{(b)}. \end{aligned} \tag{3.2.11}$$

The port voltage and current are a linear combination of the incident and reflected voltages and currents:

$$\begin{aligned} &V_n = V_n^+ + V_n^-; \quad n = 1, 2 \qquad \text{(a)} \\ &I_n = \frac{1}{Z_0}\left(V_n^+ - V_n^-\right) \qquad \text{(b)}. \end{aligned} \tag{3.2.12}$$

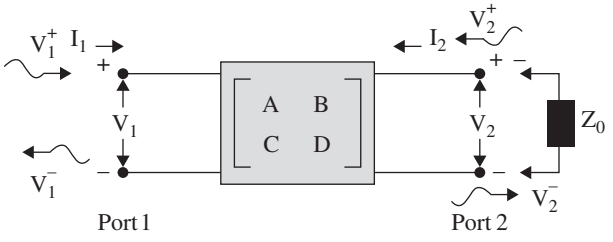

Figure 3.19 Network for [ABCD] parameter.

On substituting equation (3.2.11) in equation (3.2.12):

$$V_1 = V_1^+ + V_1^- = A\left(V_2^+ + V_2^-\right) - B\frac{\left(V_2^+ - V_2^-\right)}{Z_0} \quad (a)$$

$$I_1 = \frac{1}{Z_0}\left(V_1^+ - V_1^-\right) = C\left(V_2^+ + V_2^-\right) - D\frac{\left(V_2^+ - V_2^-\right)}{Z_0} \quad (b). \quad (3.2.13)$$

To define the [S] parameters, port-2 is terminated in the reference impedance Z_0 giving $V_2^+ = 0$, i.e. the reflection from the matched terminated load is zero. The voltage V_2^- is the incident wave on the load ($Z_L = Z_0$), whereas the voltage V_2^+ is the reflected wave from the load. The above equations are reduced to the following expressions:

$$V_1^+ + V_1^- = \left(A + \frac{B}{Z_0}\right)V_2^- \quad (a)$$

$$V_1^+ - V_1^- = (C\,Z_0 + D)\,V_2^- \quad (b). \quad (3.2.14)$$

On adding the above equations, the following expression is obtained:

$$2\,V_1^+ = (\,A + B/Z_0 + CZ_0 + D\,)\,V_2^-. \quad (3.2.15)$$

Equation (3.2.15) provides the transmission coefficient S_{21}, defined as follows:

$$S_{21} = \left.\frac{\text{Response at port-2}}{\text{Excitation at port-1}}\right|_{V_2^+ = 0} = \left.\frac{V_2^-}{V_1^+}\right|_{V_2^+ = 0}$$

$$\Rightarrow S_{21} = \frac{2}{A + B/Z_0 + CZ_0 + D}. \quad (3.2.16)$$

The following expression is obtained from equation (3.2.14):

$$\frac{V_1^+ + V_1^-}{V_1^+ - V_1^-} = \frac{A + B/Z_0}{CZ_0 + D}. \quad (3.2.17)$$

Equation (3.2.17) gives the following reflection coefficient S_{11} at the port-1, while port-2 is terminated in the matched load Z_0:

$$S_{11} = \left.\frac{\text{Response at port-1}}{\text{Excitation at port-1}}\right|_{V_2^+ = 0} = \left.\frac{V_1^-}{V_1^+}\right|_{V_2^+ = 0}$$

$$\Rightarrow S_{11} = \frac{A + B/Z_0 - CZ_0 - D}{A + B/Z_0 + CZ_0 + D}. \quad (3.2.18)$$

Similarly, the following expressions are obtained from equation (3.2.13), where the port-1 is terminated in the matched load Z_0, i.e. $V_1^+ = 0$:

$$V_1^- = (A - B/Z_0)V_2^+ + (A + B/Z_0)V_2^- \quad (a)$$

$$-V_1^- = (CZ_o - D)V_2^+ + (CZ_0 + D)V_2^- \quad (b). \quad (3.2.19)$$

On eliminating V_1^- the S_{22} is obtained, whereas S_{12} is obtained eliminating V_2^-:

$$S_{22} = \left.\frac{V_2^-}{V_2^+}\right|_{V_1^+ = 0} = \frac{-A + B/Z_0 - CZ_0 + D}{A + B/Z_0 + CZ_0 + D} \quad (a)$$

$$S_{12} = \left.\frac{V_1^-}{V_2^+}\right|_{V_1^+ = 0} = \frac{2(AD - BC)}{A + B/Z_0 + CZ_0 + D} \quad (b). \quad (3.2.20)$$

If the network is reciprocal, $AD - BC = 1$, i.e. $S_{12} = S_{21}$. For the symmetrical network, $S_{11} = S_{22}$ leading to $A = D$. The known [S] parameters can also be converted to the [A, B, C, D] parameters. Similarly, the [Z], [Y], [ABCD] and [S] parameters are also converted among themselves [B.1, B.3, B.5].

3.2.2 De-Embedding of True S-Parameters

A transmission line section could be treated as a device and its performance can be evaluated by using a VNA. The device is connected to the VNA through connecting cables and connectors. The S-parameters of a device is measured at the external circuit ports that include the effect of the cables and connectors on the S-parameters of the device. Thus, the true S-parameter of a device is *embedded* in the measured S-parameters of the device. However, it is desired to obtain the true S-parameters of the device under test (DUT). The line section could be the DUT. The process of extracting the S-parameters of the device at the *internal device ports* (1_{in}, 2_{in}), from the measured S-parameters, at the *external circuit ports* (1_{ex}, 2_{ex}) is known as the *de-embedding* process. It is achieved through a *calibration process* in which the S-parameters of two *error boxes* are quantified. The error box represents errors in the S-parameters due to cables and connectors connecting the device to the external circuit ports [B.1]. The S or [ABCD] parameter representation of the device at internal ports (1_{in}, 2_{in}) along with the error boxes is shown in Fig (3.20a). The location of the measurement ports, i.e. the external ports (1_{ex}, 2_{ex}) and the device internal ports (1_{in}, 2_{in}), are further shown in Fig (3.20b).

Once the error boxes are characterized through their S-parameters, it can be converted to the [A^e B^e C^e D^e] parameters. Similarly, the measured S-parameters of the device and the error box combined are available at the external ports. These can be converted to the measured [A^m B^m C^m D^m] parameters. The device [A^d B^d C^d D^d] parameters are related to the other two parameters by the following equation:

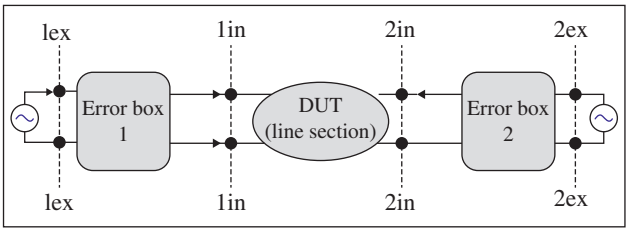

(a) Representation of measurement process with external measurement ports and internal device ports.

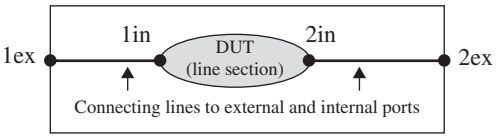

(b) Location of ports.

Figure 3.20 Calibration process in the measurement of S-parameters of a device.

$$\begin{bmatrix} A^m & B^m \\ C^m & D^m \end{bmatrix} = \begin{bmatrix} A^e & B^e \\ C^e & D^e \end{bmatrix} \begin{bmatrix} A^d & B^d \\ C^d & D^d \end{bmatrix} \begin{bmatrix} A^e & B^e \\ C^e & D^e \end{bmatrix}^{-1}. \tag{3.2.21}$$

The error box 2 is the mirror image of the error box 1 with respect to the DUT. So in the above-given matrix sequence, the third matrix is inverse of the first matrix [B.11]. At the internal device ports, the device [A^d B^d C^d D^d] parameters are de-embedding as follows:

$$\begin{bmatrix} A^d & B^d \\ C^d & D^d \end{bmatrix} = \begin{bmatrix} A^e & B^e \\ C^e & D^e \end{bmatrix}^{-1} \begin{bmatrix} A^m & B^m \\ C^m & D^m \end{bmatrix} \begin{bmatrix} A^e & B^e \\ C^e & D^e \end{bmatrix}. \tag{3.2.22}$$

The de-embedded device [A^d B^d C^d D^d] parameters are converted to the de-embedded S-parameters of the device. The de-embedded S-parameters could be further converted to the Z and Y-parameters. Thus, any two-port device can be characterized through measurements using suitable parameters- S, Z, or Y. In the case of a transmission line section, the de-embedded S-parameters can be converted to the propagation parameters and the characteristic impedance of the line.

The above-mentioned concept of de-embedding of the device S-parameters at the internal port of a device is equally applicable to the EM-Simulators – both 2.5D and 3D simulators [B.10]. In EM-simulators, the *delta-gap voltage source* could be used to launch the wave on a line section or a device. It also generates the non-propagating evanescent modes at the ports. They cause a discontinuity at the external circuit ports, i.e. at the ports of simulation. The port discontinuity affects the S-parameters of the device that is removed by the process of de-embedding [J.2]. The EM-simulators could be used to extract the propagation parameters and the characteristic impedance of a line.

3.2.3 Extraction of Propagation Characteristics

The true S-parameters of the line section, i.e. its de-embedded S-parameters over a range of frequencies are known either through the measurement or through the EM-simulation. This information can be converted to the [ABCD] parameters of a line section as follows [B.1]:

$$\begin{bmatrix} A & B \\ C & D \end{bmatrix} = \begin{bmatrix} \dfrac{(1+S_{11})(1-S_{22})+S_{12}S_{21}}{2S_{21}} & Z_o \dfrac{(1+S_{11})(1+S_{22})-S_{12}S_{21}}{2S_{21}} \\ \dfrac{1}{Z_o} \dfrac{(1-S_{11})(1-S_{22})-S_{12}S_{21}}{2S_{21}} & \dfrac{(1-S_{11})(1+S_{22})+S_{12}S_{21}}{2S_{21}} \end{bmatrix}. \tag{3.2.23}$$

Usually, $S_{11} = S_{22}$ and $S_{12} = S_{21}$ because a section of the transmission line is treated as the symmetrical and reciprocal network. The frequency-dependent [ABCD] parameters of a lossy line of length ℓ are used to compute the characteristic impedance Z_0 and propagation constant $\gamma = \alpha + j\beta$ over a range of frequencies [B.1]:

$$Z_{0l} = \sqrt{\frac{B}{C}} \quad (a), \quad \gamma = \alpha + j\beta = \frac{1}{\ell} \cosh^{-1}(A) = \frac{1}{\ell} \ln\left(A \pm \sqrt{A^2 - 1}\right) \quad (b). \tag{3.2.24}$$

The frequency-dependent secondary line parameters are extracted to get the dispersion characteristics of a line. Once the secondary line parameters of a line section are known, their frequency-dependent primary constants are computed as follows:

$$R = \mathrm{Re}(\gamma Z_0) \quad (a), \quad L = \frac{\mathrm{Im}(\gamma Z_0)}{\omega} \quad (b)$$
$$G = \mathrm{Re}\left(\frac{\gamma}{Z_0}\right) \quad (c), \quad C = \frac{\mathrm{Im}(\gamma/Z_0)}{\omega} \quad (d). \tag{3.2.25}$$

3.3 Wave Velocity on Transmission Line

In a communication network, several kinds of electrical signals propagate on a transmission line. The signal could be a modulated or unmodulated carrier wave, the baseband analog signal, or the digital pulses. The TEM mode transmission lines, and also various kinds of non-TEM waveguide structures support wave propagation. The parameters defining these transmitting media could be either frequency-independent or frequency-dependent. The property of the medium has a significant impact on the nature of wave propagation through a medium. The wave velocity has no simple or unique meaning, like the meaning of the velocity of a particle. There are several kinds of wave velocities – *phase velocity, group velocity, energy velocity, signal velocity,* etc., applied to wave propagation. The significance of several types of wave velocities is inherent both in the complexity of a signal and also in the complexity of the wave supporting medium. This section focuses attention on the meaning of the phase and group velocities only. Section (3.4) demonstrates these two wave velocities as applied to several kinds of the *artificial linear dispersive transmission lines.*

3.3.1 Phase Velocity

The concept of phase velocity is applicable to a single frequency wave, i.e. to a *monochromatic* wave discussed in Section (2.1) of chapter 2. The phase velocity is just the movement of the *wavefront*. The wavefront is a surface of constant phase, like maximum, minimum, or zero-level points shown in Fig (2.3). It is given by equation (2.1.8) of chapter 2 and reproduced below:

$$v_p = \frac{\omega}{\beta}. \tag{3.3.1}$$

The propagation constant β is influenced by the wave-supporting medium. For a lossless TEM transmission line and lossless unbounded space, β is given by

$$\beta = \omega\sqrt{LC} \ (a), \ \ \beta = \omega\sqrt{\mu\varepsilon} \ (b), \tag{3.3.2}$$

where ε and μ are permittivity and permeability of a medium. Thus, pairs (L, C) and (ε, μ) are the parameters that characterize the electrical property of the wave supporting-media. The unbounded medium supports the plane wave propagation. If these parameters are not frequency-dependent, the medium is known as *nondispersive*. In such a medium, the phase velocity remains constant at every frequency. However, if any of these parameters are frequency-dependent, the propagation constant β is frequency-dependent and consequently, the phase velocity is frequency-dependent. The medium that supports the frequency-dependent phase velocity is known as the *dispersive* medium. Normally, the characteristic impedance or intrinsic impedance of a dispersive medium is also frequency-dependent. The parameters (L, C) and (ε, μ) are usually independent of signal strength. Such a medium is called a *linear* medium, whereas the signal strength dependent medium is a *nonlinear* medium. The characteristics of the medium are discussed in Section (4.2) of chapter 4. The present discussion is only about the linear and dispersive transmission lines.

Why a medium becomes dispersive? One reason for dispersion is the loss associated with a medium. The geometry of a wave supporting inhomogeneous structures, commonly encountered in the planar technology, is another source of the dispersion. In the case of a transmission line, the parameters R and G are associated with losses and they make propagation constant β frequency-dependent. Likewise, losses make permittivity ε and permeability μ of material medium frequency-dependent complex quantities. However, a low-loss dielectric medium can be nondispersive in the useful frequency band. For such cases, the attenuation and propagation constants are given by

$$\alpha = \frac{\omega\varepsilon_r''\sqrt{\mu_r/\varepsilon_r'}}{2c} \quad (a), \quad \beta = \frac{\omega}{c}\sqrt{\mu_r\varepsilon_r'}\left[1 + \frac{1}{8}\left(\frac{\varepsilon_r''}{\varepsilon_r'}\right)^2\right] \quad (b). \tag{3.3.3}$$

In equation (3.3.3), c is the velocity of EM-wave in free space. The above expressions are obtained from equations (4.5.16) and (4.5.19) of chapter 4. The complex permittivity is given by $\varepsilon = \varepsilon' - j\varepsilon''$. The imaginary part, showing a loss in a medium, is related to the conductivity of a medium through relation $\sigma = \omega\varepsilon''$. If ε' and ε'' are not frequency-dependent, the propagation constant β is not frequency-dependent and the phase velocity is also not frequency-dependent. However, if they are frequency dependent, the phase velocity is also frequency-dependent. The phase velocity in the low-loss dielectric medium is

$$v_p = \frac{\omega}{\beta} = \frac{1}{\sqrt{\mu\varepsilon'}}\left[1 - \frac{1}{8}\left(\frac{\varepsilon''}{\varepsilon'}\right)^2\right]. \tag{3.3.4}$$

Therefore, the presence of loss decreases the phase velocity of EM-wave. This kind of wave is known as the *slow-wave*. The slow-wave can be dispersive or non-dispersive. However, it is associated with a loss. This aspect is further illustrated through the EM-wave propagation in a high conductivity medium. The conducting medium is discussed in subsection (4.5.5) of chapter 4. The attenuation (α), phase constant (β), and phase velocity ($v_{p,con}$) of a highly conducting medium are given by equation (4.5.35b) of chapter 4 [B.3]:

$$\alpha = \beta = \sqrt{\pi f \mu \sigma}. \tag{3.3.5}$$

$$v_{p,con} = \frac{\omega}{\beta} = v_p\sqrt{\frac{2\omega\varepsilon'}{\sigma}}. \tag{3.3.6}$$

The above expressions are obtained for a highly conducting medium, $\sigma/\omega\varepsilon >> 1$. It does not apply to the lossless medium with $\sigma = 0$. The wave propagation is associated with significant loss (α) given by equation (3.3.5). Moreover, both the attenuation constant and phase velocity are frequency dependent, so a conducting medium is highly dispersive. However, the periodic structures and other mechanisms give slow-wave structures with a small loss. Such structures are useful for the development of compact microwave components and devices [B.1, B.3–B.5, B7, B.12, B.13]. The slow-wave periodic transmission line structures are discussed in chapter 19.

Some EM-wave supporting media have *cut-off* property. They support the wave propagation only above the certain characteristic frequency of a medium or a structure. These media and structures are also dispersive. For instance, the *nonmagnetic plasma* medium has such cut-off property [B.4, B.14]. The plasma medium is discussed in the subsection (6.5.2) of chapter 6. The permittivity of a plasma medium is given by equation (6.5.16):

$$\varepsilon_p = \varepsilon_0\left[1 - \left(\frac{f_p}{f}\right)^2\right] \quad (a), \quad f_p = \frac{1}{2\pi}\sqrt{\frac{Ne^2}{m_e\varepsilon_0}} \quad (b). \tag{3.3.7}$$

In the above expression, f_p is the plasma frequency that is a characteristic cut-off frequency of the plasma medium [B.4, B.14]. The permeability of nonmagnetized plasma is $\mu = \mu_0$. Other parameters are as follows-ε_0: permittivity of free space, N: electron density, e: electron charge, and m_e: electron mass. The propagation constant, phase velocity, and plasma wavelength λ_{plasma} of the EM-wave wave in a plasma medium are given below:

$$\beta = \omega\sqrt{\mu\varepsilon_0}\left[1 - \left(\frac{f_p}{f}\right)^2\right]^{\frac{1}{2}} \tag{a}$$

$$v_p = \frac{1}{\sqrt{\mu\varepsilon_0}}\left[1 - \left(\frac{f_p}{f}\right)^2\right]^{-\frac{1}{2}} = v\left[1 - \left(\frac{f_p}{f}\right)^2\right]^{-\frac{1}{2}} \tag{b}$$

$$\lambda_{plasma} = \frac{2\pi}{\beta} = \frac{v}{f}\left[1 - \left(\frac{f_p}{f}\right)^2\right]^{-\frac{1}{2}} \tag{c}$$

$$v_p = \left(\frac{\lambda_{plasma}}{\lambda}\right)v \tag{d}.$$

(3.3.8)

In equation (3.3.8), $v = 1/\sqrt{\mu\varepsilon_0}$ is the velocity of EM-wave in the homogeneous medium with parameters ε_0 and μ. The wavelength in the homogeneous medium is $\lambda = v/f$. However, the nonmagnetized plasma medium has the parameters ε_0, μ_o supporting the wavelength $\lambda_0 = c/f$. The nonmagnetized plasma medium behaves as free space.

The phase velocity of the EM-waves in a plasma medium is frequency-dependent. Therefore, it is a dispersive medium that supports a *fast-wave*. It is fast in the sense that the phase velocity is higher than the phase velocity of the EM-wave in free space given by $c = 1/\sqrt{\mu_0\varepsilon_0}$. The plasma medium exhibits the *cut-off phenomenon,* similar to the cut-off behavior of the waveguide medium. The waveguide medium is discussed in the section (7.4) of chapter 7. There is no wave propagation at the plasma frequency $f = f_p$. The plasma frequency f_p behaves like the cut-off frequency f_c of a waveguide. *Thus, the waveguide can be used to simulate the electrical behavior of plasma*. For $f < f_p$, no wave propagation takes place, as the propagation constant β becomes an imaginary quantity. Such a wave is known as an *evanescent wave*. It is an exponentially decaying nonpropagating wave ($E = E_0 e^{-\alpha z}$). The standard metallic waveguide also supports the cut-off phenomenon and has a frequency-dependent phase velocity [B.1, B.5, B.7, B.8, B.15–B.17].

The dispersion is a property of the wave-supporting medium. The phase velocity of a wave in a dispersive medium can either decrease or increase with the increase in frequency. Thus, all dispersive media could be put into two groups – (i) *normal dispersive medium* and (ii) *abnormal or anomalous dispersive medium*.

Figure 3.21 Nature of normal (positive) dispersion.

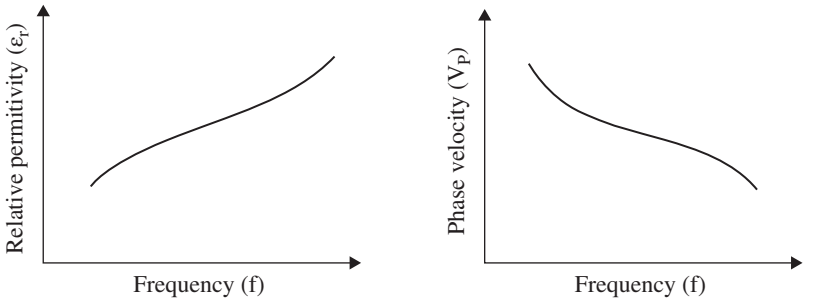

(a) Frequency-dependent relative permittivity $d\varepsilon_r / df > 0$.

(b) Frequency-dependent phase velocity $dv_p / df < 0$.

Figure (3.21a and b) show the general behavior of a medium having *normal* dispersion. The relative permittivity of such a medium increases with frequency, i.e. $d\varepsilon_r/df$ is positive, and the phase velocity decreases with frequency, i.e. dv_p/df is negative. A microstrip line provides such a medium for the normal dispersion. The effective relative permittivity of a microstrip line increases with frequency leading to a decrease in the phase velocity with an increase in frequency. The microstrip is discussed in chapter 8.

Figure (3.22a and b) show the general behavior of an *anomalous dispersive* medium. The relative permittivity of such a medium decreases with an increase in frequency, i.e. $d\varepsilon_r/df < 0$ (negative). It leads to an increase in the phase velocity with an increase in frequency, i.e. $dv_p/df > 0$ (positive). A microstrip line on a semiconductor substrate having the *Metal, Insulator, Semiconductor* (MIS) or the Schottky structure, in the transition region, is an anomalous dispersive medium [J.3, J.4].

It is emphasized that there is nothing abnormal with the anomalous dispersion. Both kinds of dispersions exist in reality. The normal dispersion is also called the *positive dispersion* as the gradient of ε_r with frequency is positive, i.e. $d\varepsilon_r/df > 0$. Similarly, the anomalous dispersion is called the *negative dispersion* with $d\varepsilon_r/df < 0$. The relative permittivity of material undergoes both kinds of dispersion depending upon the physical cause of dispersion. The dispersion is caused by several kinds of material polarizations – dipolar, ionic, electronic, and interfacial polarization. Once the frequency is varied from low-frequency to the optical frequency, the material medium undergoes these polarization changes, and the propagating wave experiences both the normal and anomalous dispersion at different frequencies [B.17, B.18]. It is discussed in chapter 6.

The concept of phase velocity applies to a single frequency signal. Now the question is to apply it to a complex baseband signal and a modulated signal. It is possible to use the phase velocity concept to such waveforms through the Fourier series of a periodic signal and using the Fourier integral for a nonperiodic signal. Any signal, periodic or nonperiodic, is composed of a large number of sinusoidal signals. They have a definite amplitude and phase relationship with the fundamental frequency of the signal. A combination of all

Figure 3.22 Nature of anomalous (negative) dispersion.

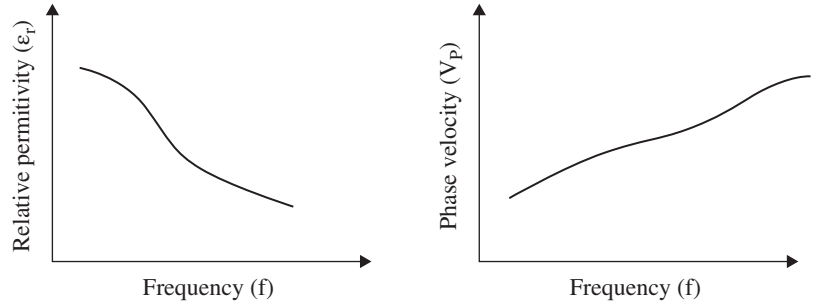

(a) Frequency-dependent relative permittivity $d\varepsilon_r / df < 0$.

(b) Frequency-dependent phase velocity $dv_p / df > 0$.

sinusoidal components gives a complex signal of definite wave-shape. If the complex waveshape travels through a dispersive medium having frequency-dependent attenuation constant $\alpha(f)$, the amplitude of each signal component changes differently. Similarly, in a dispersive medium having a frequency-dependent propagation constant $\beta(f)$, each signal component travels with a different velocity. It results in different phase-change for each frequency component of the complex wave; so the shape of the wave changes while traveling on a line or through the medium. The numerical inverse Fourier transform provides the wave-shape of a signal in the time-domain at any location in the medium. Thus, the Fourier method helps to apply the concept of phase velocity to complex waveform propagation [J.5, J.6]. Such investigations are important to maintain the signal integrity on the IC and MMIC chips.

3.3.2 Group Velocity

A complex signal composed of two or more frequency components forms a *wave-packet*. However, the frequency components should not be much different from each other like an amplitude modulated signal. Figure (3.23) shows the wave-packet formed by a group of a narrowband complex signal. The wave-packet has a central or a *carrier* frequency of higher value, superimposed with a low-frequency *envelope*. The carrier wave travels with the phase velocity v_p, whereas the envelope, i.e. the wave shape travels with the *group velocity* v_g. In a nondispersive medium, the carrier wave and envelope both travel with the same velocity without a change in the waveshape. However, in the case of a dispersive medium, velocities of the carrier and envelope are different. Depending on the nature of dispersion, the wave could be the *forward wave* or the *backward wave*. If the medium has *normal (positive) dispersion,* the phase velocity, i.e. the velocity of the carrier wave, and the velocity of the envelope, i.e. the group velocity, are in the same direction, as shown in Fig (3.23). The wave is known as the forward wave. However, in the case of a highly *anomalous (negative) dispersive* medium, under a certain condition, the phase and group velocities are in the opposite directions, forming the backward wave.

The carrier and envelope are combined to form a unified wave structure called the wave-packet. In the case of normal dispersion, the group velocity is the *energy velocity* of a signal and the information travels with the group velocity [B.1, B.4, B.5, B.7, B.14, B.16]. However, in the case of anomalous dispersion, the energy velocity and group velocity are different. In this case, group velocity is not velocity of information. Moreover, the concept of group velocity applies only to a narrow-band wave-packet, not to the wideband signal. The controversy exists at present on the travel of information with a velocity more than the velocity of light [J.7].

Formation of Two-Frequency Wave-Packet

A wave-packet is formed by a linear combination of two signals of equal magnitude with a small difference in angular frequency and phase constant. It is shown in Fig (3.24). The composite voltage wave is given by

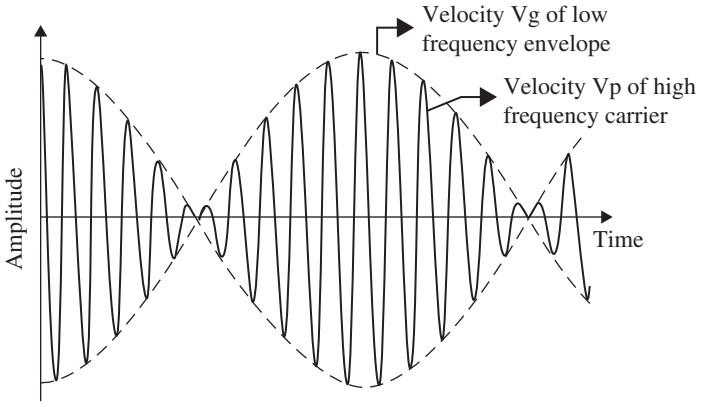

Figure 3.23 Description of phase and group velocities of a forward-moving modulated wave.